

Studying the interactions of Chikungunya virus non-structural protein 3 with *Aedes* factors

Ph.D. Thesis

By
RAMESH KUMAR



**DEPARTMENT OF BIOSCIENCES AND
BIOMEDICAL ENGINEERING
INDIAN INSTITUTE OF TECHNOLOGY
INDORE
September 2021**

Studying the interactions of Chikungunya virus non-structural protein 3 with *Aedes* factors

A THESIS

Submitted in partial fulfillment of the requirements for the award of the degree

of

DOCTOR OF PHILOSOPHY

by

RAMESH KUMAR



**DEPARTMENT OF BIOSCIENCES AND
BIOMEDICAL ENGINEERING
INDIAN INSTITUTE OF TECHNOLOGY
INDORE**

September 2021



INDIAN INSTITUTE OF TECHNOLOGY INDORE

CANDIDATE'S DECLARATION

I hereby certify that the work which is being presented in the thesis entitled **Studying the interactions of Chikungunya virus non-structural protein 3 with *Aedes* factors** in the partial fulfillment of the requirements for the award of the degree of **DOCTOR OF PHILOSOPHY** and submitted in the **DEPARTMENT OF BIOSCIENCES AND BIOMEDICAL ENGINEERING, Indian Institute of Technology Indore**, is an authentic record of my own work carried out during the time period from July 2015 till September 2021 under the supervision of Dr. Debasis Nayak, Associate Professor, Indian Institute of Technology, Indore and Dr. Sujatha Sunil, Group Leader, International Centre for Genetic Engineering and Biotechnology, New Delhi.

The matter presented in this thesis has not been submitted by me for the award of any other degree of this or any other institute.

Ramesh Kumar
03.09.2021

Signature of the student with date
(RAMESH KUMAR)

This is to certify that the above statement made by the candidate is correct to the best of my/our knowledge.

Debasis Nayak
5-9-2021

Signature of Thesis Supervisor with date

Signature of Thesis Co-supervisor with date

(Dr. DEBASIS NAYAK)

(Dr. SUJATHA SUNIL)

RAMESH KUMAR has successfully given his Ph.D. Oral Examination held on
26th December 2022

Signature of Chairperson (OEB)
Date:

Signature of External Examiner
Date:

Signature(s) of Thesis Supervisor(s)
Date:

Signature of PSPC Member #1
Date:

Signature of PSPC Member #2
Date:

Signature of PSPC Member #3
Date:

Signature of Convener, DPGC
Date:

Signature of Head of Discipline
Date:

ACKNOWLEDGEMENTS

“Take up one idea. Make that one idea your life. Think of it, dream of it, live on that idea. This is the way to success.”
-Swami Vivekananda

Firstly, I am thankful to God for blessing me with good health and strong willpower to walk in the journey of life and my Ph.D., which helped me overcome the tough times of mental stress. Lucky are those who are blessed with this.

I would like to heartily thank my thesis supervisor, Dr. Debasis Nayak, who supported me during all phases of my Ph.D. He was a constant motivator and visionary. His constant support was enough for me to focus on my work. The trust he showed and the level of patience he has been remarkable and rare. I think that is what makes him a true guru. My journey of Ph.D. would not be as smooth if he was not there. I was truly motivated for science after every interaction with him.

I want like to express my gratitude to my thesis co-supervisor, Dr. Sujatha Sunil. It was a pleasant experience to be a part of ICGEB, New Delhi. Her motivation and positivity encouraged me for science. She always gave us the freedom to plan and do experiments which can improve the understanding and interpretation of theory and it always encouraged me to think out of box ideas. I think this is the best thing that a supervisor must give to students. I was always free to discuss any work-related matter, and she was always happy for discussion. She always thought for my best, and I'll always be thankful to her for this.

I am grateful to my PSpC committee, Dr. Amit Kumar, Dr. Anjan Chakraborty and Dr. Abhijeet Joshi, for their insightful suggestions and encouragement. I am also thankful to Dr. Amit Kumar (HOD, BSBE) for his continuous support. I want to acknowledge all BSBE faculty for their support. I am thankful to all non-teaching staff of BSBE, Mr. Arif Patel, Mr. Gaurav Singh, and Mr. Murphy Bhaskar Ganveer. I would like to thanks all the academic staff, especially Mr. Tapeshe Parihar; whenever I have problems, he was always ready to help with a smile. Next, I would like to thanks all staff of the finance and account department. I am thankful to the Dean of Academic Affairs, Dean of Student Affairs, and DPGC convener for the support during the Ph.D.

I am thankful to previous directors of Indian Institute of Technology, Indore, Prof. Pradeep Mathur and Prof. Neelesh Kumar Jain, and current director Dr. Suhas Joshi and Dr. Dinakar

M. Salunki, Director, ICGEB-New Delhi, for giving me the opportunity to work at the institutes and providing me with all the required help during the Ph.D.

I would like to show affection to my lab mates at IIT Indore, Prativa majee, Ritudhwaj Tiwari, Anurag Mishra, Basant P. Sahu, Suman Bishnoi, Shruti Pyasi, Saumya Jaiswal, and at ICGEB, Priyanshu Srivastava, Ankit Kumar, Divya Mehta, Abdul Hasan, Sakshi Chaudhary, Nimisha Mishra, Geetika, Sylvester, Garvita, Dr. Dileep, Dr. Shakuntla and lab manager Mr. Dinesh Singh. I would like to acknowledge my friends Swati Gupta, Palak Babbar and others at IIT and ICGEB for their company and support all the time. I would like to recognize to all my seniors including, Dr. Jatin Shrinet, Dr. Sunil Kumar Dubey, Dr. Rahul Raina, Dr. Subodh Mishra, and Dr. Ishan Khan, for their support.

I would like to show my gratitude to Dr. Syam Prakash Somasekharan for his encouragement, guidance, and support during all the years of Ph.D. I could not continue my Ph.D. under his supervision due to some unavoidable circumstances, but he was a constant support during my Ph.D. journey.

I would like to appreciate the hard work all working members, technical staff, security personals and cleaning staff at IIT, Indore and ICGEB, New Delhi. I am thankful to IIT Indore, and ICGEB for providing the necessary facilities and infrastructure. I would like to give my regards to the Department of Biotechnology, GOI, for the Ph.D. fellowship. They were always approachable and helpful.

Lastly, I would like to shown my indebtedness to my family members, who were always supportive. My mother, Late father, brother, brother-in-law's, sisters, nephews, nieces, grandparents and all other family members, they were all supportive. As per my experience, Ph. D. journey is like roller coaster. There are times when we get results and we in the sky with happiness, but then there are times when experiments fails and we get tensed and our moral start getting down. This is the time when you need support and encouragement from supervisor and friend and family. I consider myself lucky that I was supported my supervisors, friends, and lab mates to their best.

Ramesh Kumar

Dedicated
to my family

SYNOPSIS

Title: Studying the interactions of Chikungunya virus non-structural protein 3 with *Aedes* factors

Viruses are small microscopic obligate parasites. The viruses replicate inside the cells of organisms such as bacteria, plants, and animals [1]. These contain minimum genetic material in the form of DNA or RNA, either single-stranded or double-stranded. The genetic material is encapsulated by proteins which serve the dual purpose of protection of genetic material as well as entry into the host cell [2]. Among the viruses, RNA viruses are known to cause common virus-mediated disease such as dengue fever, chikungunya fever, zika, and coronavirus disease [3,4]. A vector such as mosquitoes transmit many of these viruses like dengue, chikungunya, and zika. The last century's extensive research in basic virology and medicine led to saving countless lives. There have been attempts to develop drugs like that of bacterial infections, but due to a high mutation rate due to lack of proofreading ability of viral polymerases which causes sequence variation in proteins. These variations/ mutations make it difficult for the drugs to target the virus. The lack of specific drugs to treat these viral infections and the high rate of mutation in viruses results in outbreaks which is a concern due to its ability to impact a large population [5].

These viruses replicate inside host cells and are dependent on host machinery for their replication. Viral proteins interact with host proteins on every step of their cycle ranging from entry, replication, translation, processing, assembly, and egress. Viral growth is harmful to the host as it uses the host's resources and sometimes even kills them. In order to protect themselves from viruses, the host's immune system tries to get rid of viruses. Some immune pathways include the TLR pathway, JAK-STAT, IMD pathway, and RNAi pathway [6]. The viruses are known to interact with the host and affect them, but how they interact with mosquitoes and affect them is not well studied. Recently there were few studies that showed the impact of pathogens on mosquitoes.

Overview of the thesis

The objective of the thesis was to study the interacting partners of the chikungunya virus (CHIKV) non-structural protein 3 (nsP3). As the first step in this pursuit, the impact of chikungunya virus on *Aedes albopictus* cells' (U4.4) proteome was studied using mass spectrometry based quantitative analysis this formed the first objective of the thesis. As the next step, those proteins interacting with CHIKV-nsP3 protein were identified using co-

immunoprecipitation along with mass spectrometry. The pathway analysis revealed that proteins from pathways like translation, RNA metabolism, cellular metabolism, and gene expression were enriched. Further to this, domain analysis of nsP3 protein was also performed to understand the role of important domains in the interaction with the vector. Special attention was given to the macrodomain that was shown to possess viral suppressor activity during CHIKV infection through previous studies in our lab. Domain analysis revealed that the macrodomain has ADP ribosylhydrolase activity and sequence homology search identified three ADP ribose polymerase Aedes. The identification of these interacting partners was part of the second objective. The final objective was the validation of these interactions where two of the proteins, namely RM62F and Tankyrase were cloned and expressed in bacterial cells and purified. Further validations were performed to study the interactions of these proteins. Co-immunoprecipitation confirmed the interaction of RM62F with nsP3. Tankyrase protein was found to active in the *in vitro* assay and was capable to add ADP ribose to the protein. It was found that nsP3 was able remove the ADP ribose from the protein.

The three objectives have been categorized into three chapters. The chapter 3 discusses Objective 1, and presents the results of the global impact of chikungunya virus on proteome of *Ae. albopictus* (U4.4) cells. Chapter 4 describes the interaction study of nsP3 with *Ae. aegypti* cells' (Aag2) lysate. Chapter 5 is presented as two sub-chapters, chapter 5a presents the results of the interacting partners of nsP3 protein were validated using western blot and chapter 5b describes the characterization of *Ae. aegypti* Tankyrase protein and its interaction with nsP3 that was achieved using western blot analysis.

Chapter 1: Introduction and review of literature about chikungunya virus, its replication, transmission, and interaction with host and vector

This chapter describes the detailed information regarding chikungunya virus, its phylogeny, history of global spread, structural and genome organization. This chapter will also give a brief overview of the viral replication, mode of transmission in the host, and vector. The chapter will also cover the information about the vector of the virus, i.e., *Aedes sp.* This will further give an overview of host-pathogen interactions and the role of post-translational modifications focusing on ADP ribosylation.

Chapter 2: Materials and methodology and techniques involved the study

This chapter describes the materials, reagents, kits which were used in the study. It has protocols for the preparation of basic reagents/buffer needed for the work. It will describe basic information about the techniques used in the study and about the protocol used in the study, such as PCR, cloning, ligation, transformation, lysis, SDS-PAGE, western blot, immunofluorescence analysis, mass spectrometry, protein purification, and antibody generation. Additionally, the chapter also describes protocols such as virus propagation and viral infection.

Chapter 3: Impact of CHIKV on the proteome of *Aedes albopictus* (U4.4) cell

This chapter involves the study of the global proteome of *Ae. albopictus* cell line (U4.4) upon chikungunya virus infection. The work involves CHIKV E1 gene cloning, protein expression in *Escherichia coli* cells, and its purification. The polyclonal antibodies were raised against recombinant CHIKV E1 protein in mice and were validated with western blot and immunofluorescence assay with CHIKV infected cells or their lysate. Then the time point kinetics of CHIKV infection in U4.4 cells was done. Based on the plaque assay and western blot analysis, early time points and late time of 12 hpi and 60 hpi were chosen to study the pathways significantly modulated. Mass-spectrometry based analysis was done for early time point and late time point. The pathway analysis of significantly modulated proteins was taken further for the pathway analysis. The pathway analysis of upregulated and downregulated proteins showed that at early time point, pathways like translation, RNA processing, ribosome biogenesis, and cellular metabolic processes were downregulated. In contrast, pathways like molecule transport, RNA stability, and oxidation-reduction process were upregulated. At late time point of infection, when the infection was going down from its peak, pathways belonging to various cellular metabolic processes such as nucleotide biosynthesis, phosphate synthesis, nitrogen compound metabolic process, and others such as translation were downregulated, whereas pathways such as RNA splicing, transcription, ribonucleoprotein complex biogenesis, and ncRNA processing were upregulated.

Chapter 4: Identification of CHIKV non-structural protein 3 (nsP3) interacting partners in *Ae. aegypti* (Aag2) cells

This chapter describes the interacting partners of CHIKV nsP3 protein in Aag2 cells. Previous work from the lab showed that CHIKV nsP3 acts as a viral suppressor of RNAi (VSR) in Aag2 cells. This study was the extension of that study to find the interacting partners. In this study,

the CHIKV nsP3 protein was cloned, expressed, and purified in the bacterial cells. The purified protein was used to generate antibodies in the rabbit. The co-immunoprecipitation of nsP3 with Aag2 lysate coupled with mass spectrometry showed protein from pathways such as translation, oxidation-reduction process, RNA metabolism, stress response, and cellular metabolism. Previous work identified that the macrodomain of CHIKV nsP3 act as a VSR. Macrodomain possesses ADP ribosylhydrolase activity. ADP ribose polymerases have the capability to attach ADP ribose chains to the target molecules. ADP ribosylation plays a role in processes like DNA repair, protein-protein interactions, and apoptosis. The sequence homology search has revealed that the *Ae. aegypti* have three ADP ribose polymerases. Domain analysis of the sequences revealed that one protein has domains that play a role in protein-protein interaction and is named Tankyrase. The second protein has zinc finger domains that play role in DNA repair and is called poly ADP ribose polymerase. The third protein has only catalytic domains and is involved in mono ADP ribosylation.

Chapter 5: Characterization of *Ae. aegypti* interacting partners

This chapter is presented as two sub chapters and involves the characterization of CHIKV nsP3 protein interacting partners. The pathways analysis of nsP3 interacting partners showed that various RNA binding proteins were also interacting with nsP3 protein. One of them was RM62F, a DEAD-box RNA helicase. It is a member of the RNAi pathway. The western blot analysis of the co-immunoprecipitated sample showed RM62F as an interacting partner of CHIKV nsP3.

Since *Ae. aegypti* Tankyrase has domains such as Ankyrin and SAM domain which play a role in protein interaction and oligomerization. The catalytic domain of the Tankyrase was cloned, expressed, and purified from bacterial cells. The *in vitro* PARylation assay showed that the catalytic domain could add PAR (poly ADP ribose). The nsP3 co-incubation has shown that the nsP3 can remove the ADP ribose from the target protein. We believe that nsP3 macrodomain hydrolyzes the ADP ribose chains from host proteins, which form large complexes, thereby destabilizing these complexes. Antiviral immune pathways such as the RNAi pathway form the protein complex, e.g., the RISC complex. It is possible that, like stress granules, the CHIKV nsP3 macrodomain destabilizes the RISC complex by hydrolyzing the PAR chains, thereby destabilizing it.

Chapter 6: Scope of the thesis work and future perspective

Viruses infect almost all domains of life. They cause various diseases in organisms and are the reason for medical complications. Viruses are dependent on hosts for their replication as they lack all the proteins crucial for their replication. Viruses control the host resources and divert them to favor their growth and survival. Viruses are spread by a medium that could be either air, or direct blood contact or a vector such as mosquitoes. Chikungunya is one such virus belonging to the *Togaviridae* family. It is an enveloped positive-sense (+) single stranded (ss) RNA virus and spread from infected to the uninfected organism by mosquito bite. It is not well known that how the CHIKV virus affects the mosquito at the cells level during the infection. This work highlighted that how the virus is affecting the *Aedes* cells during the infection. Mass-spectrometry based analysis of early time points and late time points of infection. Several pathways were found to be upregulated and downregulated at early time points and late infection time points, thereby promoting cell survival and controlling the virus growth.

The viral replication occurs in the replication complex formed by non-structural protein 3 (nsP3). The protein's hypervariable domain is a highly variable domain and is intrinsically disordered. The domain act as a hub for the binding of host proteins, which helps the virus in replication. In this study, nsP3 was co-immunoprecipitated with Aag2 lysate to identify its interacting partners. The mass spectrometry analysis of elutes revealed that proteins belonging to pathways such as translation, oxidation-reduction, stress response, and RNA metabolism. One of the proteins was RM62F which is a DEAD-box helicase and also a member of the RNAi pathway.

Further, the study identified *Ae. aegypti* ADP ribose polymerases using sequence homology alignment search. A total of three ADP ribose polymerase were found. Among them, one was Tankyrase, which has domains for protein interaction and oligomerization. Other protein called Poly ADP ribose polymerase (PARP) have Zinc finger domain and play role in DNA repair. The third protein is Mono ADP ribose polymerase (MARF), which is involved in mono ADP ribosylation. Among the three proteins, Tankyrase was selected for characterization due to its role in protein interaction. The recombinant catalytic domain of Tankyrase expressed in *E. coli* cells was catalytically active and was able to add poly ADP ribose units to the proteins, whereas incubation of recombinant nsP3 protein hydrolyzed the ADP ribose chains, showing that nsP3 macrodomain is capable of removing ADP ribose moieties from the target protein.

Future work will help from the study will help to identify and validate the protein from pathways modulated during CHIKV infection, thus helping the cells counter the viral infection by reducing oxidative stress, and controlling viral titer. The CHIKV macrodomain is an ADP ribosylhydrolase and is crucial for viral replication. The ADP ribosylation based post translational-modification plays a crucial role in various cellular processes. How viral macrodomain affect the host immune pathways is not known. Future work can help to elucidate how the macrodomain affects the immune pathways and the targets of the CHIKV macrodomain. This will shed light on the viral mechanisms to counter the host immune systems.

REFERENCES

- Wolf YI, Kazlauskas D, Iranzo J, Lucia-Sanz A, Kuhn JH, Krupovic M, Dolja VV, Koonin EV (2018) Origins and Evolution of the Global RNA Virome. *mBio* 9 (6). doi:10.1128/mBio.02329-18
- Strauss JH, Strauss EG (1994) The alphaviruses: gene expression, replication, and evolution. *Microbiol Rev* 58 (3):491-562. doi:10.1128/mr.58.3.491-562.1994
- Weaver SC, Lecuit M (2015) Chikungunya virus and the global spread of a mosquito-borne disease. *N Engl J Med* 372 (13):1231-1239. doi:10.1056/NEJMra1406035
- Goodman AG, Rasmussen AL (2019) Editorial: Host-Pathogen Interactions During Arboviral Infections. *Front Cell Infect Microbiol* 9:77. doi:10.3389/fcimb.2019.00077
- Duffy S (2018) Why are RNA virus mutation rates so damn high? *PLoS Biol* 16 (8):e3000003. doi:10.1371/journal.pbio.3000003
- Kumar A, Srivastava P, Sirisena P, Dubey SK, Kumar R, Shrinet J, Sunil S (2018) Mosquito Innate Immunity. *Insects* 9 (3). doi:10.3390/insects9030095

LIST OF PUBLICATIONS

Publications from PhD thesis work:

1. **Kumar R**, Mehta D, Mishra N, Nayak D, Sunil S. Role of Host-Mediated Post-Translational Modifications (PTMs) in RNA Virus Pathogenesis. *Int J Mol Sci.* 2020 22(1):323. doi: 10.3390/ijms22010323 (**Impact factor 5.923**).
2. **Kumar R**, Srivastava P, Mathur, K. et al. Chikungunya virus non-structural protein nsP3 interacts with *Aedes aegypti* DEAD-box helicase RM62F. *VirusDis.* 2021. <https://doi.org/10.1007/s13337-021-00734-y> (**Impact factor 1.23**).
3. **Kumar R**, Mehta D, Chaudhary S, Nayak D, Sunil S. Impact of CHIKV Replication on the Global Proteome of *Aedes albopictus* Cells. *Proteomes.* 2022; 10(4):38. <https://doi.org/10.3390/proteomes10040038> (**Cite score 5.9**).
4. **Kumar R**, Mehta D, Nayak D, Sunil S. Cloning, purification and characterization of *Aedes aegypti* Tankyrase catalytic domain. (Manuscript under preparation).

Publications during PhD:

1. Chaudhary S, Jain J, **Kumar R**, Shrinet J, Weaver SC, Auguste AJ, Sunil S. Chikungunya Virus Molecular Evolution in India Since its Re-emergence in 2005. *Virus Evolution* (2021) August 2021. doi: 10.1093/ve/veab074 (**Impact factor: 7.9**)
2. **Kumar R**, Nayak D, Somasekharan SP. SILAC-based quantitative MS approach reveals Withaferin A regulated proteins in prostate cancer. *J Proteomics.* 2021 247:104334. doi: 10.1016/j.jprot.2021.104334 (**Impact factor 4.0**).
3. Srivastava P, Kumar A, Hasan A, Mehta D, **Kumar R**, Sharma C, Sunil S. Disease Resolution in Chikungunya-What Decides the Outcome? *Front Immunol.* 2020 11:695. doi: 10.3389/fimmu.2020.00695. (**Impact factor: 6.4**).
4. Kumar A, Srivastava P, Sirisena P, Dubey SK, **Kumar R**, Shrinet J, Sunil S. Mosquito Innate Immunity. *Insects.* 2018 9(3):95. doi: 10.3390/insects9030095. (**Impact factor 2.7**).

TABLE OF CONTENTS

List of Content	viii
List of Figures	xiii
List of Tables	xiv
Nomenclature	xiv
Acronyms	xiv

1. List of Content

Chapter 1 Introduction	1-30
1.1. Introduction	1
1.2. Chikungunya virus.....	3
1.2.1. Phylogenetic classification	3
1.2.2. Chikungunya virus history	3
1.2.3. Chikungunya virus genome and proteome	5
1.2.4. Chikungunya virus structure.....	9
1.2.5. Chikungunya virus replication	9
1.3. Mosquito.....	11
1.3.1. Life stages of mosquito	12
1.3.2. Chikungunya virus life cycle.....	13
1.4. Chikungunya virus life cycle in <i>Aedes</i> mosquitoes	14
1.5. Chikungunya virus life cycle in human.....	15
1.6. Host-Pathogen interactions.....	17
1.6.1. Role of post-translation modification in virus-host interactions	18
1.6.1.1.Role of ADP ribosylation in inhibition of viral growth	20
1.6.1.2.Role of ADP ribosylation in promotion of viral growth	21
1.7. Overview of the thesis work	22
1.8. References	23

Chapter 2 Materials and methods	31-46
2.1. Materials or reagents.....	31
2.2. Solution, buffer, and media preparation	32
2.3. Methods.....	35
2.3.1. Recharging Ni-NTA (Nickel-Nitrilo Triacetic acid) beads	35
2.3.2. Cell lysis.....	36
2.3.3. Protein estimation	36
2.3.4. SDS-PAGE (Sodium Dodecyl Sulfate-Poly Acrylamide Gel Electrophoresis) and transfer.....	36
2.3.5. Western blotting.....	37
2.3.6. Protocol for the thawing frozen cells.....	37
2.3.7. DEPC treatment of plastic wares for RNA work.....	38
2.3.8. RNA isolation from mosquitoes	38
2.3.9. Reverse Transcription Polymerase Chain Reaction (RT-PCR).....	38
2.3.10. Agarose gel electrophoresis and gel extraction	39
2.3.11. Plasmid isolation and gene cloning.....	39
2.3.12. <i>Escherichia coli</i> competent cell preparation.....	41
2.3.13. Transformation.....	41
2.3.14. Protein purification	42
2.3.15. Chikungunya virus propagation.....	43
2.3.16. Virus infection	43
2.3.17. Plaque assay	43
2.3.18. Quantitative real-time PCR	43
2.3.19. Antibody generation.....	45
2.3.20. Immunofluorescence assay	46
2.4. References.....	46

Chapter 3 Impact of CHIKV on the global proteome of *Aedes albopictus*

(U4.4) cells	47-76
3.1. Introduction.....	47
3.2. Results.....	48
3.2.1. Cloning, expression, and antibody generation of CHIKV E1 protein	48

3.2.2.	Kinetics of CHIKV replication in U4.4 cells.....	51
3.2.3.	Global analysis of <i>Aedes</i> proteins during CHIKV infection time points.....	52
3.2.4.	Pathway analysis of U4.4 cell proteins during CHIKV infection.....	59
3.2.5.	Comparative analysis of upregulated and downregulated proteins at early and late infection time points.....	63
3.3.	Discussion.....	65
3.4.	Materials and methods.....	67
3.4.1.	Buffers and reagents.....	68
3.4.2.	Methods.....	68
3.4.2.1.	Cloning and expression of CHIKV E1 protein.....	69
3.4.2.2.	CHIKV E1 protein purification.....	70
3.4.2.3.	SDS-PAGE, staining, and western blotting.....	70
3.4.2.4.	Anti-CHIKV E1 antibody generation.....	71
3.4.2.5.	Chikungunya virus infection in U4.4 cells.....	71
3.4.2.6.	Immunofluorescence assay.....	72
3.4.2.7.	Plaque assay.....	72
3.4.2.8.	Cell lysis.....	72
3.4.2.9.	Sample preparation.....	73
3.4.2.10.	Mass spectrometric analysis of peptide mixtures.....	73
3.4.2.11.	Data processing.....	73
3.4.2.12.	Differential analysis.....	74
3.4.2.13.	References.....	74

Chapter 4 Identification of CHIKV non-structural protein 3 (nsP3)

interacting partners in *Ae. aegypti* (Aag2) cells..... 77-101

4.1.	Introduction.....	77
4.2.	Results.....	79
4.2.1.	Cloning and expression of CHIKV nsP3 protein and antibody generation.....	79
4.2.2.	CHIKV regulates host RNAi machinery.....	81
4.2.3.	Host interacting partners of CHIKV-nsP3.....	84
4.2.4.	Macrodomain as ADP ribosylhydrolase.....	87

4.2.5. ADP ribose polymerases in <i>Aedes aegypti</i>	89
4.3. Discussion.....	91
4.4. Materials and methods.....	92
4.4.1. Cell lines and virus	92
4.4.2. Virus infection	93
4.4.3. Plaque assay.....	93
4.4.4. Quantitative real-time PCR	93
4.4.5. Generation of plasmid constructs	94
4.4.6. Protein purification	95
4.4.7. Antibody generation	95
4.4.8. Co-immunoprecipitation (Co-IP)	95
4.4.9. Mass spectrometry	96
4.4.10. Mass spectrometric analysis of peptide mixtures	96
4.4.11. Data processing	96
4.4.12. Western blot assay	97
4.4.13. Protein sequence analysis of <i>Ae. aegypti</i> PARPs	97
4.4.14. Multiple sequence alignment of alphavirus macrodomain.....	97
4.4.15. Immunofluorescence assay.....	98
4.5. References	98

Chapter 5 Characterization of *Aedes* interacting partners..... 102-121

5.1. Confirmation of nsP3 interacting partner in <i>Aedes</i>	102
5.1.1. Introduction	102
5.1.2. Results	102
5.1.2.1. CHIKV-nsP3 interacts with RM62F	102
5.2. Isolation and characterization of <i>Ae. aegypti</i> Tankyrase protein.....	105
5.2.1. Introduction	105
5.2.2. Results	107
5.2.2.1 Cloning and expression of <i>Ae. aegypti</i> Tankyrase protein	107
5.2.2.2 <i>In vitro</i> PARylation assay of Tankyrase protein.....	109
5.2.2.3 Effect of CHIKV nsP3 macrodomain on PARylation activity of Tankyrase	110

5.3	Discussion	112
5.4	Materials and methods	114
5.4.1	Reagents	114
5.4.2	Methods	115
5.4.2.1	RM62F and Tankyrase gene cloning, protein expression and purification	115
5.4.2.2	Antibody generation	115
5.4.2.3	Quantitative real-time PCR	115
5.4.2.4	Cell lines and virus	116
5.4.2.5	Virus infection	116
5.4.2.6	Co-immunoprecipitation assay	117
5.4.2.7	Western blot assay	117
5.4.2.8	<i>In vitro</i> PARylation assay	118
5.4.2.9	CHIKV nsP3 macrodomain co-incubation assay	118
5.5	References	118
 Chapter 6 Conclusion from the thesis and future prospective		122-124
6.1.	Conclusion from the thesis	122
6.2.	Future prospective	124
 Supplementary Information 1		125-137

2. List and Description of Figures

Figure 1.1 Global distribution of different lineages of chikungunya virus and its vectors. The geographical distribution of different lineages of chikungunya virus such as ECSA, West African, Asian urban, and IOL urban, and their vectors viz. *Ae. aegypti* and *Ae. albopictus* from the first report of the case in Tanzania in 1952 till 2013 is shown4

Figure 1.2 Genome organization of chikungunya virus. The viral genome is translated as two ORFs viz. ORF1 and ORF2. The ORF1 encodes non-structural proteins nsPs including nsP1, nsP2, nsP3, and nsP4. The ORF2 encodes for structural polyproteins, including capsid, envelope protein3 (E3), envelope protein 2 (E2), 6K, and envelope protein 1 (E1)5

Figure 1.3 Domain organization of chikungunya virus non-structural protein 3 (nsP3) protein. The N-terminal domain is the macro domain, the middle domain is called as alphavirus unique domain (AUD), and the C-terminal domain is known as the hypervariable domain (HVD)7

Figure 1.4 The structural organization of alphavirus. The Outer layer is composed of multiple copies of the trimer of the heterodimer of E1E2, which forms the spikes of the virus and are involved in virus entry. The next layer is the lipid bilayer formed by the host membrane during enveloping. The last layer is the nucleocapsid layer, which has multimeric capsid units enclosing viral genomic RNA. The internal organization is icosahedral symmetry (T=4).9

Figure 1.5 Viral replication cycle. The pH changes lead to the release of the viral genome into the cytoplasm. The viral genome is then translated as two polyproteins viz. ORF1 (nonstructural) and ORF2 (structural). nsPs are processed into individual nsP by proteolytic cleavage of nsP2 in cis and trans at different times of infection. The nsPs form the replication complex and play a role in viral RNA synthesis of negative and positive strands. The structural polyproteins include capsid, E3, E2, 6K, and E1. Except for capsid, which is cleaved autoproteolytically, all are cleaved into individual subunits by host proteases upon ER-localized glycosylation. The viral RNA binds to the capsid and is then packaged into envelope protein followed by entrapment into the host's membrane and release into the extracellular environment for the next round of infection 10

Figure 1.6 Life cycle of mosquito. The female mosquito lays eggs on water surfaces that are initially white or transparent in color and converted into the black within a short time. The eggs hatch, and the long thread-like larva emerges, which are motile and feed on organic matter. The larvae then develop into pupa after skin shedding and physiological development. After

a few days, the pupae metamorphoses into adult mosquitoes, ready to fly, feed, mate, and lay eggs..... 13

Figure 1.7 Chikungunya virus life cycle. The virus generally enters inside the female mosquito body during the blood meal from a virus-infected person. Inside the mosquito body, the virus replicates and spreads to the whole body. It then enters the human body during the next meal with mosquito saliva. The virus then replicates in the human body, where it reaches to billion viral particles/ml of blood. When mosquitoes bite the infected person for a blood meal, the virus also moves the blood to the mosquito body. The cycles continue to go on depending on the density of mosquitoes and humans in that particular area. The viral spread is also dependent on hygiene practices followed by the population of that area. 14

Figure 1.8 Life cycle of virus in mosquito body. The virus moves into the mosquito body along with the blood meal. The virus then resides in the midgut, where it replicates and then spreads to other parts such as hemocoel and salivary glands. Then it is released with saliva with the bite in the next blood meal to the uninfected person 15

Figure 1.9 Chikungunya virus life cycle in human. Female mosquitoes spread the virus during the blood meals from infected to non-infected persons. Upon entry into the body, the virus infects the epidermis and skin cells, including dendritic and fibroblasts. After countering the host immune system, the virus spreads to other body parts via the blood circulation system. During the initial phase, it generates billions of virion particles that are again transferred to non-infected persons in the next blood meal of mosquitoes and is characterized by fever, rashes, body aches, and joint pain. The next phase is called as acute phase and generally lasts around a week. In this phase, the virus grows to enough number and activates the immune system, and the immune system act on it and controls the viral number. It is followed by the post-acute phase, in which the virus is cleared from the circulation system. Sometimes the patients show prolonged symptoms such as arthritis even after a week or months of infection, and the phase is called the chronic phase. 16

Figure 1.10 Overview of various post-translational modifications of virus and host proteins essential during viral infections. Based on biochemical moiety, PTMs can be categorized into modification by small protein groups (ubiquitination, ISGylation, SUMOylation, NEDDylation), carbohydrates (Glycosylation, ADP ribosylation), lipids (palmitoylation, myristoylation, and prenylation), and small chemical groups (phosphorylation, methylation, acetylation, oxidation). The protein is modified to gain in function, which modulates the virus's life cycle and host response to virus infection. 19

Figure 3.1 Cloning, expression, and antibody generation of CHIKV E1 protein. A) The internal region of CHIKV E1 gene was amplified using gene-specific primers from CHIKV infected total RNA. The total E1 gene has length around 1.3 kb, but for recombinant protein generation, a 0.8 kb region was selected; B) The gene was cloned in pET29a plasmid as shown in map (left), and checked by restriction digestion, followed by separation of uncut and double digested product on agarose gel (right). The resulting clone have S-tag at N-terminal and His-tag at C-terminal; C) Coomassie-stained SDS-PAGE gel of purified CHIKV E1 protein after affinity chromatography (left image). Western blot of purified CHIKV E1 protein on nitrocellulose membrane probed with HRP conjugated anti-HIS antibody at dilution of 1:4000 (middle image), western blot of purified recombinant CHIKV E1 protein with mice pre-bleed sera (right image); and D) Western blot of uninfected and CHIKV infected Vero cells at MOI of 1 with mice raised anti-CHIKV E1 serum. The nitrocellulose membrane was incubated with anti-CHIKV E1 mice serum at 1:3000 dilution, and after washing, the membrane was probed with anti-mice HRP antibody at 1:6000 dilution. Actin antibody was used as a loading control at 1:4000 dilution49

Figure 3.2 Immunofluorescence assay of CHIKV infected Vero cells. Vero cells were infected with CHIKV at MOI of 1 for 12 h and 24 h and then fixed and permeabilized. Cells were then incubated with anti-CHIKV E1 mice serum at 1:200 dilution and Alexa 488 labelled anti-mice antibody at 1:400 dilution. Cells were incubated with DAPI (1µg/ml) for 5 min and then visualized at 100X oil immersion (Scale bar=20 µm) 51

Figure 3.3 CHIKV kinetics in U4.4 cells. A) Plaque assay of different time points of CHIKV infection in U4.4 cells at MOI of 1, error bars represent SEM; real time PCR analysis of CHIKV E1 gene using gene specific primers for the CHIKV infected U4.4 cells; and C) Western blot expression profiling of different infection time points of CHIKV (E1) in U4.4 cells52

Figure 3.4 Schematic representation of workflow of mass-spectrometric analysis of U4.4 cells for proteome analysis upon CHIKV infection.....53

Figure 3.5 Analysis of the proteome of CHIKV infected U4.4 cells. A) Principal component analysis PCA of triplicate samples of uninfected, 12 hpi and 60 hpi U4.4 samples. B) Z-score analysis of triplicate samples of uninfected, 12 hpi, and 60 hpi CHIKV infected U4.4 cell lysate54

Figure 3.6 Comparison of global abundance of U4.4 cell proteins among triplicates. A) Heat map of global comparison of 12 hpi triplicates with control triplicates (uninfected), B) Heat map of global comparison of 60 hpi triplicates with control triplicates (uninfected); C) Heat map of global comparison of 60 hpi triplicate samples with 12 hpi triplicate samples; D) Correlation coefficient analysis of 12 hpi and control sample; E) Correlation

coefficient analysis of 60 hpi and control sample, and F) Correlation coefficient analysis of 60 hpi and 12 hpi triplicate samples56

Figure 3.7 Comparison of abundance of U4.4 cell proteins at 12 hpi and 60 hpi. A) The log₂ abundance comparison of 12 hpi/untreated U4.4 cell proteins upon CHIKV infection, B) The log₂ abundance comparison of 60 hpi/untreated U4.4 cell proteins upon CHIKV infection, C) The log₂ abundance comparison of 60 hpi/ 12 hpi U4.4 cell proteins upon CHIKV infection58

Figure 3.8 Pathway analysis of CHIKV infected U4.4 cells. A) Downregulated pathways at 12 hpi in comparison to uninfected cells; B) Upregulated pathways at 12 hpi in comparison to uninfected cells; C) Downregulated pathways at 60 hpi in comparison to uninfected cells; and D) Upregulated pathways at 60 hpi in comparison to uninfected cells.....62

Figure 3.9 Comparative analysis of proteins. A) Comparison of exclusive downregulated proteins at 12 hpi (blue color) and 60 hpi (yellow color) and proteins downregulated at both 12 hpi and 60 hpi show at the center of two circles. B) Comparison of exclusive upregulated proteins at 12 hpi (blue color) and 60 hpi (yellow color) and proteins upregulated at both 12 hpi and 60 hpi show at the center of two circles.....63

Figure 4.1 Cloning, expression, antibody generation, and its validation for CHIKV nsP3 gene. A) Region of 1512 bp of 1560 bp was amplified using specific primers; B) Plasmid map of CHIKV nsP3 in pET29a vector and restriction digestion of nsP3-pET29a; C) SDS-PAGE followed by Coomassie staining and western blotting of purified recombinant CHIKV nsP3 protein (left) and pre-bleed sera testing with recombinant CHIKV nsP3 proteins via western blotting for any non-specific binding (right); D) Western blot of uninfected and CHIKV infected cell lysate with anti-CHIKV nsP3 serum (1:2000), probes with anti-rabbit HRP conjugated antibody; and E) Immunofluorescence assay of uninfected and 12 hpi and 24 hpi Vero cells at MOI of 1. The cells were probed with anti-CHIKV nsP3 serum (1:200), then incubated with Alexa 594 labelled IgG anti-rabbit antibody, and the nucleus was stained with DAPI80

Figure 4.2 Effects of CHIKV infection on RNAi machinery. A) CHIKV viral load (Y-axis) during infection in Aag2 cells at MOI of 0.1, 1, and 10 at different time points, B) Transcripts profiling of nsP3 at MOI of 0.1, 1, and 10 at different time points and western blot analysis of nsP3 at MOI of 0.1, 1, and 10 upon CHIKV infection, C) nsP3 protein expression profiling at MOI 0.1, 1, and 10 at different time points. D and E) Transcript profiling of Aedes RNAi factors such as Dicer-2, Ago-2, R2D2, TSN, VIG, and CHIKV E1 at MOI of 1 and 10 of CHIKV at different time points (** p-value <0.007, *** p-value < 0.0008 and **** p-value < 0.0001).....83

Figure 4.3 Sequence analysis of macrodomain of alphavirus family. The black rectangle encircles the active site residues. These include D10, G32, T113, Y114, and R144.....88

Figure 4.4 Identification of ADP ribose polymerase proteins in *Ae. aegypti*. A) Phylogenetic analysis of *Ae. aegypti* PARPs with human PARPs using MEGA software; B) Proteins sequence analysis of ADP ribose polymerase proteins for domains with ScanProsite database.89

Figure 5.1 Cloning and expression of *Ae. aegypti* RM62F N terminal domain. A) RM62F region selected for cloning in pET29a vector and vector map of RM62F domain cloned in pET29a plasmid; B) Restriction digestion of RM62F cloned in pET29a. Lane 1: 1kb DNA ladder, Lane 2: double digested RM62F-pET29a and Lane 3 uncut RM62F-pET29a; and C) western blot of purified recombinant RM62F domain. For western blot, anti-His HRP tagged antibody (1:4000 dilution)..... 103

Figure 5.2 Interaction of *Ae. aegypti* host factor RM62F with CHIKV-nsP3 protein. A) Expression profiling of RM62F transcript upon CHIKV post-infection in Aag2 cells. 0 hpi samples and different infection time points like 12, 24, 36, 48, 60, and 72 hpi at MOI of 10 were checked with the antibody against RM62F and RPS17 as an internal control. Relative comparison of RM62F expression levels at different infection time points; B) Expression profiling of RM62F protein upon CHIKV post-infection in Aag2 cells. Control (Uninfected) samples along with different infection time points like 12, 24, 36, and 48 hpi at MOI of 10 were checked with the antibody against RM62F and actin (as a loading control); and C) Co-IP of Aag2 lysate with recombinant nsP3 using anti-CHIKV nsP3 antibody. Immunoblotting was done with anti-CHIKV-nsP3 antibody and anti RM62F antibody. Lane1: Prestained protein ladder, lane 2: negative control (NC) represent elution of uninfected Aag2 lysate incubated with anti nsP3 antibody immobilized beads, and then probing with nsP3 specific antibody lane 3: positive control (PC) represent elution of recombinant nsP3 with anti-nsP3 antibody immobilized beads and probing with nsP3 specific antibody, lane 4: Pure CHIKV-nsP3 protein, probed with nsP3 specific antibody, lane 5: wash fraction after CHIKV-nsP3 incubation and lane 6: Co-IP of Aag2 lysate with recombinant nsP3 which is bound to the anti-nsP3 antibody immobilized beads and blotted with nsP3 and RM62F specific antibodies.104

Figure 5.3 Mechanism of protein ADP ribosylation by poly ADP ribose polymerases (PARPs). PARPs modify the nascent proteins, and in the process, these enzymes use NAD (nicotinamide adenine dinucleotide) to act as a donor for ADP ribose moieties to the proteins.106

Figure 5.4 Cloning and expression of *Ae. aegypti* Tankyrase catalytic domain. A) Tankyrase region selected for cloning in pET32a vector and

vector map of Tankyrase catalytic domain cloned in pET32a plasmid; B) Restriction digestion of Tankyrase catalytic domain cloned in pET32a. Lane 1: 1kb DNA ladder, Lane 2: uncut Tankyrase-pET32a, and Lane 3: double digested Tankyrase-pET32a; and C) Coomassie staining and western blot of purified recombinant Tankyrase catalytic domain. For western blot anti-His HRP tagged antibody (1:4000 dilution). Lane 1: Prestained protein ladder and Lane 2: Purified Tankyrase protein.....108

Figure 5.5 *In vitro* PARylation assay of Tankyrase catalytic domain. A) Schematic diagram of *in vitro* PARylation assay and gel run on SDS PAGE of unmodified and ADP ribose modified sample; B) *In vitro* PARylation assay with Tankyrase alone (negative control), NAD⁺ alone (negative control) and Tankyrase with NAD⁺. The samples were run on SDS-PAGE and transferred onto nitrocellulose membrane and probed with mice anti-pADPr antibody; and C) Western blot of time points (30 and 60 min) of *in vitro* PARylated Tankyrase catalytic domain. The samples were separated on SDS-PAGE and then transferred onto a nitrocellulose membrane. The membrane was then probed with an anti-pADPr mice antibody. It was then incubated with an anti-mice IgG HRP antibody, washed, and visualized in the gel documentation system after brief exposure to the chemiluminescent substrate109

Figure 5.6 *In vitro* PARylation assay and effect of CHIKV nsP3 on PARylation. A) *In vitro* PARylation assay was done with NAD⁺ alone (lane 1) as negative control, Tankyrase with NAD⁺ (lane 2) as positive control), CHIKV nsP3 with NAD⁺ as negative protein control (lane 3), Tankyrase with NAD⁺ for 15 min (lane 4 and 5), and Tankyrase with nsP3 and NAD⁺ (lane 6); B) The *in vitro* PARylation assay was performed for 30 and 60 min (lane 1 and lane 2 from the left side). The impact of nsP3 protein on PARylation was checked by co-incubation of nsP3 protein and PARylation buffer having Tankyrase protein for 30 and 60 min (lane 3 and 4). The reaction mixture was run on SDS PAGE and transferred to a nitrocellulose membrane. The membrane was probed with anti-pADPr antibody. The membrane was then incubated with anti-mice HRP antibody, and then it was visualized in the ChemiDoc MP system; C) diagram of EGFP and CHIKV macrodomain cloned in insect vector (pIB/V5-His). These two EGFP and CHIKV nsP3 macrodomain-pIB clones were transfected into Aag2 cells and then infected with CHIKV at MOI of 1 for different time points to observe the impact on viral growth via plaque assay; and D) the cells collected at 36 hpi were lysed and protein lysate was separated on SDS-PAGE which was then transferred and blotted with different antibodies such as anti-V5 antibody for EGFP and CHIKV macrodomain, house raised anti-CHIKV E1 mice sera for CHIKV E1 protein and anti-actin HRP antibody for actin protein111

Figure 5.7 Proposed model of Macrodomain CHIKV nsP3) mediated hydrolysis of PAR chains in ADP ribosylated proteins. Poly AD ribose modified proteins interact with each other and form protein complexes. The ADP ribosylhydrolase such as nsP3 macrodomain hydrolyzes the PAR chains, resulting in the weakened interaction leading to disintegration of complexes if protein complexes are exposed to macrodomain for a long time as virus infection.114

3. LIST OF TABLES

Table 1: Major pathways and their components involved in interaction with nsP384

4. NOMENCLATURE

Å	Angstrom (10^{-10} m)
e.g.	exempli gratia
etc.	Et cetera
pH	potential of hydrogen
V	volts
°C	degree Celsius
µl	microliter

5. ACRONYMS

ADP	Adenosine diphosphate
AUD	Alphavirus unique domain
CCL2	C-C motif ligand 2
cGAS	cyclic GMP-AMP synthase
CHIKV	Chikungunya virus
C-terminal	Carboxy terminal
CSE	Conserved sequence element
DAPI	4',6-diamidino-2-phenylindole
DC-SIGN	dendritic cell-specific ICAM-grabbing non-integrin
DEAD box	Asp-Glu-Ala-Asp box

DNA	Deoxyribonucleic acid
ds	Double stranded
ECSA	Eastern Central South Africa
g	grams
h	hour
HVD	Hypervariable domain
HRP	horse radish peroxidase
IFN	interferon
IgG	Immunoglobulin G
IOL	Indian ocean lineage
Kb	kilo basepairs
KCl	potassium chloride
kDa	kilo daltons
MAR	mono ADP ribose
Min	minute
ml	milli liter
mM	milli molar
NaCl	sodium chloride
ng	nanograms
Ni-NTA	Nickel Nitrilo Triacetic acid
NK cells	natural killer cells
N-terminal	Amino terminal
nsP	non-structural protein
OAS	2'-5'-oligoadenylate synthase
OD	optical density
ORF	Open reading frame
PARPs	Poly ADP ribose polymerase
PBS-T	phosphate buffer saline Triton-X-100
PCR	polymerase chain reaction
pfu	plaque-forming units
PKR	protein kinase R
PTM	Post-translational modifications
RNA	Riboxy nucleic acid

RNase	ribonuclease
rpm	rotation per minute
RSE	Reserved sequence alignment
s	second
SDS-PAGE	Sodium dodecylsulphate poly acrylamide gel electrophoresis
ss	Single stranded
TF	transframe
UTR	Untranslated region
UV-Vis	ultra violet visible

Chapter 1

Chapter 1

Introduction

1.1. Introduction

Viruses are microscopic-sized opportunistic pathogens that replicate inside the host cells. They infect all domains of life, including single-cell bacteria, to multicellular organisms such as algae, plants, animals, insects, and birds (Fermin, 2018). These possess genetic material as DNA or RNA, which are both single-stranded or double-stranded and positive or negative sense. In the case of positive sense viruses, nucleic acid acts as a template for replicating genetic material. In the case of negative sense, the strand is first used to synthesize the complementary strands, which are then used for translation (HR, 1996). The viruses contain a minimum genome that fulfills its requirement proteins for replication and envelops the virus's genome and further transmission. They need host proteins for their replication and hence affect the host's cells during infection by controlling host translation machinery to favors their growth. In contrast, the host uses various immune mechanisms such as innate and adaptive immune pathways to control viral growth (Nagy & Pogany, 2011; Walsh & Mohr, 2011).

Viruses are classified based on their genetic material (DNA or RNA) and the type of strand of genetic material (single-stranded or double-stranded and positive or negative sense). They are also classified based on the host (bacteriophages, plant, animal), morphology, presence of envelope (naked or enveloped), the shape of virus (bullet, filamentous), mode of transmission (respiratory, blood transfusion, zoonotic, and sexual) (Nasir et al., 2014). The most accepted classification was developed by David Baltimore in the early 1970s. In this classification, viruses were classified into seven groups based on their genetic content and morphology (Baltimore, 1971).

Group I: These viruses possess double-stranded DNA (dsDNA) genome. Their transcription is similar to that of cellular DNA, e.g., Adenoviruses, Herpesviruses, and Poxviruses.

Group II: These viruses have single-stranded DNA (ssDNA) genome. These first convert their genome into a dsDNA intermediate before its transcription to mRNA, e.g., Parvoviruses.

Group III: These viruses have a dsRNA genome. One of the strand is used as a template for generating mRNA using the RNA-dependent RNA polymerase encoded by the virus, e.g., Reoviruses.

Group IV: This group of viruses has ssRNA as their genome with a positive sense. Positive sense means that the genomic RNA can be directly used as mRNA, e.g., Picornaviruses and Togaviruses.

Group V: These viruses contain ssRNA as their genome which has negative polarity. It means that their sequence is complementary to the mRNA. In this case, the negative-stranded genome can be converted directly to mRNA by RNA-dependent RNA polymerase. The positive RNA strands serve as template for producing the negative-stranded genome, e.g., Orthomyxoviruses and Rhabdoviruses.

Group VI. This group of viruses has ssRNA genome. These encode the reverse transcriptase, which can convert RNA to dsDNA; the dsDNA then enters into the host cell's nucleus and inserts into the host genome. The integrated viral DNA can produce mRNA by transcription, e.g., Retroviruses.

Group VII: The group of viruses has dsDNA genome with the capability to make reverse transcriptase. The transcription process makes ssRNA intermediates which are also converted back into dsDNA genomes by reverse transcriptase activity and is necessary for genome replication, e.g., Hepadnaviruses.

Among the viruses, RNA viruses have a small genome (typically <14 kb), with the exception of coronavirus, toroviruses, and roniviruses which have larger genome sizes (24–30 kb) (Campillo-Balderas et al., 2015; Chaitanya, 2019). Alphaviruses are arboviruses that spread among animals, insects, and fish. They can spread in both urban (human–mosquito–human) and sylvatic environments (primate–mosquito–primate) (Valentine et al., 2019). They are spherical virions with lipid bilayer having heterodimeric enveloped spike proteins (Gould et al., 2010). Alphaviruses are categorized into old and new world alphaviruses. Old world viruses such as Ross River, Barmah Forest, Mayaro, O'nyong-nyong, Chikungunya, and Sindbis cause rashes, fever, arthritis, and diseases. In contrast, new world viruses such as Venezuelan Equine Encephalitis Virus (VEEV), Eastern Equine Encephalitis Virus (EEEV), and Western Equine Encephalitis Virus (WEEV) causes encephalitis (Baxter

& Heise, 2018). These viruses are maintained between vector (mosquito) and host via blood meals of female mosquitoes (Gould et al., 2010; Suhrbier et al., 2012).

1.2. Chikungunya virus

Among the RNA viruses that received the attention of the public and health experts include coronavirus, dengue virus, Nipah virus, and zika virus. Chikungunya virus (CHIKV) is one of them due to its worldwide spread and repeated outbreaks. It was first isolated in Tanzania in 1952. Since then, there have been regular outbreaks in Africa, Asia and Europe, and America (Suhrbier et al., 2012). Every year thousands or millions of chikungunya virus infection cases come, e.g., till now, there have been 85,304 cases this year till 30 July 2021 (*Chikungunya worldwide overview*, 2021).

1.2.1. Phylogenetic classification

Chikungunya virus is classified into Kingdom, Phylum, Class, Order, Family, Genus, and species by the International Committee on Taxonomy of Viruses (ICTV) classification (Viruses, 2021). It belongs to the *Togaviridae* family. The family of *Togaviridae* consists of two genera: *Alphavirus* and *Rubivirus*.

Taxonomical Classification	
Kingdom	<i>Orthornavirae</i>
Phylum	<i>Kitrinoviricota</i>
Class	<i>Alsuviricetes</i>
Order	<i>Martellivirales</i>
Family	<i>Togaviridae</i>
Genus	<i>Alphavirus</i>
Species	<i>Chikungunya</i>

1.2.2. Chikungunya virus history

Chikungunya virus historically circulated in sub-Saharan Africa, involving non-human primates as hosts and mosquitoes as vectors (Tsetsarkin et al., 2016). The deforestation followed by urbanization led to the virus's emergence and spread in and beyond the African region. The spread was also favored by ships involved in the movement of goods on water roads. The period of this rapid emergence ranges between mid of nineteenth and twentieth-century via eastern, central, and southern African (ECSA) lineage, with the first report in Tanzania in 1953 (Wimalasiri-Yapa et al., 2019; Zeller et al., 2016). The ECSA lineages evolved during the later years as Asian lineage with *Ae. aegypti* as vector. The other ECSA, Indian ocean lineage

(IOL), successfully incorporated mutation in envelope protein 1 (E1) from alanine to valine at 226th position (E1 A226V), which allowed it to amplify in both *Ae. aegypti* and *Ae. albopictus* as vector. The *Ae. albopictus* was able to better survive in cold temperatures and rural areas; the vector caused the spread to temperate regions such as Italy while *Ae. aegypti* better adapt to urban. The adaptability of these two vectors to different conditions led to their spread to wiser areas (Li et al., 2014; Wahid et al., 2017).

Till 2004 there were occasional outbreaks of the virus, when the virus emerged in many countries of Africa, Europe, and Asia. The outbreak started on Lamu Island, Kenya. The outbreak then spread to other Islands. La Reunion, Madagascar, Mayotte, and Seychelles experienced the epidemic from March 2005 and May 2006 and *Ae. albopictus* was the primary vector responsible and ECSA lineage with E1-A226V. In Asia, more than a million cases were reported between October 2005 and October 2006. In other countries like Sri Lanka and Malaysia, Thailand, Singapore, Cambodia, and China in subsequent years till 2009. Other countries like Indonesia, Papua Guinea, Bhutan, and Philippines also experienced CHIKV outbreaks in the coming years (Pulmanusahakul et al., 2011; Schwartz & Albert, 2010; Vazeille et al., 2007).

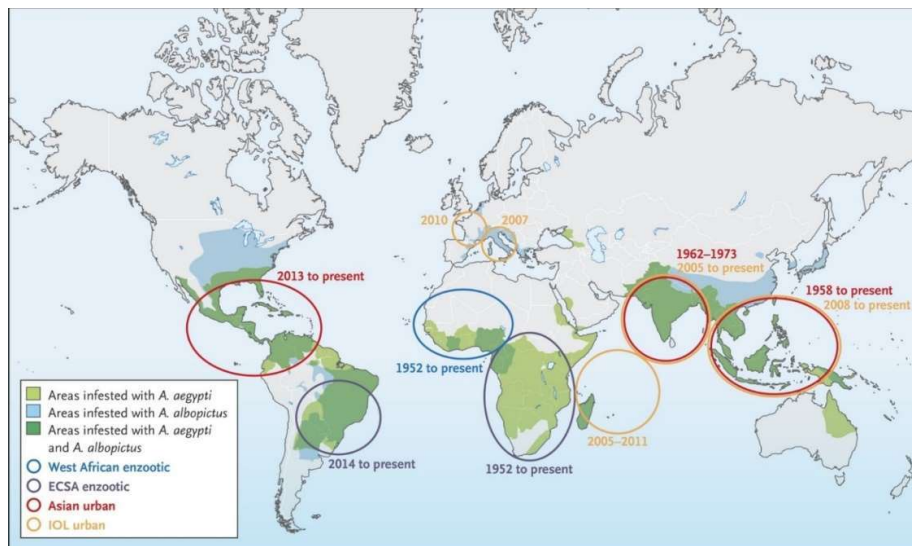


Figure 1.1 Global distribution of different lineages of chikungunya virus and its vectors. The geographical distribution of different lineages of chikungunya virus such as ECSA, West African, Asian urban, and IOL urban, and their vectors viz. *Ae. aegypti* and *Ae. albopictus* from the first report of the case in Tanzania in 1952 till 2013 is shown. Adapted from (Weaver & Lecuit, 2015).

In Europe, the outbreak was first reported in Italy in 2007. The ECSA strain with E1-A226V mutation and *Ae. albopictus*. The virus was then spread to countries like France, Croatia with chronic cases reported every year. In America, cluster of cases were reported in St Martin Island in around December 2013. The rapid movement of people resulted in the spread of the virus to different Islands and Central, South, and North America (Amraoui & Failloux, 2016; Vega-Rua et al., 2015; Weaver & Lecuit, 2015).

1.2.3. Chikungunya virus genome and proteome

Chikungunya virus is a positive sense (+) single-stranded (ss) RNA virus and the size of the genome is about 11.8 kb. At the extreme side are untranslated regions (UTR) called 5'- and 3'-UTR. The 5'-UTR has a type 0 cap (N7mGppp), and length ranges around 80 nucleotides. The cap plays a role in translation as well as pathogenicity. The 3'-UTR region's length varies around 200 to 700 nucleotides. The reserved sequence elements (RSE) are located just after structural proteins, stretching 18-102 nucleotides. Their exact role is not known but is essential to viral replication. Conserved sequence elements (CSE) are located after RSE and are 19-24 bases long. These serve as a promotor for negative-strand synthesis, and immediately after the CSE is the polyadenylation tail. The proteins are translated into two ORFs (Open reading frames): ORF1 and ORF2, which encodes for non-structural and structural polyproteins (Hoornweg et al., 2020) (Figure 1.2). The polyproteins are then cleaved into individual proteins by protease activity of nsP2 or by host proteins such as furin (Hyde et al., 2015; Ozden et al., 2008).

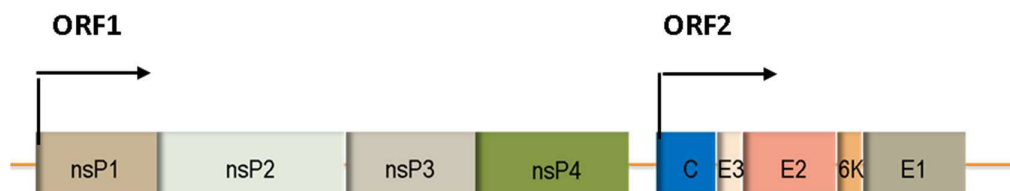


Figure 1.2 Genome organization of chikungunya virus. The viral genome is translated as two ORFs viz. ORF1 and ORF2. The ORF1 encodes non-structural proteins nsPs including nsP1, nsP2, nsP3, and nsP4. The ORF2 encodes for structural polyproteins, including capsid, envelope protein3 (E3), envelope protein 2 (E2), 6K, and envelope protein 1 (E1).

ORF1: ORF1 of CHIKV encodes for non-structural polyprotein, which is then cleaved to individual proteins: nsP1, nsP2, nsP3, and nsP4. nsPs are cleaved by protease activity of nsP2 into individual proteins. These possess enzymatic activity, which is crucial for viral RNA capping, protease, helicase, and RNA-dependent RNA polymerase activity. These proteins are briefly explained here:

nsP1: non-structural protein 1 (nsP1) is a viral RNA capping enzyme having methyltransferase (MTase) and guanylyltransferase (GTPase) activity. It introduces cap via two steps: first, the enzyme via its MTases activity, methylate GTP (Guanosine-5'-triphosphate) by transferring the methyl group from S-adenosyl methionine (SAM), which acts as the methyl donor, to GTP. The methylated m7GMP moiety is then transferred to dephosphorylated 5' end of RNA by GTPase activity of the nsP1 enzyme (Tero Ahola, 2016). The protein form channel complex at membrane having 12 subunits forming ring structure with 75 Å internal diameter (Zhang et al., 2021). The N-terminal region of nsP1 is palmitoylated, which helps it to bind to the plasma membrane and form a replication complex (Lampio et al., 2000; Zhang et al., 2019).

nsP2: non-structural protein 2 (nsP2) protein possesses two domains to have helicase activity (N-terminal) and protease domain (C-terminal). The helicase domain functions to unwind secondary structures of viral RNA formed during replication. The NTPase activity removes γ -phosphate from nascent viral RNA yielding diphosphate moieties at 5' terminus, which is a substrate for the addition of capping reaction of nsP1 (Tero Ahola, 2016). The C-terminal protease domain is involved in proteolytic processing of non-structural polyprotein (P1234), and within that, 3/4 cleavage occurs at early infection while 2/3 cleavage at later in infection. As 2/3 junction is distant from the site, thus cleavage occurs in *trans*. The cleavage occurs in *cis*, but as the infection increases, the *trans* cleavage becomes prominent. CHIKV nsP2 also acts as a transcription factor by binding to the subgenome promoter. It also regulates host transcription by targeting the RNA Pol II CTD subunit (Akhrymuk et al., 2012; Gao et al., 2019; Garmashova et al., 2006; Tero Ahola, 2016).

nsP3: non-structural protein 3 (nsP3) has got the attention of researchers during the last decades, as its role in the viral growth cycle was not clear. It has a role in RNA synthesis, and mutations in the protein affect the subgenomic RNA synthesis and

minus-strand synthesis. It contains three domains: Macrodomain, alphavirus unique domain, and hypervariable domain (HVD). The macrodomain has exhibits nucleic acid binding and ADP ribosylhydrolase activity. Its function in viral replication is not clear. It is known to catalyze the hydrolysis of mono ADP ribose subunits. The domain is conserved among the alphaviruses. The mutations in the active site of the macrodomain hamper viral replication. The AUD is localized to the central part of nsP3 and, similar to the macrodomain, is conserved among alphaviruses (Meshram et al., 2018; Tero Ahola, 2016) (Figure 1.3). Mutational analyses have revealed the importance of macrodomain and AUD, resulting in defective subgenomic and minus-strand RNA synthesis. The HVD is the C-terminal domain of the nsP3 protein. It is characterized by a region of the variability of length and amino acid sequence. The HVD domain is disordered, has multiple phosphorylation sites, and has a crucial role in viral RNA synthesis (Abraham et al., 2018; Gao et al., 2019; McPherson et al., 2017; Meshram et al., 2018; Tero Ahola, 2016).

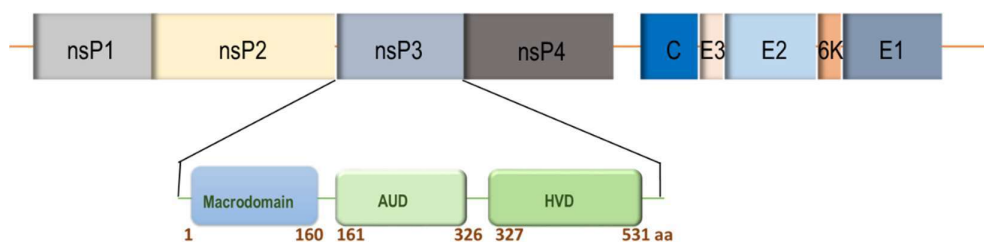


Figure 1.3 Domain organization of chikungunya virus non-structural protein 3 (nsP3) protein. The N-terminal domain is the macro domain, the middle domain is called as alphavirus unique domain (AUD), and the C-terminal domain is known as the hypervariable domain (HVD).

nsP4: non-structural protein 4 (nsP4) is the only RNA-dependent RNA polymerase (RdRp) of CHIKV and is responsible for the RNA synthesis in the viral replication complex. The N-terminal 100 amino acids are unique to alphaviruses, while the rest of the 500 amino acids are possessed the RdRp structure with palm, finger, and thumb domains. The protein is synthesized less than other non-structural proteins and is stabilized by incorporation into replication complex (Chen et al., 2017; Tan et al., 2021; Tero Ahola, 2016).

ORF2: Open Reading Frame 2 (ORF2) encodes structural polyproteins, including capsid, E3, E2, 6K, and E1 proteins. These are translated from 26S subgenomic mRNA. These proteins play a role in nucleocapsid assembly, protection of viral RNA, viral entry, and viral budding and release. These are explained here briefly:

Capsid: Capsid proteins are located at the N-terminal of ORF2. It consists of around 263 amino acids. It contains both NLS (nuclear localization signal) and NES (nuclear export signal), thus allowing active transport out and from the nucleus. Upon translation, the capsid is auto-catalytically cleaved at the C-terminal, leading to insertion into ER (endoplasmic reticulum) and interaction with the cytoplasmic tail of E2. The region of 1-113 amino acids is involved in the encapsulation of viral RNA and dimerization. The C-terminal region is highly conserved among alphaviruses and functions as proteinases involved in self-cleavage (Brown et al., 2020; Mendes & Kuhn, 2018; Zheng & Kielian, 2013).

E3: Envelope 3 (E3) is a peripheral glycoprotein with a molecular weight of around 7 kDa. Its inhibition negatively impacts spike protein heterodimer formation and E1 and E2 to the membrane (Snyder & Mukhopadhyay, 2012; Uchime et al., 2013). In the Sindbis virus, Cys19 and Cys25 of the capsid are involved in disulfide bond formation, and mutation causes attenuation (Parrott et al., 2009).

E2 and E1: Envelope proteins 2 and 1 (E2 and E1) are of about similar size. These are generated by proteolytic cleavage of signalase and furin, resulting in the generation of E2, E1, and a small 6K protein. The N-terminal region of E2 between 11th and 14th residues is a signal for carbohydrate attachment. The C-terminal region act as a stop-transfer signal and acts as an anchor for membrane attachment. The glycoproteins form a heterodimer with E2 and E3 form the virus's envelope (Holmes et al., 2020).

6K/TF: The 6K polypeptide is a small protein of around 60 amino acids. It forms a cation channel, which helps maintain ionic strength, which is crucial for virus assembly and budding. At the C-terminal region, -1 frameshift mutation of 6K yields, a novel protein called transframe (TF). The TF is not crucial for virus production but its release (Snyder et al., 2013). The N-terminal region of TF is palmitoylated, which is necessary for its incorporation into virion (Ramsey et al., 2019; Ramsey et al., 2017).

1.2.4. Chikungunya virus structure

The alphaviruses are almost spherical particles of 60-70 nm diameter and have envelope proteins as spikes that help receptor binding. These viruses have three layers of substructures: an outer glycoprotein shell, a lipid bilayer, and viral RNA containing core (Figure 1.4)

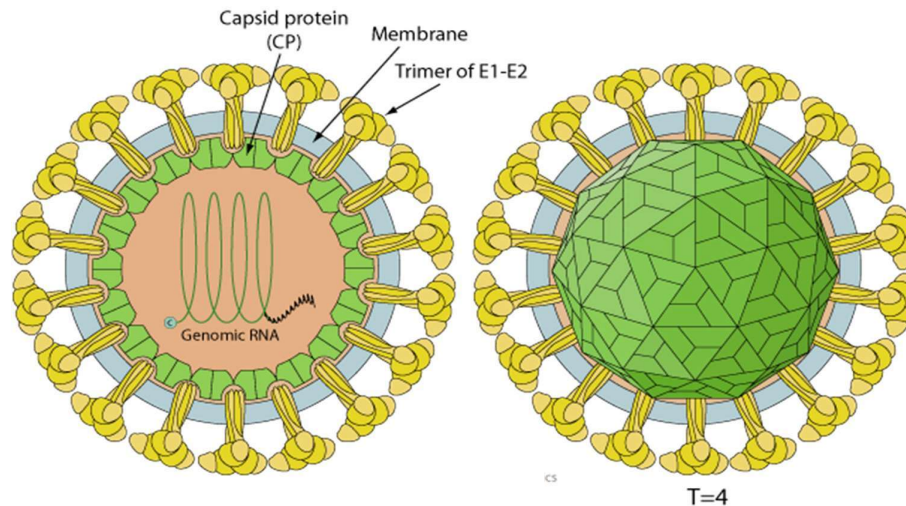


Figure 1.4 The structural organization of chikungunya virus particle. The Outer layer is composed of multiple copies of the trimer of the heterodimer of E1E2, which forms the spikes of the virus and are involved in virus entry. The next layer is the lipid bilayer formed by the host membrane during enveloping. The last layer is the nucleocapsid layer, which has multimeric capsid units enclosing viral genomic RNA. The internal organization is icosahedral symmetry (T=4). (Source: ViralZone www.expasy.ch/viralzone, Swiss Institute of Bioinformatics).

1.2.5. Chikungunya virus replication

The replication of alphavirus begins with the entry of the virus into the cell. The process is mediated by the binding of viral spike proteins with host receptors such as Mxra8 and CD147 in humans (De Caluwe et al., 2021; Song et al., 2019), while in the case of *Aedes*, the mechanism is not known. The receptor binding and low pH leads to membrane fusion and internalization of the virus. The E1 protein is a membrane fusion protein and is E2 dependent heterodimer that is crucial for regulating fusion and transport. Upon entry into the cytoplasm, the virus particle undergoes disassembly, followed by genomic RNA released into the cytoplasm. The viral genome is then translated into two ORFs which ultimately generate non-structural and

structural proteins. In the early infection, P1234 is *cis* (protease activity on one molecule cleave the same molecule) cleaved between P123 and P4, thereby generating P123 and nsP4. It is important to note that due to the leaky stop codon after nsP3, the synthesis of full P1224 occurs at the rate of 10-20%, leading to excess P123 and depletion nsP4 relative to other nsPs. Both form an initial replication complex involved in synthesizing the minus-strand of the viral RNA genome. Later cleavage of P123 to nsP1 and P23 occurs in *trans* (protease domain of one molecule cleave the other molecule only), which is favored at the later stage of infection as the number of polyproteins is enough. As the cleavage to individual nsP1, P23, and nsP4 is over, the involved in the negative stand synthesis inactivated and the positive strand synthesis and subgenomic RNA synthesis begins (Leung et al., 2011; Silva & Dermody, 2017; Tero Ahola, 2016).

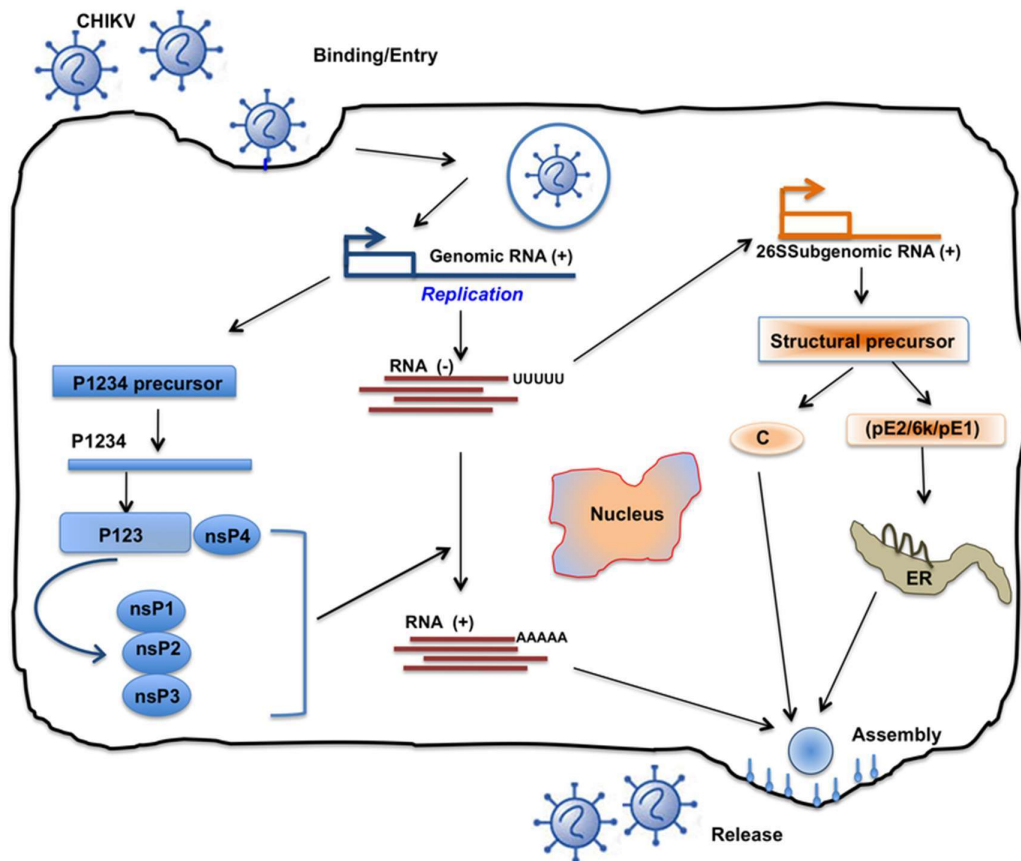


Figure 1.5 Viral replication cycle. CHIKV enters inside the cell via the receptor-mediated or endocytosis-mediated process. The pH changes lead to the release of the viral genome into the cytoplasm. The viral genome is then translated as two polyproteins viz. ORF1 (nonstructural) and ORF2 (structural). nsPs are processed into

individual nsP by proteolytic cleavage of nsP2 in cis and trans at different times of infection. The nsPs form the replication complex and play a role in viral RNA synthesis of negative and positive strands. The structural polyproteins include capsid, E3, E2, 6K, and E1. Except for capsid, which is cleaved autoproteolytically, all are cleaved into individual subunits by host proteases upon ER-localized glycosylation. The viral RNA binds to the capsid and is then packaged into envelope protein followed by entrapment into the host's membrane and release into the extracellular environment for the next round of infection. Adapted from ref. (Thiboutot et al., 2010).

The cleavage of structural polyproteins in alphaviruses occurs co-translationally. It begins with the autoproteolytic cleavage of capsid from the structural polyprotein. The capsid protein then associates with viral RNA, with the help of packaging signals such as only one genome of the virus is packed in one viral particle. The E3 protein act as a signal sequence for the insertion of polyprotein into the ER for processing by host endopeptidases. 6K proteins act as a signal sequence for processing. The E2 precursor and E1 interact with each other to form a heterodimer. The heterodimer complex is then transported from ER to cell surface. During the later stage of transport, the pE2 precursor is cleaved by furin to mature E2 and E3. This cleavage induces a conformational change between E2 and E1, resulting in weaker interaction in the heterodimer. The interaction between capsid protein and E2 protein cytoplasmic domain drives the viral budding process via envelope formation around nucleocapsid by heterodimer. During the release process, the virion acquires the host membrane around it (Strauss & Strauss, 1994; Yap et al., 2017).

1.3. Mosquito

Mosquito belongs to the Animalia kingdom, and Arthropoda family, and Insect class. Mosquitoes belong to the family of *Culicidae*. The word mosquito means little fly (from Spanish language *mosca* little, and *it* means fly). The mosquito has a segmented body, pair of halteres, three pairs of long hair-like legs, elongated mouthparts, and pair of wings. The mosquito is classified into two subfamilies: *Anophelinae* and *Culicidae*. Some of the common names include *Aedes*, *Culex*, and *Anopheles*.

Taxonomical Classification	
Kingdom	Animalia
Phylum	Arthropoda
Class	Insecta
Order	Diptera
Family	Culicidae
Tribe	Aedini
Genus	<i>Aedes</i>

1.3.1. Life stages of mosquito

The mosquito's life cycle has four stages such as egg, larva, pupa, and adult. The female mosquito lays eggs (up to 100) on the water surface, hatching into the larva within 48. The larva is motile and feeds on aquatic algae and other organic matter. There are four stages in larval development, and each of them sheds skin and grows in size to help them breathe. At the end of the larva stage, it develops into pupa. The non-feeding stage of development characterizes the pupal stage. The pupae are mobile, respond to light, and moves with the flip with their tails. The mosquito then metamorphoses into adults.

Moreover, similar to butterflies, the mosquito skin splits, and the adults come out. The freshly emerged adult mosquitoes rest at the surface of the water for some time to allow them to dry and harden body parts. The wings spread out to fly properly. After a particular day, the mosquitoes are ready to mate and blood feed (Costa et al., 2010; Prevention, 2021).

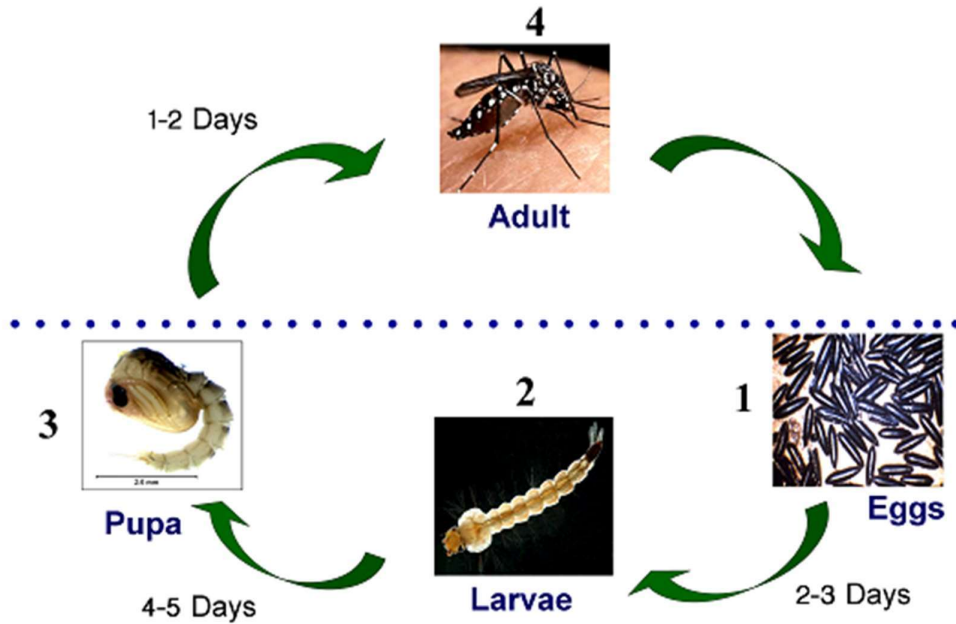


Figure 1.6 The life cycle of the mosquito. The female mosquito lays eggs on water surfaces that are initially white or transparent in color and converted into the black within a short time. The eggs hatch, and the long thread-like larva emerges, which are motile and feed on organic matter. The larvae then develop into pupa after skin shedding and physiological development. After a few days, the pupae metamorphoses into adult mosquitoes, ready to fly, feed, mate, and lay eggs. Adapted from: <http://www.dengue.health.gov.lk/web/index.php/en/information/dengue-mosquitoes>).

1.3.2. Chikungunya virus life cycle

Arboviruses use one organism as a host (to replicate) and the other as a vector (to transmit). The virus enters inside the mosquito's body from an infected person during the blood meal of female *Aedes* mosquitoes. Females need blood proteins for egg development. The virus grows inside the mosquito for a few days to make enough population. Then during the next blood meal, it enters into the body of other humans, probably uninfected. The virus will grow inside the human body to make billions of virus particles. If humans live in an ideal habitat for mosquitoes, then there are good chances that other mosquitoes will bite and take the virus along with blood. This cycle continuously continues, and the percentage of the population infected with the virus increases with time (Figure 1.7). The ideal temperature and humidity conditions such

as rainy and humid environments favor the mosquito population, leading to viral spread (Conway et al., 2014; Huang et al., 2019; Lim et al., 2018).

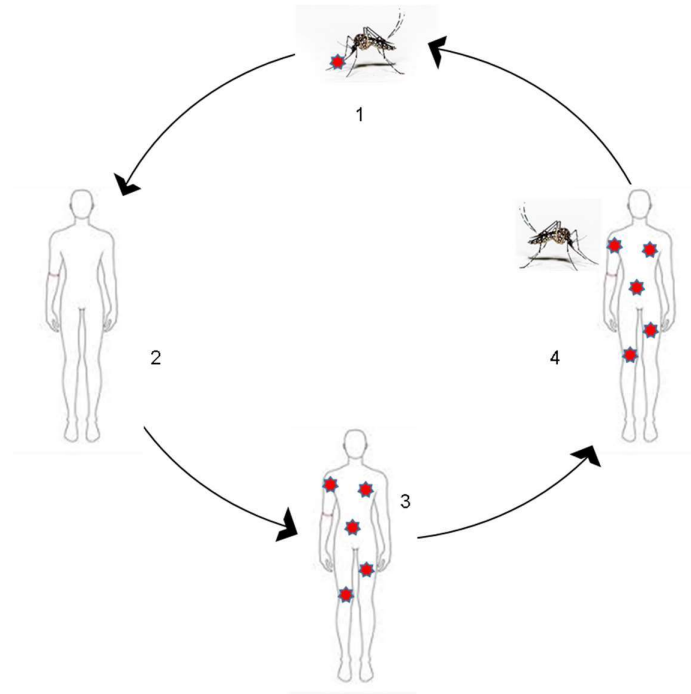


Figure 1.7 Chikungunya virus life cycle. The virus generally enters inside the female mosquito body during the blood meal from a virus-infected person. Inside the mosquito body, the virus replicates and spreads to the whole body. It then enters the human body during the next meal with mosquito saliva. The virus then replicates in the human body, where it reaches to billion viral particles/ml of blood. When mosquitoes bite the infected person for a blood meal, the virus also moves the blood to the mosquito body. The cycles continue to go on depending on the density of mosquitoes and humans in that particular area. The viral spread is also dependent on hygiene practices followed by the population of that area.

1.4. Chikungunya virus life cycle in *Aedes* mosquitoes

The mosquitoes pose a significant health burden to the world population due to their ability to transmit various pathogens including viruses such as zika, dengue, yellow fever, and chikungunya. The rapid urbanization, globalization, climate change, poverty resulting in unhygienic practices, lack of sufficient medical facilities led to the rapid spread of pathogens. Most viral pathogens utilize *Aedes* sp. for their transmission being *Ae. aegypti* and *Ae. albopictus* as significant vectors. *Ae. aegypti*

was a dominant vector for CHIKV transmission, but in the later outbreaks, *Ae. albopictus* became a significant vector, which could be attributed to the E1 A226V mutation of CHIKV (Tsetsarkin et al., 2007).

The female mosquito takes a blood meal and ingests the virus. Inside the mosquito, the virus reaches the midgut cells and replicate then it disseminates to other organs such as hemocoel, and salivary glands. It penetrates the basal lamina of salivary glands and is deposited into the apical cavities, which act as a store for the virus before its release during blood feeding (Figure 1.8).

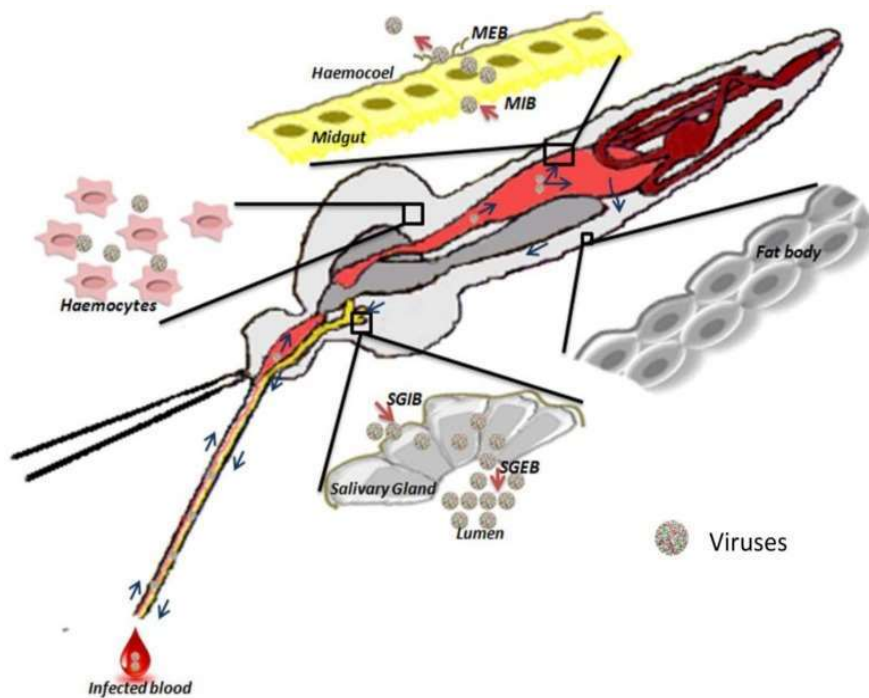


Figure 1.8 The life cycle of the virus in mosquito body. The virus moves into the mosquito body along with the blood meal. The virus then resides in the midgut, where it replicates and then spreads to other parts such as hemocoel and salivary glands. Then it is released with saliva with the bite in the next blood meal to the uninfected person. Adapted from (Kumar et al., 2018).

1.5. Chikungunya virus life cycle in human

The CHIKV infection cycle begins with the bite of virus infected female mosquito to the uninfected human. The virus enters the human body via skin along with mosquito saliva. The virus enters the human body through mosquito proboscis, the mosquito mouth system of six thin, needle-like mouthparts. This pierces the skin, finds blood

vessels, and makes it easy for mosquitoes to suck blood. Once inside the skin, virus. The viruses are deposited into the epidermis and dermis layer of the skin. The puncture of blood vessels during the blood meal allows the entry of the virus into the bloodstream. The mosquito bite site has resident cells of the immune system such as lymphocytes, dendritic cells, and monocytes. There have been reports that there are mannose-rich carbohydrates on mosquitoes' cells. The virus produced by these cells binds strongly to cells expressing DC-SIGN/L-SIGN, such as dendritic cells. As the virus infects the cells at the site of bite and replicates. The initial phase of infection is called the acute phase and generally lasts for 7-14 days. Its hallmarks are peak viremia, the manifestation of clinical symptoms, and the synthesis of neutralizing antibodies. Interferons and downstream signaling molecules limit the infection. These interferons help to recruit virus-sensing immune cells which use specific pathogen recognition receptors such as cGAS (cyclic GMP-AMP synthase), PKR (protein kinase R), OAS (2'-5'-oligoadenylate synthase) (Schwartz & Albert, 2010; Srivastava et al., 2020)

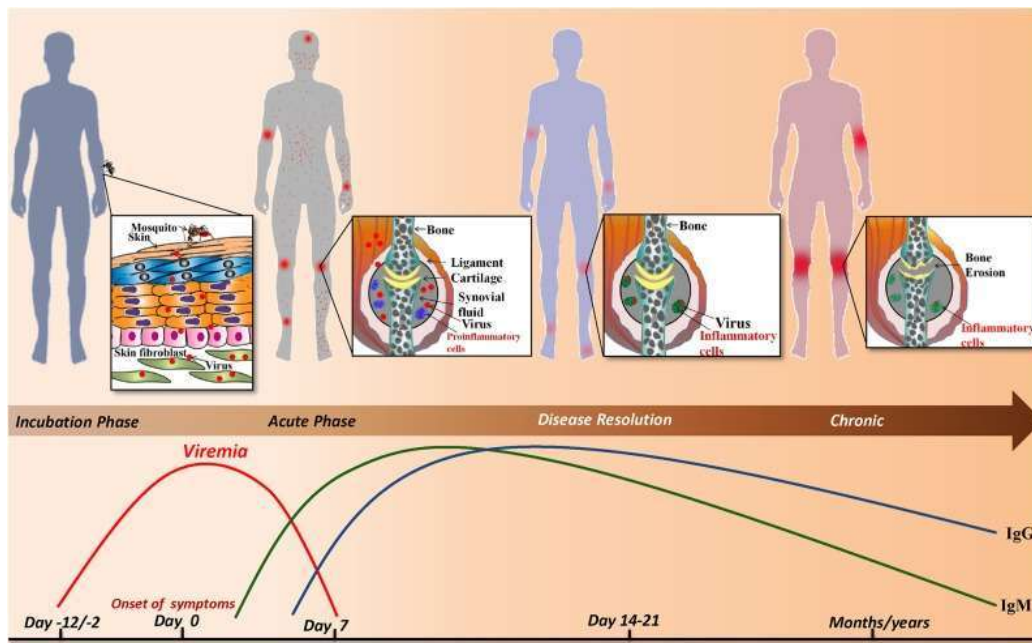


Figure 1.9 Chikungunya virus life cycle in humans. Female mosquitoes spread the virus during the blood meals from infected to non-infected persons. Upon entry into the body, the virus infects the epidermis and skin cells, including dendritic and fibroblasts. After countering the host immune system, the virus spreads to other body parts via the blood circulation system. During the initial phase, it generates billions of virion particles that are again transferred to non-infected persons in the next blood

meal of mosquitoes and is characterized by fever, rashes, body aches, and joint pain. The next phase is called as acute phase and generally lasts around a week. In this phase, the virus grows to enough number and activates the immune system, and the immune system act on it and controls the viral number. It is followed by the post-acute phase, in which the virus is cleared from the circulation system. Sometimes the patients show prolonged symptoms such as arthritis even after a week or months of infection, and the phase is called the chronic phase. Image adapted from ref.(Srivastava et al., 2020).

Despite a quick and effective immune response, the virus evades the cellular system by translational shutoff and apoptosis. The fibroblast, endothelial cells, microglial cells release cytokines such as CCL2, which attracts other cells such as macrophages, neutrophils, lymphocytes, and natural killer (NK) cells to the site of infection. In the acute phase, the IgM antibodies' level also starts going up, and the IgG level goes up later. In the late acute phases, all immune pathways cumulatively help to clear the virus from the body (Srivastava et al., 2020).

1.6. Host-Pathogen interactions

Viruses, whether with a genome of 10 kb or 30 kb, are not self-sufficient in carrying out crucial processes for their continuous growth and survival. The viruses encode only a set of enzymes and depend on the host for viral proteins during the replication process. The translation process interacts with various mosquito proteins and affects several proteins' expression levels to favors viral growth and virus survival. The host proteins interact with viral proteins from entry to replication, translation, post-translational processing, etc.(Goodman & Rasmussen, 2019). Host proteins such as proteases interact and cleave viral proteins and thus are crucial for viral growth. Similarly, helicases bind to viral RNA and play a role in replication and processing (Matkovic et al., 2019; Zaragoza et al., 2006). The outcome of the virus-host interaction generally results in eliciting an immune response. Almost all viral protein interacts with the host protein at one stage of the viral life cycle. One of the hubs of interaction is CHIKV non-structural protein 3 (nsP3). It is the most enigmatic protein of CHIKV, and least is known about its importance except that it forms the replication complex with viral RNA and host proteins. Various studies in human cell lines studied the host proteins that interact with nsP3 and are part of the replication

complex. Several factors were identified, including DEAD-box helicases, translation factors, ribosomes, etc. (Gao et al., 2019; Meshram et al., 2018).

1.6.1. Role of post-translation modification in virus-host interactions

Post-translational modifications (PTMs) of proteins are essential for the housekeeping functions of the cells. These involve attaching small groups to a protein such as ubiquitination, lipidation, glycosylation, methylation, phosphorylation, acetylation, and oxidation (Rahnefeld et al., 2014; Santos & Lindner, 2017; Zhang et al., 2017). These modifications are specific to proteins, amino acid residue, as well as bio/physicochemical conditions. PTMs are carried out by specialized enzymes (Bharaj et al., 2017; Santos & Lindner, 2017), such as Ubiquitin E3 ligase, glycosyltransferase, poly ADP ribose polymerase, acetyltransferase, kinases, etc. PTMs result in enhancing solubilization, conformation (by altering charge or hydrophobicity), interactions, signaling, degradation, and playing a crucial role in cell growth (Ryslava et al., 2013). During infection, the host overcomes viral infection by inactivating viral proteins by attaching small molecules such as ubiquitin, leading to their inactivation and/or proteasome-mediated degradation and activating immune response involving interferon response inhibit viral growth. The virus adopts a similar kind of approach to growing where its proteins either cleave host proteins involved in immune response and remove PTMs from its proteins which otherwise hinders its growth by targeting them to proteasomal degradation. Based on the size/chemical nature, PTMs can be broadly categorized into four categories, 1) Protein-based modification involving Ubiquitin, SUMO, ISG, NEDD8, 2) carbohydrate molecule-based modification such as glycosylation, ADP ribosylation, 3) lipid molecule-based modifications such as palmitoylation, myristylation, prenylation, and 4) chemical/ionic group such acetyl, phosphate, methyl, and oxidation to nascent proteins (Figure 1.10).

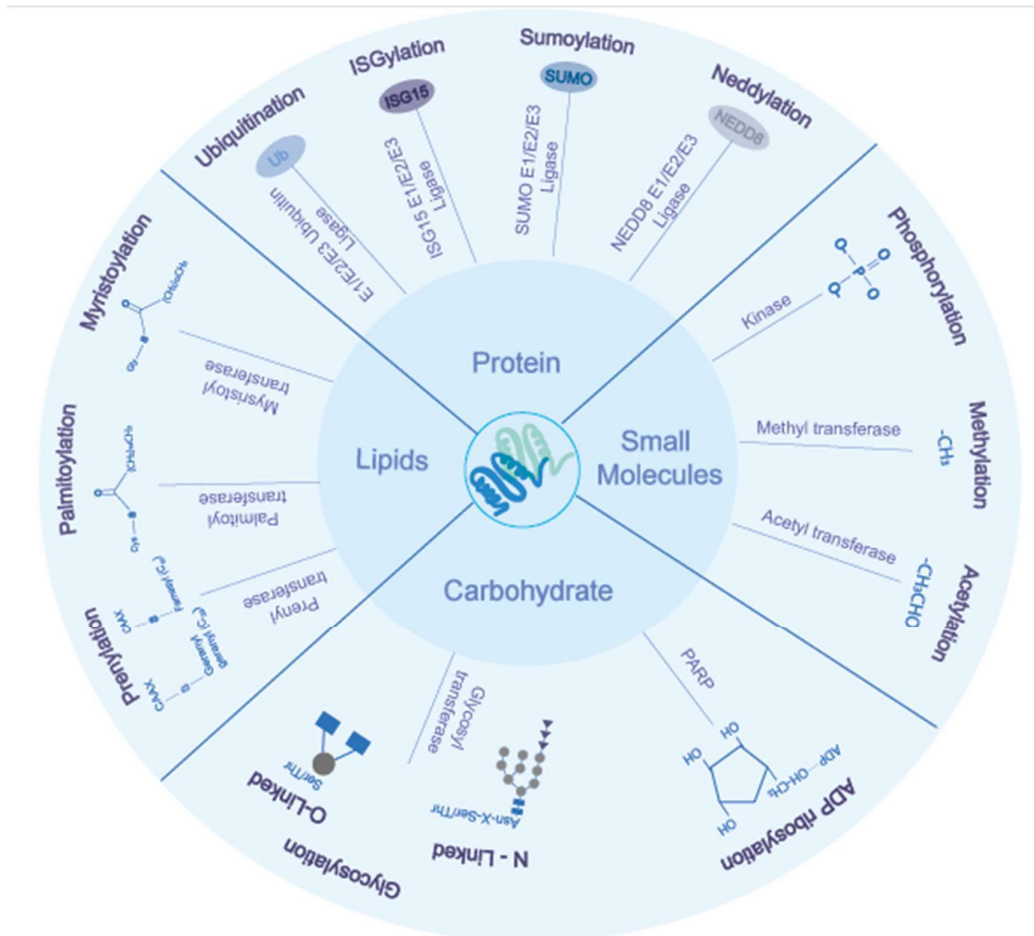


Figure 1.10 Overview of various post-translational modifications of virus and host proteins essential during viral infections. Based on biochemical moiety, PTMs can be categorized into modification by small protein groups (ubiquitination, ISGylation, SUMOylation, NEDDylation), carbohydrates (Glycosylation, ADP ribosylation), lipids (palmitoylation, myristoylation, and prenylation), and small chemical groups (phosphorylation, methylation, acetylation, oxidation). The protein is modified to gain in function, which modulates the virus's life cycle and host response to virus infection. Image from the published review paper in IJMS journal (Kumar et al., 2020).

ADP-ribosylation is a ubiquitous modification across all life domains ranging from viruses to eukaryotic organisms (Cohen & Chang, 2018; Grunewald et al., 2018; Hottiger et al., 2010). ADP-ribosylation utilizes nicotinamide adenine dinucleotide (NAD^+) as a cofactor to transfer ADP-ribose nucleotide onto proteins and DNA (Cohen & Chang, 2018). The reaction is catalyzed by the enzyme ADP-ribosyl transferases known as ARTDs (ADP-ribosyltransferase, diphtheria toxin-like) or

PARPs (Poly ADP ribose polymerase) (Cohen & Chang, 2018). The ADP-ribosylation plays an essential role in multiple biological processes such as viral translation and replication, signal transduction, epigenetics, cellular stress response, protein degradation (Bai, 2015). Modification by PARPs occurs mainly on acidic amino acid residues such as glutamate and aspartate, but other residues such as serine, arginine, lysine, and cysteines can also be acceptors (Hottiger et al., 2010).

1.6.1.1. Role of ADP ribosylation in inhibition of viral growth

PARPs regulate innate immune response at various viral infection steps and use MARylating and non-enzymatic PARPs to suppress IFN (interferon) response and pro-inflammatory cytokine induction. PARP binds to the RIG1 receptor and promotes its oligomerization and initialization of signaling cascade (Fehr et al., 2020). In addition to its role in cells' functioning, ribosylation negatively affects viral replication and infection outcomes (Atasheva et al., 2014). Some PARPs which are known to show antiviral properties are shown below.

PARP1 leads to transcriptional silencing of the integrated HIV (human immunodeficiency virus) genome in host cells either by the integration of HIV genome in transcriptionally disfavored regions (Centromere) or by epigenetic mechanisms, thereby repressing viral infection (Bueno et al., 2013; Gutierrez et al., 2016). Using a VEEV (Venezuelan Equine Encephalitis Virus) mutant based model, Atasheva et al. (2012) identified PARP12, among others PARP proteins, as an essential ISG involved in cellular defense against numerous alphavirus (Atasheva et al., 2012). PARP12 exhibited suppression of cellular translation, and this suppression was partially dependent on the catalytic activity of the carboxy-terminal PARP domain of the protein (Welsby et al., 2014). Further, PARP12 was identified to interact with ribosomes. PARP domain of the protein, however, was not involved in interactions with cellular translational machinery. The results of this study indicated a more complex and synergistic mechanism of PARP12 mediated inhibition of viral replication (Welsby et al., 2014). Zika virus-encoded NS1 and NS3 proteins underwent PARP12-mediated PAR. The PAR modification further recruited E3 ubiquitin ligase for ubiquitination. Thus, these two modifications were found to work synchronously to bring about proteasomal degradation of zika virus proteins (NS1 and NS3) (Li et al., 2018).

PARP13 is one of the first PARP enzymes for which antiviral function was identified. Two isoforms are ZAP-S (N-terminal tandem zinc-finger motifs that bind RNA) and ZAP-L (N-terminal tandem zinc-finger with C-terminal PARP inactive catalytic domain). PARP13/ZAP-S via N-terminal domain inhibits viral replication by promoting viral RNA degradation by recruiting RNA processing exosomes in HIV-1, Semliki forest virus (Kerns et al., 2008; Zhu et al., 2011), Sindbis, and Moloney murine leukemia virus (MLV); alternatively, it also binds to 3'UTR of IFN and causes degradation of IFN (IFNL1, IFNL2, and IFNB) mRNA (Schwerk et al., 2019). PARP13/ZAPL associate with ADP ribose moieties via its C-terminal PARP domain and mediates ubiquitination and subsequent IAV polymerase PB2 and PA (Liu et al., 2015). Other PARPs known to inhibit viral growth include PARP5a, PARP7, PARP9, PARP10, PARP12, and PARP13, which inhibit viral growth in one way, such as increasing IFNs, ISGs, binding to viral RNA, and preventing its translation (Fehr et al., 2020).

1.6.1.2. Role of ADP ribosylation in promotion of viral growth

During IAV replication, PARP1 is localized to the cytosol, where it mediates the degradation of the IFN receptor resulting in impaired host antiviral defense. PARP1 mediated IFNAR degradation depended on PAR-enzymatic activity, although the mechanism is still unclear (Fig. 3) (Xia et al., 2020). This suggests that ADP ribosylation has a potential pro-viral role during influenza virus infection. PARP1 is activated upon double-stranded breaks and modifies nuclear histones leading to chromatin de-condensation and enhanced access to repair enzymes. The enzyme facilitates HIV1 integration within the host genome by mediating DNA repair events during viral integration (Ha et al., 2001). PARP11 induced during VSV infection causes mono ADP ribosylation of ubiquitin E3 ligase β -transducin repeat-containing protein (β -TCP), leading to ubiquitination of IFNAR1 and its degradation. This results in reduced IFN and antiviral response (Guo et al., 2019). To counter host PARPs mediated immune response, several RNA viruses such as alphaviruses, hepatitis E virus, coronavirus (Grunewald et al., 2019; Malet et al., 2009; Parvez, 2015) has a macrodomain and possess the ability to recognize and reverse the effect of ADP ribosylation. Macrodomain from the RNA virus families bind both mono and poly-ADP-ribose and can hydrolyze and remove mono-ADP-ribose from proteins (Li et al., 2016) and promote the replication of viruses (Abraham et al., 2018; Grunewald et al.,

2019). CHIKV nsP3 protein macrodomain mutants showed that ADP-ribose binding caused the initiation of viral replication, while hydrolase activity is essential for amplifying replication complexes (Abraham et al., 2018).

Moreover, the mutant of the SARS-CoV macrodomain induced a robust pro-inflammatory cytokine response and increased the virus sensitivity to IFN-1 treatment (Grunewald et al., 2019). One study showed the importance of macrodomain in HEV replication where it was found that mutants (Asn809Ala' and His812Leu) were nonviable, whereas RNA replication was abrogated in mutants (Gly816Ala and Gly817Ala) (Parvez, 2015). Another study by Li et al. showed a strong correlation between viral replication and enzymatic activity of the mutant (Fehr et al., 2018). These findings suggest that the macro domain is not only crucial in replication but also post RNA replication.

1.7. Overview of the thesis work

The current work was focused on studying the interacting partners of chikungunya virus (CHIKV) nsP3 protein. For this, as first objective, the global impact on the proteome of *Ae. albopictus* cells (U4.4) upon CHIKV infection was studied. The mass spectrometric-based global impact on U4.4 cells' proteome was studied during chikungunya's early and late course. Since U4.4 cells have an active siRNA pathway, which helps them to grow while being infected. The study was critical as it showed how the infection modulates mosquito cells' pathways to facilitate its replication and survival at the cell level. The virus will establish infection, whereas the host immune system will be activated by viral RNA, leading to active surveillance for the virus. Whereas during the late infection time point study will give information about pathways responsible for maintaining virus number at check while maintaining cell growth.

The second objective of the study was to study the interacting partners of the CHIKV non-structural protein 3 (nsP3) using co-immunoprecipitation assay. The CHIKV nsP3 protein was cloned in pET29a vector and expressed in bacterial cells. Polyclonal antibodies were generated against nsP3 protein and validated using infected lysate. The antibodies were then used to immunoprecipitate the interacting partners of nsP3 in *Ae. aegypti* cells (Aag2) lysate. The mass spectrometry analysis of immunoprecipitated proteins revealed that proteins belonging to pathways such as

translation, RNA metabolism, oxidation-reduction gene expression were enriched. CHIKV nsP3 has three domains: macrodomain, AUD, and hypervariable domains (HVD). HVD act as recruiter of host proteins. Previous study from the lab identified that macrodomain interact with host immune pathways proteins and act as VSR (viral suppressor of RNAi). The domain has ADP ribosylhydrolase activity. There are no studies about the *Aedes* ADP ribose polymerases. The Sequence homology search with the human ADP ribose polymerases revealed presence of three ADP ribose polymerases in *Ae. aegypti*. Of these, Tankyrase was having domain crucial for protein interaction.

The third objective of my thesis work was to characterize the *Aedes* protein involved in interaction with nsP3. The objective was divided into two parts. First part was to validate the interacting partners of nsP3 protein using western blot analysis. Among the proteins interacting with the snP3, the focus was on RNAi pathway. Of the two RNAi pathway proteins RM62F was selected for validation as it was also found to be interacting in the previous pull-down experiments in the lab. The western blot analysis of nsP3 co-immunoprecipitated *Ae. aegypti* cell (Aag2) lysate revealed that RM62F interacts with nsP3. In the second part of the objective, the Tankyrase catalytic domain was cloned and expressed in bacteria. The purified protein was able to add ADP ribose chains in the *in vitro* poly ADP ribosylation (PAR) assay. It was also found that nsP3 protein was able to hydrolyze these long chains indicating that nsP3 negatively impact ADP ribosylation of host proteins, indicating that viral proteins control host machinery by targeting the post-translational modification.

1.8. References

- Abraham, R., Hauer, D., McPherson, R. L., Utt, A., Kirby, I. T., Cohen, M. S., . . . Griffin, D. E. (2018). ADP-ribosyl-binding and hydrolase activities of the alphavirus nsP3 macrodomain are critical for initiation of virus replication. *Proc Natl Acad Sci U S A*, *115*(44), E10457-E10466. <https://doi.org/10.1073/pnas.1812130115>
- Akhrymuk, I., Kulemzin, S. V., & Frolova, E. I. (2012). Evasion of the innate immune response: the Old World alphavirus nsP2 protein induces rapid degradation of Rpb1, a catalytic subunit of RNA polymerase II. *J Virol*, *86*(13), 7180-7191. <https://doi.org/10.1128/JVI.00541-12>
- Amraoui, F., & Failloux, A. B. (2016). Chikungunya: an unexpected emergence in Europe. *Curr Opin Virol*, *21*, 146-150. <https://doi.org/10.1016/j.coviro.2016.09.014>

- Atasheva, S., Akhrymuk, M., Frolova, E. I., & Frolov, I. (2012). New PARP gene with an anti-alphavirus function. *J Virol*, 86(15), 8147-8160. <https://doi.org/10.1128/JVI.00733-12>
- Atasheva, S., Frolova, E. I., & Frolov, I. (2014). Interferon-stimulated poly(ADP-Ribose) polymerases are potent inhibitors of cellular translation and virus replication. *J Virol*, 88(4), 2116-2130. <https://doi.org/10.1128/JVI.03443-13>
- Bai, P. (2015). Biology of Poly(ADP-Ribose) Polymerases: The Factotums of Cell Maintenance. *Mol Cell*, 58(6), 947-958. <https://doi.org/10.1016/j.molcel.2015.01.034>
- Baltimore, D. (1971). Expression of animal virus genomes. *Bacteriol Rev*, 35(3), 235-241. <https://doi.org/10.1128/br.35.3.235-241.1971>
- Baxter, V. K., & Heise, M. T. (2018). Genetic control of alphavirus pathogenesis. *Mamm Genome*, 29(7-8), 408-424. <https://doi.org/10.1007/s00335-018-9776-1>
- Bharaj, P., Atkins, C., Luthra, P., Giraldo, M. I., Dawes, B. E., Miorin, L., . . . Rajsbaum, R. (2017). The Host E3-Ubiquitin Ligase TRIM6 Ubiquitinates the Ebola Virus VP35 Protein and Promotes Virus Replication. *J Virol*, 91(18). <https://doi.org/10.1128/JVI.00833-17>
- Brown, R. S., Anastasakis, D. G., Hafner, M., & Kielian, M. (2020). Multiple capsid protein binding sites mediate selective packaging of the alphavirus genomic RNA. *Nat Commun*, 11(1), 4693. <https://doi.org/10.1038/s41467-020-18447-z>
- Bueno, M. T., Reyes, D., Valdes, L., Saheba, A., Urias, E., Mendoza, C., . . . Llano, M. (2013). Poly(ADP-ribose) polymerase 1 promotes transcriptional repression of integrated retroviruses. *J Virol*, 87(5), 2496-2507. <https://doi.org/10.1128/JVI.01668-12>
- Campillo-Balderas, J. A., Lazcano, A., & Becerra, A. (2015). Viral Genome Size Distribution Does not Correlate with the Antiquity of the Host Lineages. *Frontiers in Ecology and Evolution*, 3. <https://doi.org/10.3389/fevo.2015.00143>
- Chaitanya, K. V. (2019). Structure and Organization of Virus Genomes. *Genome and Genomics*, 1(30). https://doi.org/10.1007/978-981-15-0702-1_1
- Chen, M. W., Tan, Y. B., Zheng, J., Zhao, Y., Lim, B. T., Cornvik, T., . . . Luo, D. (2017). Chikungunya virus nsP4 RNA-dependent RNA polymerase core domain displays detergent-sensitive primer extension and terminal adenylyltransferase activities. *Antiviral Res*, 143, 38-47. <https://doi.org/10.1016/j.antiviral.2017.04.001>
- Chikungunya worldwide overview*. (2021). European Centre for Disease Prevention and Control. <https://www.ecdc.europa.eu/en/chikungunya-monthly>
- Cohen, M. S., & Chang, P. (2018). Insights into the biogenesis, function, and regulation of ADP-ribosylation. *Nat Chem Biol*, 14(3), 236-243. <https://doi.org/10.1038/nchembio.2568>
- Conway, M. J., Colpitts, T. M., & Fikrig, E. (2014). Role of the Vector in Arbovirus Transmission. *Annu Rev Virol*, 1(1), 71-88. <https://doi.org/10.1146/annurev-virology-031413-085513>
- Costa, E. A. P. d. A., Santos, E. M. d. M., Correia, J. C., & Albuquerque, C. M. R. d. (2010). Impact of small variations in temperature and humidity on the reproductive activity and survival of *Aedes aegypti* (Diptera, Culicidae). *Revista Brasileira de Entomologia*, 54(3), 488-493. <https://doi.org/10.1590/s0085-56262010000300021>

- De Caluwe, L., Coppens, S., Vereecken, K., Daled, S., Dhaenens, M., Van Ostade, X., . . . Bartholomeeusen, K. (2021). The CD147 Protein Complex Is Involved in Entry of Chikungunya Virus and Related Alphaviruses in Human Cells. *Front Microbiol*, *12*, 615165. <https://doi.org/10.3389/fmicb.2021.615165>
- Fehr, A. R., Jankevicius, G., Ahel, I., & Perlman, S. (2018). Viral Macrodomains: Unique Mediators of Viral Replication and Pathogenesis. *Trends Microbiol*, *26*(7), 598-610. <https://doi.org/10.1016/j.tim.2017.11.011>
- Fehr, A. R., Singh, S. A., Kerr, C. M., Mukai, S., Higashi, H., & Aikawa, M. (2020). The impact of PARPs and ADP-ribosylation on inflammation and host-pathogen interactions. *Genes Dev*, *34*(5-6), 341-359. <https://doi.org/10.1101/gad.334425.119>
- Fermin, G. (2018). *Chapter 5 - Host Range, Host-Virus Interactions, and Virus Transmission* (G. F. Paula Tennant, Jerome E. Foster, Ed.). Academic Press. <https://doi.org/10.1016/B978-0-12-811257-1.00005-X>
- Gao, Y., Goonawardane, N., Ward, J., Tuplin, A., & Harris, M. (2019). Multiple roles of the non-structural protein 3 (nsP3) alphavirus unique domain (AUD) during Chikungunya virus genome replication and transcription. *PLoS Pathog*, *15*(1), e1007239. <https://doi.org/10.1371/journal.ppat.1007239>
- Garmashova, N., Gorchakov, R., Frolova, E., & Frolov, I. (2006). Sindbis virus nonstructural protein nsP2 is cytotoxic and inhibits cellular transcription. *J Virol*, *80*(12), 5686-5696. <https://doi.org/10.1128/JVI.02739-05>
- Goodman, A. G., & Rasmussen, A. L. (2019). Editorial: Host-Pathogen Interactions During Arboviral Infections. *Front Cell Infect Microbiol*, *9*, 77. <https://doi.org/10.3389/fcimb.2019.00077>
- Gould, E. A., Coutard, B., Malet, H., Morin, B., Jamal, S., Weaver, S., . . . Canard, B. (2010). Understanding the alphaviruses: recent research on important emerging pathogens and progress towards their control. *Antiviral Res*, *87*(2), 111-124. <https://doi.org/10.1016/j.antiviral.2009.07.007>
- Grunewald, M. E., Chen, Y., Kuny, C., Maejima, T., Lease, R., Ferraris, D., . . . Fehr, A. R. (2019). The coronavirus macrodomain is required to prevent PARP-mediated inhibition of virus replication and enhancement of IFN expression. *PLoS Pathog*, *15*(5), e1007756. <https://doi.org/10.1371/journal.ppat.1007756>
- Grunewald, M. E., Fehr, A. R., Athmer, J., & Perlman, S. (2018). The coronavirus nucleocapsid protein is ADP-ribosylated. *Virology*, *517*, 62-68. <https://doi.org/10.1016/j.virol.2017.11.020>
- Guo, T., Zuo, Y., Qian, L., Liu, J., Yuan, Y., Xu, K., . . . Zheng, H. (2019). ADP-ribosyltransferase PARP11 modulates the interferon antiviral response by mono-ADP-ribosylating the ubiquitin E3 ligase beta-TrCP. *Nat Microbiol*, *4*(11), 1872-1884. <https://doi.org/10.1038/s41564-019-0428-3>
- Gutierrez, D. A., Valdes, L., Serguera, C., & Llano, M. (2016). Poly(ADP-ribose) polymerase-1 silences retroviruses independently of viral DNA integration or heterochromatin formation. *J Gen Virol*, *97*(7), 1686-1692. <https://doi.org/10.1099/jgv.0.000466>

- Ha, H. C., Juluri, K., Zhou, Y., Leung, S., Hermankova, M., & Snyder, S. H. (2001). Poly(ADP-ribose) polymerase-1 is required for efficient HIV-1 integration. *Proc Natl Acad Sci U S A*, *98*(6), 3364-3368. <https://doi.org/10.1073/pnas.051633498>
- Holmes, A. C., Basore, K., Fremont, D. H., & Diamond, M. S. (2020). A molecular understanding of alphavirus entry. *PLoS Pathog*, *16*(10), e1008876. <https://doi.org/10.1371/journal.ppat.1008876>
- Hoorweg, T. E., Bouma, E. M., van de Pol, D. P. I., Rodenhuis-Zybert, I. A., & Smit, J. M. (2020). Chikungunya virus requires an intact microtubule network for efficient viral genome delivery. *PLoS Negl Trop Dis*, *14*(8), e0008469. <https://doi.org/10.1371/journal.pntd.0008469>
- Hottiger, M. O., Hassa, P. O., Luscher, B., Schuler, H., & Koch-Nolte, F. (2010). Toward a unified nomenclature for mammalian ADP-ribosyltransferases. *Trends Biochem Sci*, *35*(4), 208-219. <https://doi.org/10.1016/j.tibs.2009.12.003>
- HR, G. (1996). *Structure and Classification of Viruses* (B. S., Ed. Vol. 4). <https://www.ncbi.nlm.nih.gov/books/NBK8174>
- Huang, Y. S., Higgs, S., & Vanlandingham, D. L. (2019). Arbovirus-Mosquito Vector-Host Interactions and the Impact on Transmission and Disease Pathogenesis of Arboviruses. *Front Microbiol*, *10*, 22. <https://doi.org/10.3389/fmicb.2019.00022>
- Hyde, J. L., Chen, R., Trobaugh, D. W., Diamond, M. S., Weaver, S. C., Klimstra, W. B., & Wilusz, J. (2015). The 5' and 3' ends of alphavirus RNAs--Non-coding is not non-functional. *Virus Res*, *206*, 99-107. <https://doi.org/10.1016/j.virusres.2015.01.016>
- Kerns, J. A., Emerman, M., & Malik, H. S. (2008). Positive selection and increased antiviral activity associated with the PARP-containing isoform of human zinc-finger antiviral protein. *PLoS Genet*, *4*(1), e21. <https://doi.org/10.1371/journal.pgen.0040021>
- Kumar, A., Srivastava, P., Sirisena, P., Dubey, S. K., Kumar, R., Shrinet, J., & Sunil, S. (2018). Mosquito Innate Immunity. *Insects*, *9*(3). <https://doi.org/10.3390/insects9030095>
- Kumar, R., Mehta, D., Mishra, N., Nayak, D., & Sunil, S. (2020). Role of Host-Mediated Post-Translational Modifications (PTMs) in RNA Virus Pathogenesis. *Int J Mol Sci*, *22*(1). <https://doi.org/10.3390/ijms22010323>
- Lampio, A., Kilpelainen, I., Pesonen, S., Karhi, K., Auvinen, P., Somerharju, P., & Kaariainen, L. (2000). Membrane binding mechanism of an RNA virus-capping enzyme. *J Biol Chem*, *275*(48), 37853-37859. <https://doi.org/10.1074/jbc.M004865200>
- Leung, J. Y., Ng, M. M., & Chu, J. J. (2011). Replication of alphaviruses: a review on the entry process of alphaviruses into cells. *Adv Virol*, *2011*, 249640. <https://doi.org/10.1155/2011/249640>
- Li, C., Debing, Y., Jankevicius, G., Neyts, J., Ahel, I., Coutard, B., . . . Perlman, S. (2016). Viral Macro Domains Reverse Protein ADP-Ribosylation. *Journal of Virology*, *90*(19), 8478-8486. <https://doi.org/10.1128/jvi.00705-16>
- Li, L., Zhao, H., Liu, P., Li, C., Quanquin, N., Ji, X., . . . Cheng, G. (2018). PARP12 suppresses Zika virus infection through PARP-dependent degradation of NS1 and NS3 viral proteins. *Sci Signal*, *11*(535). <https://doi.org/10.1126/scisignal.aas9332>

- Li, Y., Kamara, F., Zhou, G., Puthiyakunnon, S., Li, C., Liu, Y., . . . Chen, X. G. (2014). Urbanization increases *Aedes albopictus* larval habitats and accelerates mosquito development and survivorship. *PLoS Negl Trop Dis*, 8(11), e3301. <https://doi.org/10.1371/journal.pntd.0003301>
- Lim, E. X. Y., Lee, W. S., Madzokere, E. T., & Herrero, L. J. (2018). Mosquitoes as Suitable Vectors for Alphaviruses. *Viruses*, 10(2). <https://doi.org/10.3390/v10020084>
- Liu, C. H., Zhou, L., Chen, G., & Krug, R. M. (2015). Battle between influenza A virus and a newly identified antiviral activity of the PARP-containing ZAPL protein. *Proc Natl Acad Sci U S A*, 112(45), 14048-14053. <https://doi.org/10.1073/pnas.1509745112>
- Malet, H., Coutard, B., Jamal, S., Dutartre, H., Papageorgiou, N., Neuvonen, M., . . . Canard, B. (2009). The crystal structures of Chikungunya and Venezuelan equine encephalitis virus nsP3 macro domains define a conserved adenosine binding pocket. *J Virol*, 83(13), 6534-6545. <https://doi.org/10.1128/JVI.00189-09>
- Matkovic, R., Bernard, E., Fontanel, S., Eldin, P., Chazal, N., Hassan Hersi, D., . . . Briant, L. (2019). The Host DHX9 DExH-Box Helicase Is Recruited to Chikungunya Virus Replication Complexes for Optimal Genomic RNA Translation. *J Virol*, 93(4). <https://doi.org/10.1128/JVI.01764-18>
- McPherson, R. L., Abraham, R., Sreekumar, E., Ong, S. E., Cheng, S. J., Baxter, V. K., . . . Leung, A. K. (2017). ADP-ribosylhydrolase activity of Chikungunya virus macrodomain is critical for virus replication and virulence. *Proc Natl Acad Sci U S A*, 114(7), 1666-1671. <https://doi.org/10.1073/pnas.1621485114>
- Mendes, A., & Kuhn, R. J. (2018). Alphavirus Nucleocapsid Packaging and Assembly. *Viruses*, 10(3). <https://doi.org/10.3390/v10030138>
- Meshram, C. D., Agback, P., Shiliaev, N., Urakova, N., Mobley, J. A., Agback, T., . . . Frolov, I. (2018). Multiple Host Factors Interact with the Hypervariable Domain of Chikungunya Virus nsP3 and Determine Viral Replication in Cell-Specific Mode. *J Virol*, 92(16). <https://doi.org/10.1128/JVI.00838-18>
- Nagy, P. D., & Pogany, J. (2011). The dependence of viral RNA replication on co-opted host factors. *Nat Rev Microbiol*, 10(2), 137-149. <https://doi.org/10.1038/nrmicro2692>
- Nasir, A., Forterre, P., Kim, K. M., & Caetano-Anolles, G. (2014). The distribution and impact of viral lineages in domains of life. *Front Microbiol*, 5, 194. <https://doi.org/10.3389/fmicb.2014.00194>
- Ozden, S., Lucas-Hourani, M., Ceccaldi, P. E., Basak, A., Valentine, M., Benjannet, S., . . . Seidah, N. G. (2008). Inhibition of Chikungunya virus infection in cultured human muscle cells by furin inhibitors: impairment of the maturation of the E2 surface glycoprotein. *J Biol Chem*, 283(32), 21899-21908. <https://doi.org/10.1074/jbc.M802444200>
- Parrott, M. M., Sitarski, S. A., Arnold, R. J., Picton, L. K., Hill, R. B., & Mukhopadhyay, S. (2009). Role of conserved cysteines in the alphavirus E3 protein. *J Virol*, 83(6), 2584-2591. <https://doi.org/10.1128/JVI.02158-08>
- Parvez, M. K. (2015). The hepatitis E virus ORF1 'X-domain' residues form a putative macrodomain protein/Appr-1"-pase catalytic-site, critical for viral RNA replication. *Gene*, 566(1), 47-53. <https://doi.org/10.1016/j.gene.2015.04.026>

- Prevention, C. f. D. C. a. (2021, March 5, 2020). <https://www.cdc.gov/mosquitoes/about/life-cycles/aedes.html>.
- Pulmanausahakul, R., Roytrakul, S., Auewarakul, P., & Smith, D. R. (2011). Chikungunya in Southeast Asia: understanding the emergence and finding solutions. *International Journal of Infectious Diseases*, *15*(10), e671-e676. <https://doi.org/10.1016/j.ijid.2011.06.002>
- Rahnefeld, A., Klingel, K., Schuermann, A., Diny, N. L., Althof, N., Lindner, A., . . . Voigt, A. (2014). Ubiquitin-like protein ISG15 (interferon-stimulated gene of 15 kDa) in host defense against heart failure in a mouse model of virus-induced cardiomyopathy. *Circulation*, *130*(18), 1589-1600. <https://doi.org/10.1161/CIRCULATIONAHA.114.009847>
- Ramsey, J., Chavez, M., & Mukhopadhyay, S. (2019). Domains of the TF protein important in regulating its own palmitoylation. *Virology*, *531*, 31-39. <https://doi.org/10.1016/j.virol.2019.02.016>
- Ramsey, J., Renzi, E. C., Arnold, R. J., Trinidad, J. C., & Mukhopadhyay, S. (2017). Palmitoylation of Sindbis Virus TF Protein Regulates Its Plasma Membrane Localization and Subsequent Incorporation into Virions. *J Virol*, *91*(3). <https://doi.org/10.1128/JVI.02000-16>
- Ryslava, H., Doubnerova, V., Kavan, D., & Vanek, O. (2013). Effect of posttranslational modifications on enzyme function and assembly. *J Proteomics*, *92*, 80-109. <https://doi.org/10.1016/j.jprot.2013.03.025>
- Santos, A. L., & Lindner, A. B. (2017). Protein Posttranslational Modifications: Roles in Aging and Age-Related Disease. *Oxid Med Cell Longev*, *2017*, 5716409. <https://doi.org/10.1155/2017/5716409>
- Schwartz, O., & Albert, M. L. (2010). Biology and pathogenesis of chikungunya virus. *Nat Rev Microbiol*, *8*(7), 491-500. <https://doi.org/10.1038/nrmicro2368>
- Schwerk, J., Soveg, F. W., Ryan, A. P., Thomas, K. R., Hatfield, L. D., Ozarkar, S., . . . Savan, R. (2019). RNA-binding protein isoforms ZAP-S and ZAP-L have distinct antiviral and immune resolution functions. *Nat Immunol*, *20*(12), 1610-1620. <https://doi.org/10.1038/s41590-019-0527-6>
- Silva, L. A., & Dermody, T. S. (2017). Chikungunya virus: epidemiology, replication, disease mechanisms, and prospective intervention strategies. *J Clin Invest*, *127*(3), 737-749. <https://doi.org/10.1172/JCI84417>
- Snyder, A. J., & Mukhopadhyay, S. (2012). The alphavirus E3 glycoprotein functions in a clade-specific manner. *J Virol*, *86*(24), 13609-13620. <https://doi.org/10.1128/JVI.01805-12>
- Snyder, J. E., Kulcsar, K. A., Schultz, K. L., Riley, C. P., Neary, J. T., Marr, S., . . . Kuhn, R. J. (2013). Functional characterization of the alphavirus TF protein. *J Virol*, *87*(15), 8511-8523. <https://doi.org/10.1128/JVI.00449-13>
- Song, H., Zhao, Z., Chai, Y., Jin, X., Li, C., Yuan, F., . . . Gao, G. F. (2019). Molecular Basis of Arthritogenic Alphavirus Receptor MXRA8 Binding to Chikungunya Virus Envelope Protein. *Cell*, *177*(7), 1714-1724 e1712. <https://doi.org/10.1016/j.cell.2019.04.008>

- Srivastava, P., Kumar, A., Hasan, A., Mehta, D., Kumar, R., Sharma, C., & Sunil, S. (2020). Disease Resolution in Chikungunya-What Decides the Outcome? *Front Immunol*, *11*, 695. <https://doi.org/10.3389/fimmu.2020.00695>
- Strauss, J. H., & Strauss, E. G. (1994). The alphaviruses: gene expression, replication, and evolution. *Microbiol Rev*, *58*(3), 491-562. <https://doi.org/10.1128/mr.58.3.491-562.1994>
- Suhrbier, A., Jaffar-Bandjee, M. C., & Gasque, P. (2012). Arthritogenic alphaviruses--an overview. *Nat Rev Rheumatol*, *8*(7), 420-429. <https://doi.org/10.1038/nrrheum.2012.64>
- Tan, Y. B., Lello, L. S., Liu, X., Law, Y.-S., Kang, C., Lescar, J., . . . Luo, D. (2021). A crystal structure of alphavirus nonstructural protein 4 (nsP4) reveals an intrinsically dynamic RNA-dependent RNA polymerase. *BioRxiv*. <https://doi.org/10.1101/2021.05.27.445971>
- Tero Ahola, A. M. (2016). *Functions of Chikungunya Virus Nonstructural Proteins*. Springer, Cham. https://doi.org/10.1007/978-3-319-42958-8_6
- Thiboutot, M. M., Kannan, S., Kawalekar, O. U., Shedlock, D. J., Khan, A. S., Sarangan, G., . . . Muthumani, K. (2010). Chikungunya: a potentially emerging epidemic? *PLoS Negl Trop Dis*, *4*(4), e623. <https://doi.org/10.1371/journal.pntd.0000623>
- Tsetsarkin, K. A., Chen, R., & Weaver, S. C. (2016). Interspecies transmission and chikungunya virus emergence. *Curr Opin Virol*, *16*, 143-150. <https://doi.org/10.1016/j.coviro.2016.02.007>
- Tsetsarkin, K. A., Vanlandingham, D. L., McGee, C. E., & Higgs, S. (2007). A single mutation in chikungunya virus affects vector specificity and epidemic potential. *PLoS Pathog*, *3*(12), e201. <https://doi.org/10.1371/journal.ppat.0030201>
- Uchime, O., Fields, W., & Kielian, M. (2013). The role of E3 in pH protection during alphavirus assembly and exit. *J Virol*, *87*(18), 10255-10262. <https://doi.org/10.1128/JVI.01507-13>
- Valentine, M. J., Murdock, C. C., & Kelly, P. J. (2019). Sylvatic cycles of arboviruses in non-human primates. *Parasit Vectors*, *12*(1), 463. <https://doi.org/10.1186/s13071-019-3732-0>
- Vazeille, M., Moutailler, S., Coudrier, D., Rousseaux, C., Khun, H., Huerre, M., . . . Failloux, A. B. (2007). Two Chikungunya isolates from the outbreak of La Reunion (Indian Ocean) exhibit different patterns of infection in the mosquito, *Aedes albopictus*. *PLoS One*, *2*(11), e1168. <https://doi.org/10.1371/journal.pone.0001168>
- Vega-Rua, A., Lourenco-de-Oliveira, R., Mousson, L., Vazeille, M., Fuchs, S., Yebakima, A., . . . Failloux, A. B. (2015). Chikungunya virus transmission potential by local *Aedes* mosquitoes in the Americas and Europe. *PLoS Negl Trop Dis*, *9*(5), e0003780. <https://doi.org/10.1371/journal.pntd.0003780>
- Viruses, I. C. o. T. o. (2021). *Togaviridae*. Retrieved 10 July 2021 from https://talk.ictvonline.org/taxonomy/p/taxonomy-history?taxnode_id=202005082
- Wahid, B., Ali, A., Rafique, S., & Idrees, M. (2017). Global expansion of chikungunya virus: mapping the 64-year history. *Int J Infect Dis*, *58*, 69-76. <https://doi.org/10.1016/j.ijid.2017.03.006>

- Walsh, D., & Mohr, I. (2011). Viral subversion of the host protein synthesis machinery. *Nat Rev Microbiol*, 9(12), 860-875. <https://doi.org/10.1038/nrmicro2655>
- Weaver, S. C., & Lecuit, M. (2015). Chikungunya virus and the global spread of a mosquito-borne disease. *N Engl J Med*, 372(13), 1231-1239. <https://doi.org/10.1056/NEJMra1406035>
- Welsby, I., Hutin, D., Gueydan, C., Krusys, V., Rongvaux, A., & Leo, O. (2014). PARP12, an interferon-stimulated gene involved in the control of protein translation and inflammation. *J Biol Chem*, 289(38), 26642-26657. <https://doi.org/10.1074/jbc.M114.589515>
- Wimalasiri-Yapa, B., Stassen, L., Huang, X., Hafner, L. M., Hu, W., Devine, G. J., . . . Frentiu, F. D. (2019). Chikungunya virus in Asia - Pacific: a systematic review. *Emerg Microbes Infect*, 8(1), 70-79. <https://doi.org/10.1080/22221751.2018.1559708>
- Xia, C., Wolf, J. J., Sun, C., Xu, M., Studstill, C. J., Chen, J., . . . Hahn, B. (2020). PARP1 Enhances Influenza A Virus Propagation by Facilitating Degradation of Host Type I Interferon Receptor. *J Virol*, 94(7). <https://doi.org/10.1128/JVI.01572-19>
- Yap, M. L., Klose, T., Urakami, A., Hasan, S. S., Akahata, W., & Rossmann, M. G. (2017). Structural studies of Chikungunya virus maturation. *Proc Natl Acad Sci U S A*, 114(52), 13703-13707. <https://doi.org/10.1073/pnas.1713166114>
- Zaragoza, C., Saura, M., Padalko, E. Y., Lopez-Rivera, E., Lizarbe, T. R., Lamas, S., & Lowenstein, C. J. (2006). Viral protease cleavage of inhibitor of kappaBalpha triggers host cell apoptosis. *Proc Natl Acad Sci U S A*, 103(50), 19051-19056. <https://doi.org/10.1073/pnas.0606019103>
- Zeller, H., Van Bortel, W., & Sudre, B. (2016). Chikungunya: Its History in Africa and Asia and Its Spread to New Regions in 2013-2014. *J Infect Dis*, 214(suppl 5), S436-S440. <https://doi.org/10.1093/infdis/jiw391>
- Zhang, K., Law, Y. S., Law, M. C. Y., Tan, Y. B., Wirawan, M., & Luo, D. (2021). Structural insights into viral RNA capping and plasma membrane targeting by Chikungunya virus nonstructural protein 1. *Cell Host Microbe*, 29(5), 757-764 e753. <https://doi.org/10.1016/j.chom.2021.02.018>
- Zhang, N., Zhao, H., & Zhang, L. (2019). Fatty Acid Synthase Promotes the Palmitoylation of Chikungunya Virus nsP1. *J Virol*, 93(3). <https://doi.org/10.1128/JVI.01747-18>
- Zhang, T., Ye, Z., Yang, X., Qin, Y., Hu, Y., Tong, X., . . . Ye, X. (2017). NEDDylation of PB2 Reduces Its Stability and Blocks the Replication of Influenza A Virus. *Sci Rep*, 7, 43691. <https://doi.org/10.1038/srep43691>
- Zheng, Y., & Kielian, M. (2013). Imaging of the alphavirus capsid protein during virus replication. *J Virol*, 87(17), 9579-9589. <https://doi.org/10.1128/JVI.01299-13>
- Zhu, Y., Chen, G., Lv, F., Wang, X., Ji, X., Xu, Y., . . . Gao, G. (2011). Zinc-finger antiviral protein inhibits HIV-1 infection by selectively targeting multiply spliced viral mRNAs for degradation. *Proc Natl Acad Sci U S A*, 108(38), 15834-15839. <https://doi.org/10.1073/pnas.1101676108>

Chapter 2

Chapter 2

Materials and methods

2.1. Materials or reagents

All the primers used in this study were designed in Snapgene software (for cloning) and Prime Quest tool (for quantitative PCR) from Integrated DNA Technologies for respective DNA templates and procured from Sigma-Aldrich Chemical Ltd. The chemicals used in the study are as follows: Tris base, glycine, Ethylene diamine tetraacetic acid (EDTA), Potassium hydrogen phosphate K₂HPO₄, Potassium chloride, Sodium chloride, 2-Mercaptoethanol, Chloroform, Methanol, glycerol, LB agar, terrific broth, Trimethylethylene diamine (TEMED), Leibovitz's L-15 medium, fetal bovine serum (FBS), TRIzol, Isopropanol, Glacial acetic acid, Bromophenol blue, Coomassie Brilliant Blue R-250, Nonidet P-40, Imidazole, IPTG (Isopropyl β-D-1-thiogalactopyranoside), formaldehyde, Phenylmethylsulfonylfluoride (PMSF), QuantiTect SYBR Green PCR Kit, and Kanamycin, Ampicillin. All the chemicals were of molecular biology grade and were procured from Sigma-Aldrich Chemical Pvt. Ltd., Invitrogen Pvt. Ltd., Amresco LLC, Roche, Himedia Laboratories Pvt. Ltd.

The pET29a plasmid was used for the expression of proteins. *Escherichia coli* (*E. coli*) DH5α as cloning cells while *E. coli* BL21-CodonPlus competent cells were used for the expression of recombinant proteins. *Aedes albopictus* cells (U4.4) and *Aedes aegypti*-derived cell line (Aag2) were used in the study. Aag2 cells were a kind gift from Dr. Alain Kohl (University of Glasgow, United Kingdom). Vero and C6/36 cells were used for virus propagation, and Vero cells were used for plaque assay.

The plasmid isolation and PCR/gel purification kits were purchased from Genetix, India, T4 DNA ligase kit, Prestained protein ladder, and 1kb DNA ladder were from Thermo Fisher. All restriction enzymes were from New England Biolabs, USA. PrimeScript™ One-Step RT-PCR Kit Ver.2 from Takara Bio companies. Cell culture media (DMEM, Leibovitz's L-15 medium), SYBR green master mixture were purchased from Qiagen. Antibodies such as anti-His IgG-HRP, anti-mice IgG-HRP, anti-rabbit IgG-HRP, anti-mice alexa 488 labelled IgG antibody, and anti-rabbit alexa 594 labelled IgG antibody, DAPI were from either Sigma Aldrich Chemicals Pvt. Ltd, Abcam, Santa Cruz, Invitrogen, and Cell signaling Technology.

2.2. Solution, buffer, and media preparation

Phosphate buffer Saline (PBS) protocol

Solute		1X	10X
NaCl	137 mM	8 g	80 g
KCl	2.7 mM	0.2 g	2 g
Na ₂ HPO ₄	10 mM	1.44 g	14.4 g
KH ₂ PO ₄	2 mM	0.24 g	2.4 g

All the components were dissolved in 800 ml water, and the pH was adjusted to 7.4. Distilled water was added to make the final volume 1L. It was sterilized by autoclaving for 20 min at 15 psi or by filter sterilization. The buffer was stored at room temperature.

Luria-Bertani (LB) Media

2.5 g LB media was dissolved in 100 ml distilled water. The media was autoclaved and then kept at room temperature until used.

LB agar

2.5 g LB broth+1.5 g agar was added in 100 ml distilled water. The media was autoclaved, and then desired antibiotics were added at specific concentrations when the temperature reached around 45°C and then poured into petri plates for solidifying.

Terrific broth

Terrific broth (TB) 1:

Yeast extract	24 g/L
Tryptone	12 g/L
Glycerol	4 g/L

TB-1 was prepared by combining the ingredients in a final volume to 900 ml with MilliQ water and then autoclaved.

TB-2:

KH ₂ PO ₄	2.3 g
K ₂ HPO ₄	16.4 g

TB-2 was prepared by combining the ingredients in a final volume to 100 ml with MilliQ water and then autoclave. To prepare TB, mix 900 ml of TB-A with 100 ml of TB-2.

10X SDS running buffer

30.0 g of Tris base, 144.0 g of glycine, and 10.0 g of SDS were dissolved in 1000 ml of H₂O. pH adjustment was not required. The running buffer was stored at room temperature and diluted to 1X by adding 100 ml buffer to 900 ml MilliQ water before use.

Tris-Cl buffer

Tris-Cl buffer was added to MilliQ water and dissolved completely. The pH was adjusted with HCl. The final volume was adjusted with MilliQ water. The buffer was autoclaved and kept at room temperature.

Acrylamide/bisacrylamide solution

29 g acrylamide was added with 1 g of bisacrylamide and dissolved in the amber color bottle. The final volume was adjusted with MilliQ water, and the bottle was kept at 4°C.

Ammonium persulfate solution

0.1 g of ammonium persulfate powder was added to 1ml of MilliQ water and dissolved completely. It was wrapped in aluminum foil and stored at 4°C.

10% SDS solution

10 g of sodium dodecyl sulfate was added to 80 ml water and vortex. The final volume was adjusted to 100 ml with MilliQ water and stored at room temperature.

50x TAE (Tris acetate (EDTA) buffer

Reagent	Weight/Volume	Final concentration
Tris base	242 g	2 M
Glacial acetic acid	57.1 ml	1 M
0.5 M EDTA, pH 8.0	100 ml	0.05 M
MilliQ water	Up to 1 L.	

1X TAE was prepared from it by adding 20 ml TAE buffer to 980 ml MilliQ water.

SDS PAGE staining and destaining solution

2.5 g of Coomassie Brilliant Blue R-250 was added in 900 ml of methanol: H₂O (50:40, v/v) and 100 ml of glacial acetic acid. The solution was filtered through a Whatman No. 1 filter to remove any particulate matter.

Destaining solution: methanol (40% [v/v]), glacial acetic acid (10% [v/v]), and H₂O (50%).

Ponceau S stain

To 47.5 ml water, 2.5 ml glacial acetic acid was added. To this, 0.5 g Ponceau S powder was added and dissolved by mixing.

SDS-PAGE gel preparation

First separation gel (10%) solution was prepared by mixing the components in the following order. Volume shown here is for one 1 mm SDS-PAGE gel and was accordingly scaled up if needed.

H ₂ O	1.9 ml
Acrylamide/bis (30%)	1.7 ml
Tris-HCl (1.5 M, pH 8.8)	1.3 ml
SDS, 10%	50 µl
Ammonium persulfate (APS), 10%	50 µl
N,N,N',N'-tetramethylethylene-diamine (TEMED)	2 µl

1. After adding TEMED and APS to the SDS-PAGE separation gel solution, the gel will polymerize quickly, so add these two reagents when ready to pour.
2. The solution was poured, and ~2 cm space was left below the bottom of the comb for the stacking gel. Care was taken to remove bubbles.

3. The top of the gel was layered with isopropanol. This helped remove the air bubbles at the top of the gel and kept the polymerized gel from drying out. In about 30 min, the gel completely polymerized.
4. The isopropanol was removed.
5. The stacking gel (4%) was prepared by mixing reagents in the following order:

H ₂ O	0.68 ml
Acrylamide/bis (30%)	0.17 ml
Tris-HCl (1M, pH 6.8)	0.13 ml
SDS, 10%	10 μ l
Ammonium persulfate (APS), 10%	10 μ l
TEMED	1 μ l
6. The stacking gel was poured on top of the separation gel.
7. 10 well combs were inserted to make wells. After 20 min the gel was removed from the clamp and kept at 4°C until used.

2.3. Methods

2.3.1. Recharging Ni-NTA (Nickel Nitrilo Triacetic acid) beads

1. Wash Ni-NTA beads were washed in 6 column volumes of MilliQ water.
2. Beads were washed in ~4 column volumes of strip buffer.
Strip buffer
20 mM Tris, pH 8.0
100 mM EDTA,
500 mM NaCl,
3. The Beads turned white. Beads were washed in MilliQ water.
4. The beads were washed in ~6 column volumes of recharge buffer (100 mM NiSO₄).
5. Beads were then washed in MilliQ water.
6. Beads were then equilibrated in the lysis buffer.
7. For long-term storage, the beads were added with 20% ethanol and stored at 4°C.

2.3.2. Cell lysis

1. Aag2 and U4.4 cells were washed with PBS in the tissue culture flask by adding cold PBS and gently rocking. The step was repeated one more time.
2. The cells were scraped from the flask and centrifuged at 200 g for 5 min.
3. The appropriate volume of ice-cold lysis buffer (with fresh protease inhibitors) was added. The vial was incubated for 30 min on ice, with gentle vortexing after 10 min.
4. The lysate was clarified to remove debris by spinning for 20 min at 12,000 g, at 4°C.
5. The supernatant was transferred to a fresh tube and stored on ice or frozen at -20°C or -80°.

2.3.3. Protein estimation

The cell lysate was kept on ice while working. Protein was estimated using Pierce™ BCA Protein assay kit. The manufacturer's protocol was followed. Briefly, the solution was prepared by mixing 10 µl of reagent B to 500 µl of reagent A and were mixed vigorously. To each well of 96 well plates, 5 µl of each sample was added in triplicate, and 200 µl of the freshly prepared BCA solution was added in each well. The plate was kept for 30 min in the dark. The plate was then taken for spectrophotometric plate reader, and 560 nm wavelength was set for detection. The absorbance was then plotted on BSA standard plots, and the final concentration was calculated.

2.3.4. SDS-PAGE (Sodium Dodecyl Sulfate-Poly Acrylamide Gel Electrophoresis) and transfer

1. Samples were mixed with SDS-PAGE loading buffer and heated to 95°C for 5 min.
2. 20-30 µg samples per lane were loaded along with a protein ladder.
3. The gel was run at 80 V for 10 min and then at 100 V till the front running dye come out from the other end, or desired separation of bands was achieved.
4. The proteins were then transferred from gel to nitrocellulose membrane at 50 V for 1 h. The membrane was checked for transfer by placing it in Ponceau S solution for 1 min and then washing the membrane with MilliQ water till a non-specific stain was washed.

2.3.5. Western blotting

1. The nitrocellulose membrane was put into a blocking solution (PBS+5% Bovine serum albumin) at 1 h at RT (room temperature). Care should be taken to use sufficient volume to keep the blot fully covered, with gentle agitation throughout.
2. The membrane was rinsed briefly in PBS.
3. It was incubated with primary antibody diluted in PBS+2.5% BSA overnight at 4°C, or for 1 h at RT.
4. The membrane was washed in PBST (0.1% tween-20) (3x10 minutes) with gentle agitation to remove a non-specific bound antibody.
5. Appropriate antibody (anti-rabbit IgG-HRP for rabbit primary antibody and anti-mice IgG-HRP for mice primary antibody) PBST+2.5% BSA was used and incubated for 1 h at RT with gentle agitation in a sufficient volume to ensure coverage.
6. The membrane was rinsed with PBST (0.1% Tween-20) for 3X10 min. The membrane was kept in PBS.
7. The membrane was transferred to the appropriate enzyme substrate solution chemiluminescent substrate and incubated for the time period recommended by the manufacturer to visualize protein bands via Bio-rad ChemiDoc MP.

2.3.6. Protocol for the thawing frozen cells

1. The cryovial containing the frozen cells was removed from liquid nitrogen storage and immediately placed into a 37°C water bath.
2. Quickly thaw the cells were quickly thawed in the 37°C water bath.
3. The vial was transferred into the laminar flow hood and wiped with ethanol from outside.
4. The cell was transferred in the 10 ml pre-warmed complete growth medium into the centrifuge tube.
5. The cells were centrifuged at approximately 200 g for 5 min.
6. After the centrifugation, the supernatant was aseptically decanted without disturbing the cell pellet.
7. Cells were re-suspended in a complete growth medium, transferred into a T-25 flask, and shifted into the incubator.

2.3.7. DEPC treatment of plastic wares for RNA work

1. 1 ml Diethylpyrocarbonate (DEPC) (0.1%) was added to 1000 ml Distilled Water
2. The solution was mixed, and microfuge tubes were added to it and allowed to sit at room temperature overnight.
3. It was autoclaved, and water was discarded.
4. The tubes were allowed to cool at room temperature before use.

For RNA work, the water was also treated with DEPC to make it RNase-free.

2.3.8. RNA isolation from mosquitoes

4-6 freshly collected uninfected or CHIKV infected *Ae. aegypti* mosquitoes were pooled into microfuge tube (DEPC treated) and were added with 1 ml Trizol solution. The mosquito was crushed using a plastic pestle for 1-2 min. The tube was centrifuged at 12,000 g for 10 min at 4°C. The upper part having pink-colored solution was removed and transferred into a fresh microfuge tube. The tube was then added with 200 µl chloroform and vortexed vigorously for 15 s. The tube was then left at RT. The tube was then centrifuged at 12,000 g for 10 min at 4°C. The upper transparent layer was carefully transferred to a new tube without disturbing the interface and preferably leaving some part of the transparent layer to avoid mixing during pipetting. The transparent portion was added with 500 µl of isopropanol. The tube was inverted a few times for mixing and then kept for 10 min at RT. The tube was then centrifuged at 12,000 g. The supernatant was discarded, and the pellet was air-dried. The pellet was dissolved in 50 µl DEPC treated autoclaved distilled water. The total RNA was quantified with a Nanodrop spectrophotometer instrument.

2.3.9. Reverse Transcription Polymerase Chain Reaction (RT-PCR)

A one-step RT-PCR kit was used to convert RNA to cDNA and then double-stranded DNA. The ingredients and protocol are shown below:

Components	Volume (µl) needed for 50 µl reaction
2X 1 step buffer	25
PrimeScript 1 step Enzyme Mix	2
Total RNA 1µg RNA	X µl
Forward primer (10 µM)	2
Reverse primer (10 µM)	2
RNase free Water	To make volume to 50 µl

PCR conditions:

50°C	30 min	cDNA synthesis	
94°C	2 min		
↓↓			
94°C	30 s.		
55 -65°C	30 s	Primer annealing	} 40 cycles
72°C	1 min/kb	Extension	
72°C	10 min	Final extension	
4°C		Storage	

2.3.10. Agarose gel electrophoresis and gel extraction

The PCR product was mixed with 6X DNA loading dye. The product was run along with 1kb DNA ladder on 1% agarose gel at 100 V for 40 min. After that, the gel was visualized in a UV trans-illuminator, and desired bands were cut and transferred to the microfuge tube. The gel piece was added with Binding buffer SET. The vial was heated at 55°C till the gel piece was dissolved. The solution containing dissolved gel, PCR product, and binding buffer were transferred to the binding column and centrifuged at 10,000 g for 1 min. The flow-through was discarded, and the column was washed by adding 600 µl Wash solution and then centrifuging for 1 min at 10,000 g. The flow-through was discarded, and then the column was run empty for 2 min to remove residual ethanol. The collection tube was discarded, and fresh microfuge was taken, and the column was put in a fresh microfuge tube. 20-30 µl DNase free water was added to the column, and it was centrifuged at 12000 g for 1 min. The eluted DNA concentration was measured with a Nanodrop spectrophotometer.

2.3.11. Plasmid isolation and gene cloning

For the plasmid isolation, the respective bacterial cultures were incubated at 37° C at 150 rpm with respective antibiotics (Kanamycin 50 µg/ml and ampicillin 100 µg/ml). The next day, the culture was pelleted at 2500 g for 10 min. The supernatant was discarded, and to the bacterial cell, 200 µl resuspension buffer was added. The pellet was suspended in it, and 300 µl lysis buffer was added. To the mix, 400 µl neutralization buffer was added. The mixture turned white from transparent. Centrifuge the mixture at 10,000 g for 10 min. The transparent supernatant was transferred into a filter column with a collection tube. The tube was centrifuged at

10,000 g for 1 min. The flow-through was discarded, and 600 μ l Wash buffer 1 was added. The tube was centrifuged at 10,000 g for 1 min. The flow-through was discarded, and the column was added with 600 μ l Wash solution 4. The tube was centrifuged at 10,000 g for 1 min. The flow-through was discarded, and the tube was run in centrifuged for 2 min to remove residual ethanol. The column was added with 30 μ l of DNase-free water. The tube was centrifuged for 1 min at 10,000 g. The eluted plasmid concentration was measured by a nanodrop spectrophotometer. The samples were also checked for 260/280 and 230/260 ratios of 1.8 and 2.0, respectively, indicating the quality of the DNA sample.

The purified plasmid and eluted PCR products were used for restriction digestion. Briefly, around 1.5 μ g plasmid and 500-800 ng of PCR product were used for digestion separately as mentioned below:

Components	Volume (μl) needed for 20 μl reaction
10X Cut smart buffer	2
Restriction enzyme 1	1
Restriction enzyme 2	1
Plasmid 1.5 μ g/ PCR product	X μ l
DNase free water	To make volume to 20 μ l

The digestion reaction was set up for 30 min and then run on the agarose gel. The gel was visualized in a UV transilluminator. The desired bands were cut and transferred into fresh microfuge tubes. The binding buffer was added at approximately 3X value, i.e., 600 μ l binding buffer for 200 μ g agarose gel piece. The DNA was eluted by the protocol as mentioned in section 2.2.3. The eluted DNA was quantified, and then overnight ligation reaction was set up as follows:

Components	Volume (μl) needed for 20 μl reaction
10X ligation buffer	2
Restricted vector DNA	~60 ng
Restricted insert DNA	~180 ng
T4 DNA ligase enzyme	0.4 μ l
DNase free water	To make volume to 20 μ l

After the addition of components, a short spin was given to the tube. The tube was kept in a cold room overnight. The next day the ligation product was transformed into *E. coli* DH5 α competent cells.

2.3.12. *Escherichia coli* competent cell preparation

Competent cells were prepared using the CaCl₂ method. For this, *E. coli* cells were grown in Luria Bertani (LB) broth tubes (10 ml each) from the culture at 37° C at 150 rpm (rotation per minute). The next day morning, 1% of the grown culture was used as secondary culture, i.e., 1 ml culture in 100 ml LB broth culture in 1000 ml capacity flask for proper aeration. The culture was allowed to grow for 3-4 hours (h) till optical density (OD) reached around 0.4 at 600 nm in UV-Vis spectrophotometer. When the desired OD was reached, the flask was kept on ice to cool the temperature of the media. The culture was pelleted at 2700 g at 4°C for 10 min. The supernatant was discarded, and to the pellet, 30 ml per 50 ml culture of ice-cold solution of 80 mM CaCl₂ and 20 mM MgCl₂ was added, and the pellet was dissolved with the help of pipetting. The culture was centrifuged at 2700 g at 4°C for 10 min. The supernatant was discarded, and tubes were kept in an inverted position for 1 min to remove traces of supernatant. The pellet was dissolved in 2 ml of 100 mM CaCl₂ and 20 % glycerol. The suspension was aliquoted as 50 μ l in 1.5 ml microfuge tubes and kept at -70°C.

2.3.13. Transformation

Before proceeding for transformation, LB agar plates with respective antibiotics were prepared. For that, 2.5 g LB broth and 1.5 g agar/100 ml water were mixed and autoclaved. The autoclaved LB agar was allowed to cool to around 45°C, and the respective antibiotics at desired concentration were added. The media was poured into 100 mm sterile Petri plates in the biosafety laminar hood and allowed to solidify.

The aliquot of competent cells was transferred to ice. 5 μ l ligation mixture/40 ng pure plasmid was added to the aliquot. It was kept on ice for 20 min. After incubation, heat shock at 42°C was given for 90 s. The vial was immediately transferred to ice. After 2 min, 1 ml LB media was added to the tube, and the tube was shifted to incubator cum shaker at 37°C with 150 rpm for one h. After the incubation, the tube was centrifuged at 2500 g for 3 min. The supernatant was discarded and left with around 200 μ l media and was spread plated onto LB agar plate having respected antibiotic. The plate was then incubated at 37°C incubator for overnight growth. The next day the colonies

were observed. The plates were kept at 4-8°C refrigerators, and in the evening, 2-4 colonies were picked and added to a glass tube having 10 ml LB media and respective antibiotics. The tubes were shifted to incubator cum shaker at 37°C with 150 rpm for overnight growth. The next morning, plasmids were isolated and checked for the desired insert by doing restriction digestion with respective restriction enzymes and running on 1% agarose gel. The gel was first visualized in a UV trans-illuminator and then imaged in a gel documentation system. The glycerol stocks were prepared for the same insert positive colonies by adding glycerol at 20% final concentration in the cryovial and stored at -70° C.

2.3.14. Protein purification

The plasmids were transformed into *E. coli* BL21-CodonPlus cells. For protein purification, the Cryo stock of cells was added with antibiotic to the glass tube having 10 ml LB media. The bacterial cultures were incubated at 37°C at 150 rpm with respective antibiotics (Kanamycin 50 µg/ml and ampicillin 100 µg/ml). The next day, the culture was transferred to large volume LB broth at 1% final volume. The culture was allowed to grow at 37°C at 150 rpm with respective antibiotics for 3-8 h till OD 0.6 in case of LB media or 2.0 in base to TB media. The culture was then transferred to 18°C and then induced with IPTG for around 16 h. The culture was then centrifuged at 4000 g for 30 min at 4°C in centrifuge bottles. The culture pellet was either stored at -70°C or directly lysed in lysis buffer having 1mM PMSF and lysozyme. The suspension was incubated in ice for 3 min for lysis. After sonication, the suspension was centrifuged at 12000 g for 30 min. The supernatant of the lysates was transferred to a fresh bottle/tube. If the protein was insoluble, then to the pellet, 8 M Urea solution was added and kept at 37° C at 150 rpm for 1 h. The solution was centrifuged at 12000 g for 30 min. The solution of both lysis buffer or urea solution was transferred to a fresh bottle/tube loaded onto an affinity column (Ni-NTA) and washed with lysis buffer containing 20 mM Imidazole. Proteins were eluted with a lysis buffer having 300 mM imidazole. The elution fraction was confirmed with SDS-PAGE and Western blot for proteins. The eluted fractions containing purified CHIKV-nsP3 and RM62F protein were confirmed by Western blot and concentrated.

2.3.15. Chikungunya virus propagation

The chikungunya virus isolated from patient serum (Shrinet et al., 2012) was propagated in Vero cells in a T-175 flask. The supernatant was collected from the flask and centrifuged at 13000 rpm for 1h at 4°C to remove any debris. The supernatant was then kept on ice, and aliquots were made. The viral titer was quantified using plaque assay. The virus was alternatively grown in C6/36 cells and Vero cells to maintain its pathogenicity.

2.3.16. Virus infection

Ae. aegypti (Aag2) cells were grown in tissue culture plates in complete L-15 media. Cells were infected with CHIKV strain at the desired multiplicity of infection (MOI). The virus was diluted in FBS and antibiotic-free L-15 media, and cells were incubated at 28°C. After 2 hours post-infection (hpi), cells were washed with phosphate-buffered saline (PBS) (pH 7.4) and grown in complete L-15 media. The cells and media were collected at different time points, and cell pellets were washed once with PBS and either resuspended in TRIzol for RNA isolation or lysis buffer for western blot.

2.3.17. Plaque assay

CHIKV was quantified with plaque assay using a previously described protocol (Sirisena et al., 2018). Briefly, Vero cells were seeded in a 96-well plate in DMEM with 10% FBS. Supernatant media collected of MOI of 0.1, 1, and 10 at different time points from CHIKV infected Aag2 cells was added at different dilutions and incubated for 1h. After the incubation, viruses containing media were removed from the wells and covered with 1% carboxymethylcellulose (CMC) in FBS-free media. Cells were incubated for 48 h at 37 °C. Post washing with PBS, cells were fixed with 4% formaldehyde and stained with 0.25% crystal violet in 30% methanol. Virus titer in infected cells was calculated by plaque-forming units (pfu) = (No. of plaques)/(Dilution × volume of the virus).

2.3.18. Quantitative real-time PCR

Expression profiles of RNAi factors and CHIKV genes were performed from infected cells from different time points. The sequences of RNAi factors were retrieved from ImmunoDB, and the CHIKV-nsP3 sequence was taken from CHIKV/IND/DEL/01 strain (Accession no. JF950631.1) (Shrinet et al., 2012). Primers for qPCR were made

using the Prime Quest tool of Integrated DNA Technologies (IDT) with amplicon lengths ranging from 90-110 nucleotides.

Primer names	Forward Primer	Reverse Primer
Ago-2	TACCCGGCTCCAACCTATTA	CTGCATTCTCTCGTACTCCTTG
Dicer-2	TTGCTACCGTTGGGAGTTATG	GTGACAGTCGAAGGGTTGAATA
RM62F	GACCACAGGTTTCGGATTT	CAACGACGCAAGTTGGTAATG
RPS17	GTGAGCGCAGAGACAACACTAC	TCCAGCTGCTTCAACATCTC
TSN	CACTGTGGTGGAAAGTGTTC	GCCTCACGTGGAGGTTTAAT
VIG	GCCGAAAGACGCCAGATTA	CGTTTGTTCCTACTCTGTGATT
R2D2	GACGAATTGCTCTGGACGAA	CGCTGTTGTCTCGTTTCATTTTC
FMR1	AGAGCTGAACAGTGTTGATAGG	CTGGACATTTCCGTTGGATTG
CHIKV-E1	TACCCATTTATGTGGGGC	GCCTTTGTACACCACGATT
CHIKV-nsP3	AAGGCGCACTGTACTCATATC	TAGGCAGACTTGCTCATTGG

Total RNA was extracted from cells using Trizol and quantified with Nanodrop. We used 300 ng RNA per reaction. The qPCR was carried out using the Quantitect SYBR green one-step real-time PCR kit (Cat. no. 204243 Qiagen). The qPCR was done with the protocol as cDNA synthesis 50°C for 30 min, initial denaturation at 95°C for 2 min, followed by 40 cycles as denaturation at 95°C for 15 s, annealing at 56°C for 30 s and extension at 72°C for 30 s, data acquisition and followed by melt curve analysis. Expression values were normalized to RPS17 housekeeping control mRNA levels. Relative log-fold expression levels were calculated using the $2^{(-\Delta\Delta CT)}$ method (Schmittgen & Livak, 2008) and represented as mean \pm SD. Statistical analysis of experimental data was conducted using GraphPad Prism (version 6). Two-tailed student's t-test and Fisher's Least Significant Difference (LSD) test were performed to check the significance of the data, and p-values < 0.001 were considered significant.

2.3.19. Antibody generation

Antibodies against proteins were raised in-house following 90 days protocol explained below in detail. Briefly, Purified CHIKV-nsP3 and RM62F proteins were injected into rabbit (500 µg /animal) and mice (100 µg/animal) with Freund's complete adjuvant. Booster doses of respective proteins with Freund's incomplete adjuvant were given in regular intervals, and serum was collected at specific times. Antibody specificity was checked against purified protein and later against cell lysate to confirm the reactivity.

Dose	Protocol day	Description
Pre-bleed collection	Day 0	Pre immune blood 200 µl for mice and 4 ml for rabbit
First injection	Day 1	Immune with antigen incomplete Freund's adjuvant 100 µg/mice and 500 µg/rabbit
First booster	Day 21	Boost with 50 µg/mice and 250 µg/rabbit antigens in Incomplete Freund's adjuvant
Second booster	Day 42	Boost with 50 µg/mice and 250 µg/rabbit antigens in Incomplete Freund's adjuvant
First bleed	Day 50	300 µl blood collection from mice and 20 ml blood collection in the rabbit.
Third booster	Day 62	Boost with 50 µg/mice and 250 µg/rabbit antigen in Incomplete Freund's adjuvant
Second bleed	Day 70	300 µl blood collection from mice and 20 ml blood collection in the rabbit.
Third bleed	Day 80	300 µl blood collection from mice and 20 ml blood collection in the rabbit.
Fourth bleed	Day 90	Final blood collection and animal termination.

After the collection of blood, the tubes were kept in a tilted position for 30 min at RT to allow the blood to clot. Then tubes were centrifuged at 2000 g. The serum was transferred to fresh vials having 0.02% sodium azide and stored at -70°C for future use.

2.3.20. Immunofluorescence assay

Cells seeded at 30–40% confluence in 6-cm/6 well culture plate containing round cover glasses. After the transfection/infection, cells were fixed in 4% paraformaldehyde (PAF) for 20 min and permeabilized with PBS-T (0.05% Triton X-100 in PBS) for 20 min. The cells were then blocked for 30 min in PBS containing 5% BSA and incubated with primary antibody at dilution for 1 h/overnight in PBS containing 2.5% BSA. Cells were washed in PBS-T for 30 min (3 × 10 min) followed by incubation with secondary antibodies (1:400) in PBS-T containing 2.5% BSA for 1 h at RT. Cells were then washed in PBS-T for 30 min (3 × 10 min). Cells were then immersed in DAPI (1 µg/ml; Thermo Fisher Scientific) for nuclear staining, mounted with FluorSave, and viewed using an inverted confocal microscope with 40× or 100× oil-immersion objective lenses. Images were processed using NIS element software.

2.4. References

- Schmittgen, T. D., & Livak, K. J. (2008). Analyzing real-time PCR data by the comparative C(T) method. *Nat Protoc*, 3(6), 1101-1108. <https://doi.org/10.1038/nprot.2008.73>
- Shrinet, J., Jain, S., Sharma, A., Singh, S. S., Mathur, K., Rana, V., . . . Sunil, S. (2012). Genetic characterization of Chikungunya virus from New Delhi reveal emergence of a new molecular signature in Indian isolates. *Virol J*, 9, 100. <https://doi.org/10.1186/1743-422X-9-100>
- Sirisena, P., Kumar, A., & Sunil, S. (2018). Evaluation of *Aedes aegypti* (Diptera: Culicidae) Life Table Attributes Upon Chikungunya Virus Replication Reveals Impact on Egg-Laying Pathways. *J Med Entomol*, 55(6), 1580-1587. <https://doi.org/10.1093/jme/tjy097>

Chapter 3

Chapter 3

Impact of CHIKV on the proteome of *Aedes albopictus* (U4.4) cells

3.1. Introduction

For the last few centuries, several epidemics, pandemics, and outbreaks of different viruses have been reported, and incidences of different viruses such as dengue, hepatitis, HIV, chikungunya, influenza, or recent coronavirus, etc., have significantly impacted the health of the human population (Chen et al., 2020; Parvez & Parveen, 2017). These have resulted in medical complications in millions of people. This leads to a massive loss to society in terms of economic and individual levels. In the last century, extensive research in virology, anti-viral therapies, and immunology gave hopes for the treatment of several viruses such as HIV, hepatitis, influenza (De Clercq, 2002; De Clercq & Li, 2016; Mohammadi Pour et al., 2019). The regular outbreaks of the vector-borne virus, e.g., Chikungunya virus (CHIKV) in Asia, Africa, and Europe, are a serious concern. Chikungunya is a single stranded (ss) positive sense (+) RNA virus from alphavirus genus and *Togaviridae* family. It is spread through bites of mosquitoes during blood meals. The virus is arthritogenic, and symptoms include fever, rashes, joint pain (Gould et al., 2010; Suhrbier et al., 2012). Viruses are known to accumulate new mutations due to the absence of proofreading ability in their polymerase. Most of the mutations have no impact on the virus fitness, but some are detrimental to the virus, and few are beneficial to it. This is becoming more concerning with new mutations in the viruses getting selected, favoring the fitness and spread of the virus (Duffy, 2018). The latest of them was CHIKV E1 A226V which increased the adaptability of the virus in the *Aedes albopictus* and cause of 2004 onwards outbreaks of the virus (Tsetsarkin et al., 2007).

Since different viruses affect the host differently, e.g., some cell lines allow persistent virus growth without showing a cytopathic effect. In contrast, some show cytopathic effects due to dependency of the particular cell type on other cells to synthesize and release cytokines to provide anti-viral immunity. This necessitates studying the impact of the virus on host cells (Abraham et al., 2013; Li et al., 2013). As earlier mentioned, the viruses use host cells to grow, and in that process, they try to take over the control of host cell machinery (Bosl et al., 2019; Nagy & Pogany, 2011). Traditionally it was difficult to study the global impact of the virus on the host,

various pathways, and processes. However, due to the development of sophisticated high throughputs technologies such as isotope labeling and label-free mass spectrometry, it is possible to study the global impact of the virus on host proteome and pathways, which play a crucial role in the protection of the host from the virus as well as promotion of virus survival (Abraham et al., 2015; Bojkova et al., 2020; Emmott et al., 2010; Trinh et al., 2013; Zhu et al., 2017). Recently few studies have shown the impact of virus infection on mosquitoes/cells using mass spectrometry (Cui et al., 2020; Vasconcellos et al., 2020).

This study was focused on to see the effect and response of *Ae. albopictus* cells (U4.4) upon CHIKV infection. First, viral kinetics was studied in U4.4 cells upon CHIKV infection at different time points using plaque assay and western blot analysis using house raised CHIKV E1 specific antibodies. The uninfected lysate was taken as a negative control to see any nonspecific binding. The time point infection study of CHIKV on U4.4 cells was done to pick early and late time points of infection to study global proteome response upon CHIKV infection in cells. Based on our initial data and available literature evidence, two time points were chosen: (early 12 hpi) and late (60 hpi). The statistically significant proteins were selected for further analysis, and pathway analysis highlighted pathways significantly up or downregulated.

3.2. Results

3.2.1. Cloning, expression, and antibody generation of CHIKV E1 protein

CHIKV glycoproteins are one of the well-studied proteins of the virus. Among them, envelope 1 (E1) protein is commonly used to study viral kinetics in cells. In this study, the primers were designed for the center region of the E1 gene (Figure 3.1A), and reverse transcription PCR was done to cloned into the pET29a vector (Figure 3.1B) with *KpnI* and *BamHI* restriction sites. The ligation mixture was transformed into *E. coli* DH5a cells. The positive cloned were then isolated and plasmid was isolated and checked for desired insert using restriction digestion. The CHIKV E1-pET29a plasmid was then cloned into *E. coli* BL21-CodonPlus cells and then grown in culture media and induced with 1 mM IPTG. The cells were lysed, and protein came as insoluble aggregate and was dissolved in 8 M urea. It was purified using an affinity chromatography column and buffer exchanged. The purified protein was run on SDS-PAGE gel and visualized through Coomassie staining, and western blot after

transferring the protein to nitrocellulose membrane and probing it with HRP conjugated anti-His antibody (Figure 3.1C). The purified and concentrated E1 protein was injected into four Balb/c mice for antibody generation after pre-bleed serum collection. The pre-bleed sera was checked for any background noise (Figure 3.1C right image) and showed no non-specific signal. The mice blood was collected for serum isolation at regular intervals as mentioned in materials and methods. The mice sera were tested for recombinant proteins and then tested against uninfected and CHIKV infected lysate of Vero cells (Figure 3.1D). Detailed protocols can be found in Chapter 2.

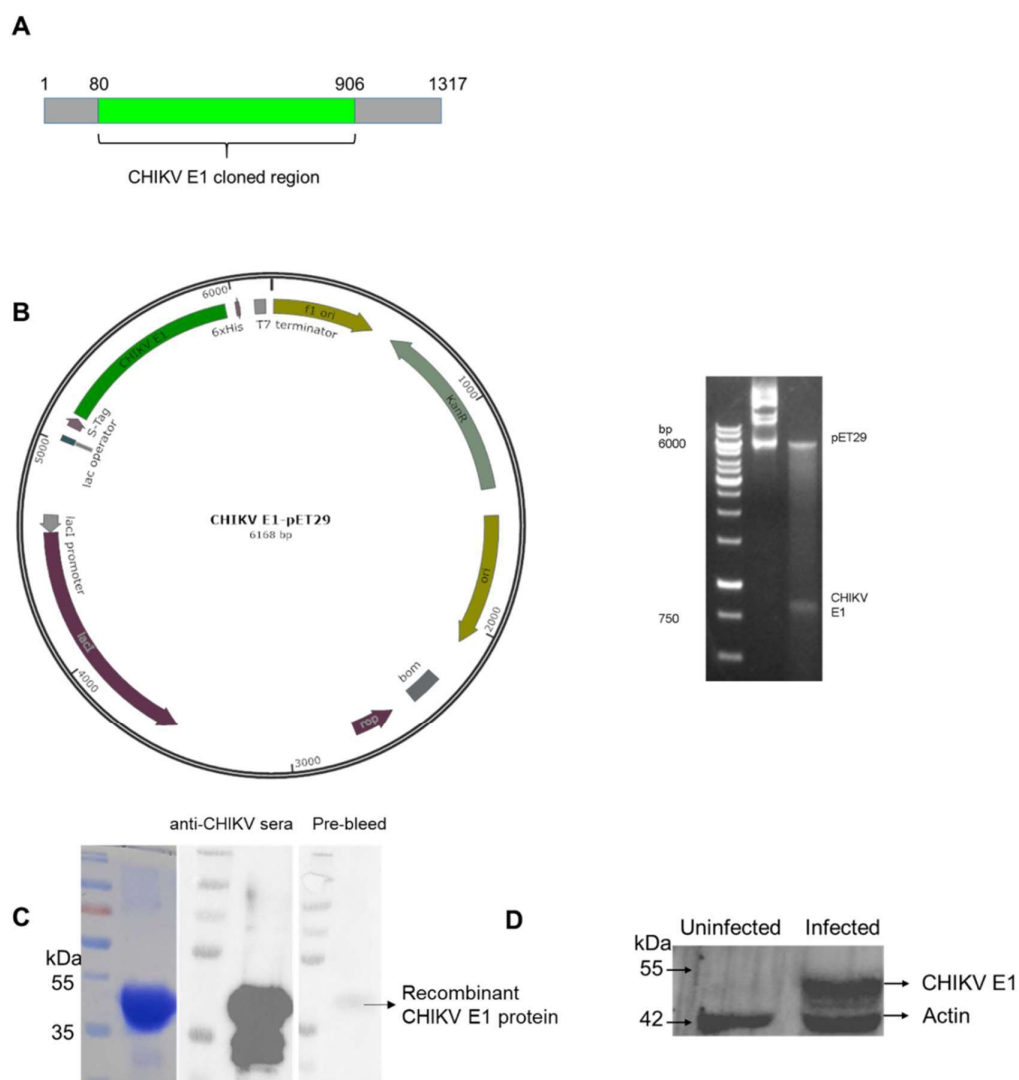


Figure 3.1 Cloning, expression, and antibody generation of CHIKV E1 protein. A) The internal region of CHIKV E1 gene was amplified using gene-specific primers

from CHIKV infected total RNA. The total E1 gene has length around 1.3 kb, but for recombinant protein generation, a 0.8 kb region was selected; B) The gene was cloned in pET29a plasmid as shown in map (left), and checked by restriction digestion, followed by separation of uncut and double digested product on agarose gel (right). The resulting clone have S-tag at N-terminal and His-tag at C-terminal; C) Coomassie-stained SDS-PAGE gel of purified CHIKV E1 protein after affinity chromatography (left image). Western blot of purified CHIKV E1 protein on nitrocellulose membrane probed with HRP conjugated anti-HIS antibody at dilution of 1:4000 (middle image), western blot of purified recombinant CHIKV E1 protein with mice pre-bleed sera (right image); and D) Western blot of uninfected and CHIKV infected Vero cells at MOI of 1 with mice raised anti-CHIKV E1 serum. The nitrocellulose membrane was incubated with anti-CHIKV E1 mice serum at 1:3000 dilution, and after washing, the membrane was probed with anti-mice HRP antibody at 1:6000 dilution. Actin antibody was used as a loading control at 1:4000 dilution.

The mouse raised anti-CHIKV E1 serum were then tested for native antigen detection using immunofluorescence assay of Vero cells. For this, Vero cells were infected with CHIKV at MOI of 1 for 12 h and 24 h. Cells were treated with reagents as mentioned in methods section. It was observed that in comparison to uninfected cells, there were few cells at 12 hpi which were showing green fluorescence (CHIKV E1 protein), while at 24 hpi, most of the cells were showing green fluorescence indicating the mice serum antibodies was binding specifically to the E1 protein of CHIKV in infected cells (Figure 3.2).

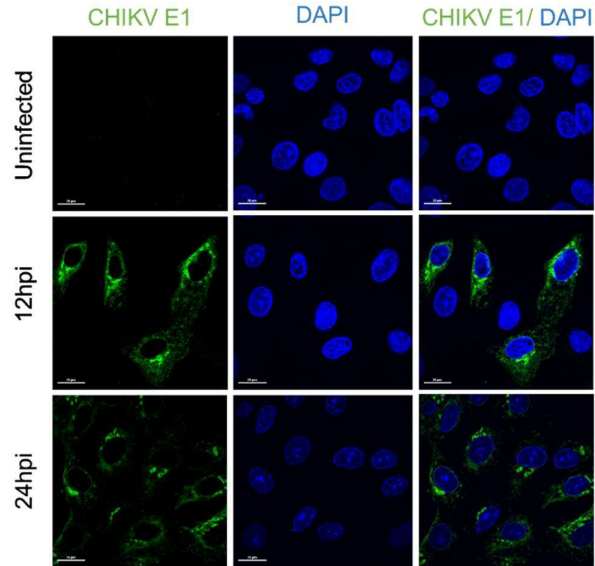


Figure 3.2 Immunofluorescence assay of CHIKV infected Vero cells. Vero cells were infected with CHIKV at MOI of 1 for 12 h and 24 h and then fixed and permeabilized. Cells were then incubated with anti-CHIKV E1 mice serum at 1:200 dilution and Alexa 488 labelled anti-mice antibody at 1:400 dilution. Cells were incubated with DAPI (1 μ g/ml) for 5 min and then visualized at 100X oil immersion (Scale bar=20 μ m).

3.2.2. Kinetics of CHIKV replication in U4.4 cells

After the protein purification and antibody generation and its validation were done, the next was to study the CHIKV viral kinetics in *Ae. albopictus* cells (U4.4). These cells have a functional RNAi system. Compared to humans, in *Aedes* cells such as Aag2 and U4.4, RNAi pathways are major anti-viral immune pathways (Blair, 2011; Goic et al., 2016; Varjak et al., 2018; Vodovar et al., 2012). U4.4. cells were infected at 1 MOI. The media and cells were collected at 12, 24, 36, 48, 60, 66 and 72 hpi. The media (representing extracellular titre) collected was used for viral titration via plaque assay whereas cells (representing intracellular viral titre) were lysed for the quantitation of CHIKV E1 proteins in these time points. The plaque assay of the time points showed that viral titre peaked from 12 hpi to 36 hpi and then lowered till 72 hpi (Figure 3.3A). Similar pattern was observed in the real time PCR of CHIKV E1 gene for the same the points (Figure 3.3B). In case of CHIKV E1 proteins quantitation, the expression of CHIKV E1 protein peaked at 60 hpi and then maintained (Figure 3.3C).

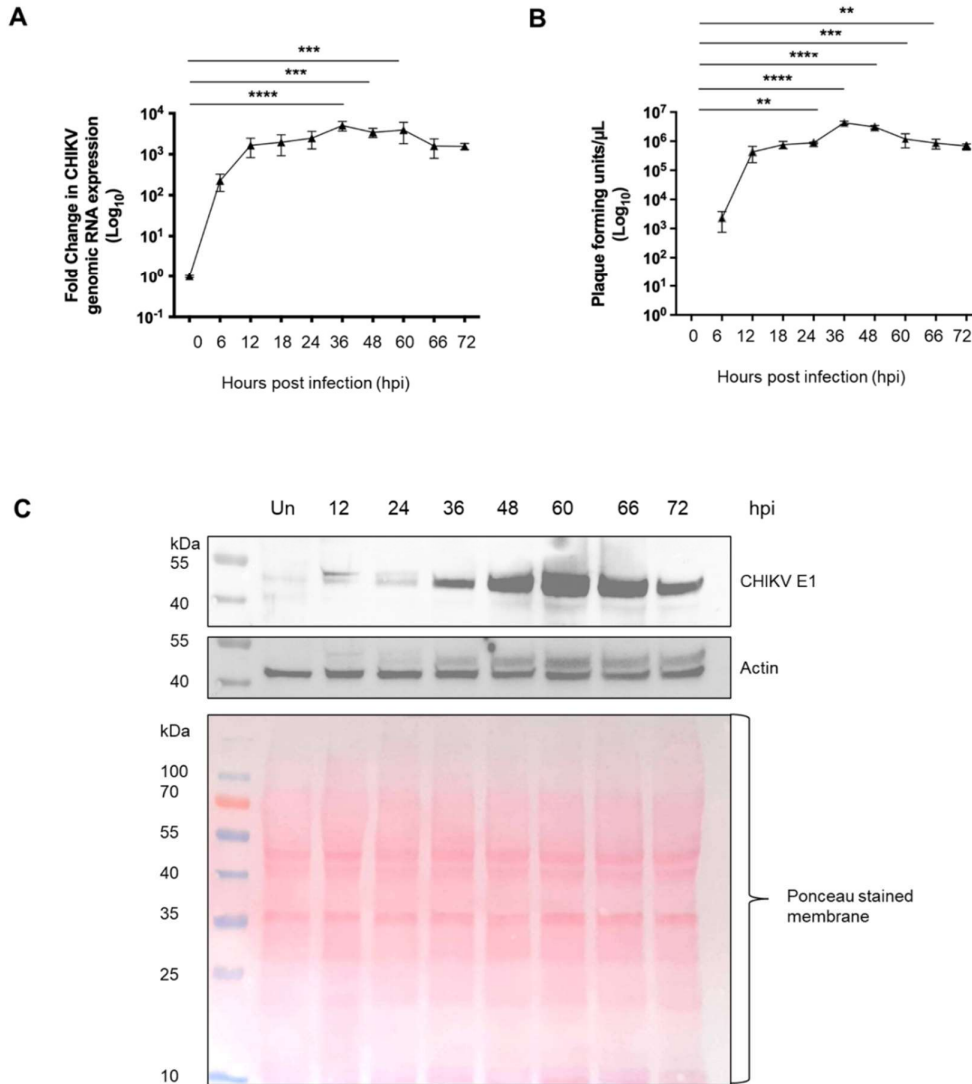


Figure 3.3 CHIKV kinetics in U4.4 cells. A) Plaque assay of different time points of CHIKV infection in U4.4 cells at MOI of 1, error bars represent SEM; real time PCR analysis of CHIKV E1 gene using gene specific primers for the CHIKV infected U4.4 cells; and C) Western blot expression profiling of different infection time points of CHIKV (E1) in U4.4 cells.

3.2.3. Global analysis of *Aedes* proteins during CHIKV infection time points

The next objective of the study was to study the global impact of CHIKV infection on U4.4 cell proteome during the course of infection. As mentioned in previous studies, that *Aedes sp.* have a fully functional RNAi system which helps it in controlling viral growth and avoiding cytopathic effect (Blair, 2011; Goic et al., 2016). From the

CHIKV plaque data and western blot data (Figure 3.3), it was clear that virus growth was visible at 12 hpi and could be an early infection time point to study the pathways which are modulated at 12 hpi. Also, from the same data, it was clear that at 1 MOI, virus growth was at the peak in 36 to 48 hpi and then was going down. To study the stress response as well as immune pathways having a role in protection against CHIKV, 60 hpi was chosen because, at that time, these pathways would be upregulated and had shown some cessation of the viral growth as visible from western data and plaque data.

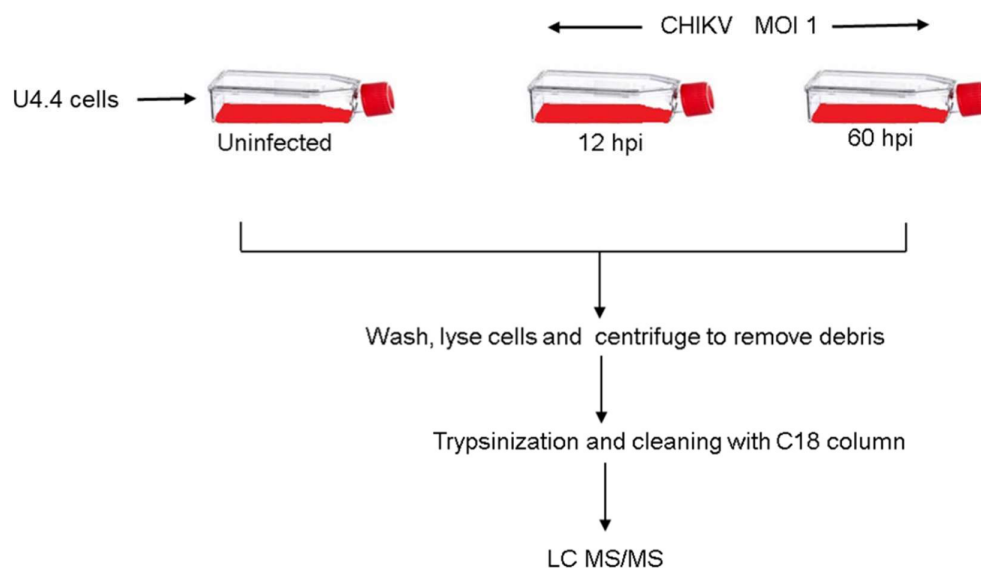
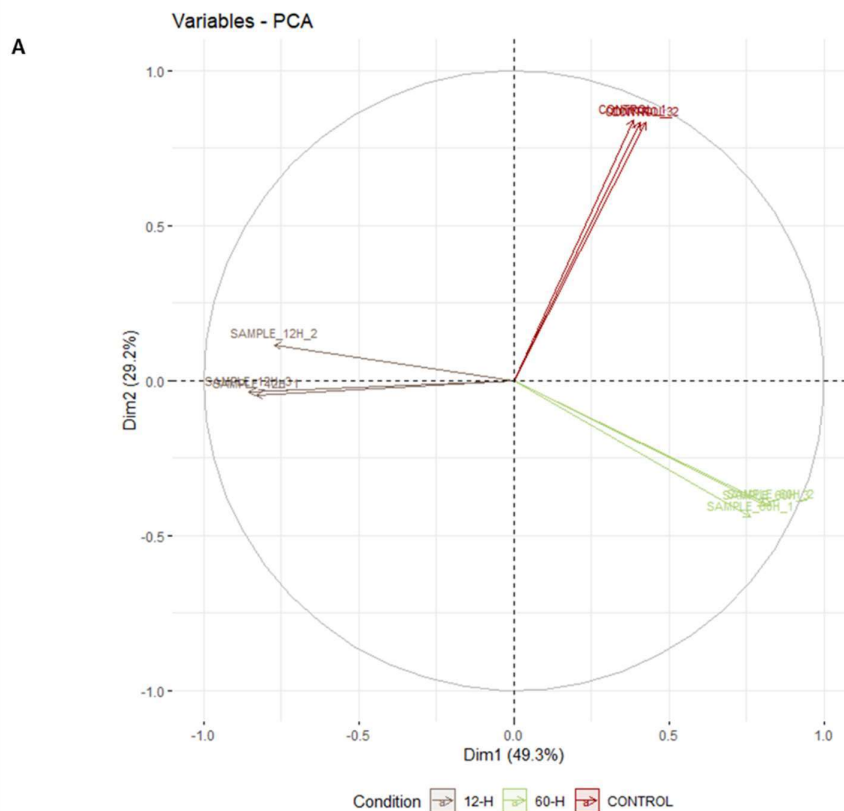


Figure 3.4 Schematic representation of workflow of mass-spectrometric analysis of U4.4 cells for proteome analysis upon CHIKV infection.

U4.4 cells were seeded in 9 T-25 flasks (2×10^6 cells/flask) and allowed to grow at 28°C with 5% CO_2 . Upon reaching 70% confluency, the cells were infected with CHIKV at MOI 1, following earlier protocol. Three times, the uninfected cells, 12 hpi cells, and 60 hpi cells were washed with ice-cold PBS. The cells were centrifuged at 100 g at 4°C for 5 min and then lysed with 1ml lysis buffer/plate for 15 min in ice. The lysate was centrifuged at 12000 g at 4°C for 15 min. The lysate was processed for mass-spectrometric analysis; detailed schematics have been shown in Figure 3.4 and the materials and methods section.

The quantitative analysis was with a label-free approach. Total 5203 proteins were found, which were present in at least 8 of 9 replicates. The principal component analysis (PCA) of the triplicate samples of untreated, 12 hpi and 60 hpi have shown that the triplicate samples are positively correlated (Figure 3.5A). The Z-score analysis, which shows standard deviation from means value, showed that triplicates variability was within the value of 2 to -2 (Figure 3.5B).



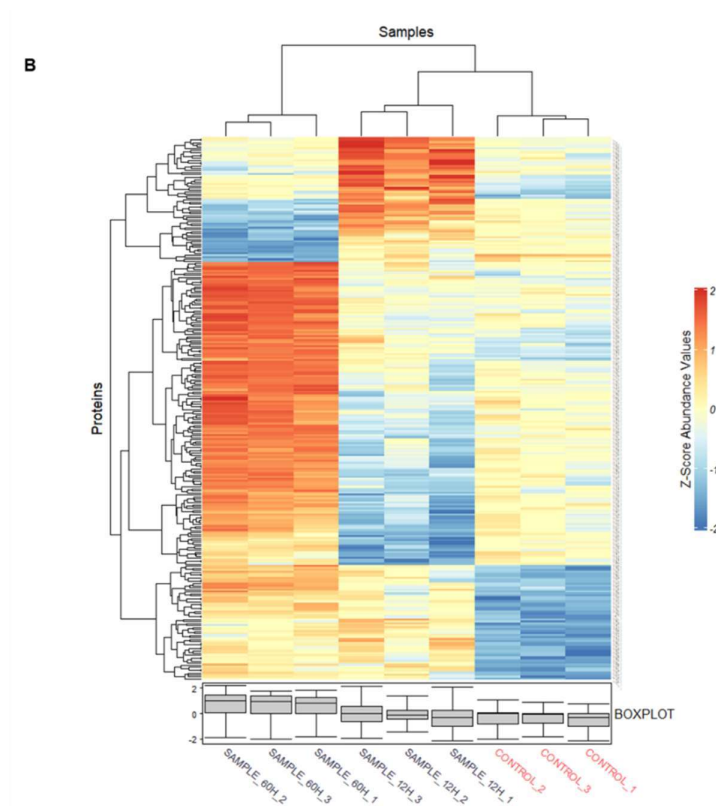
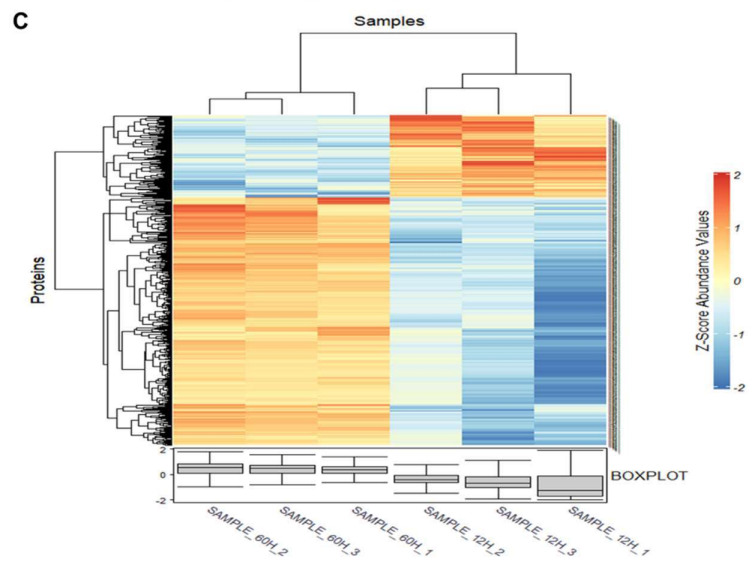
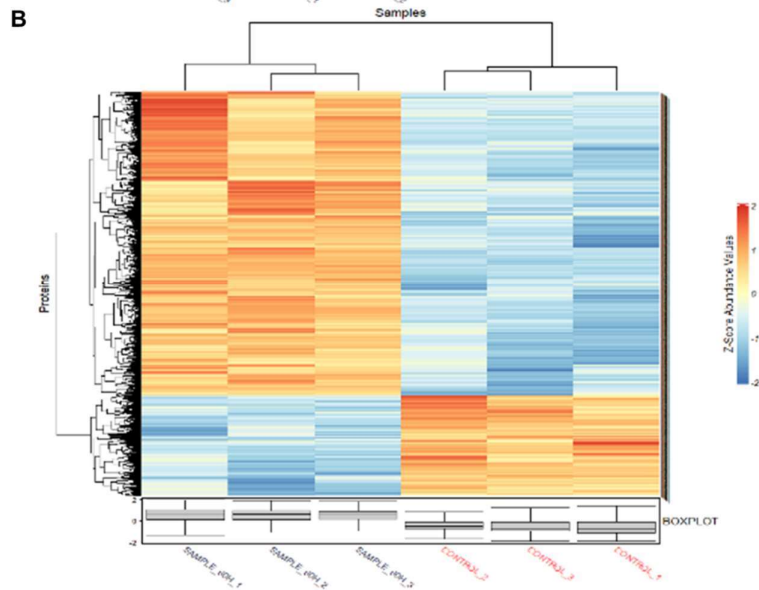
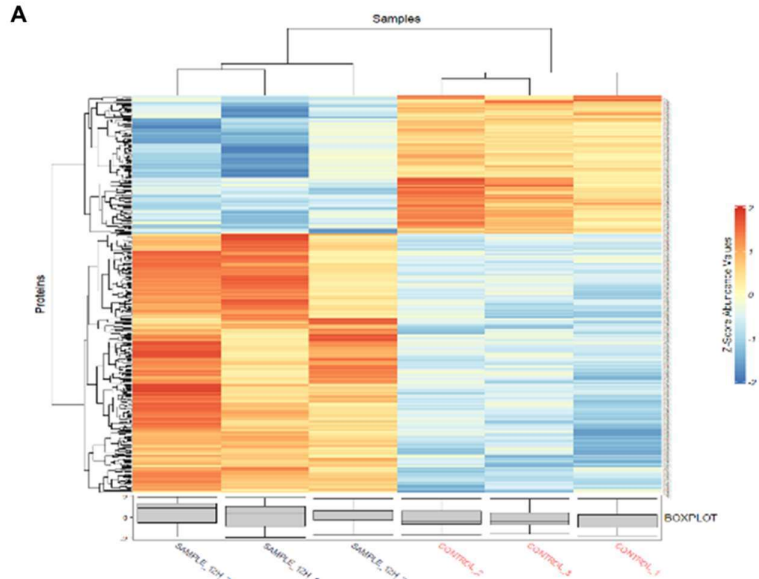


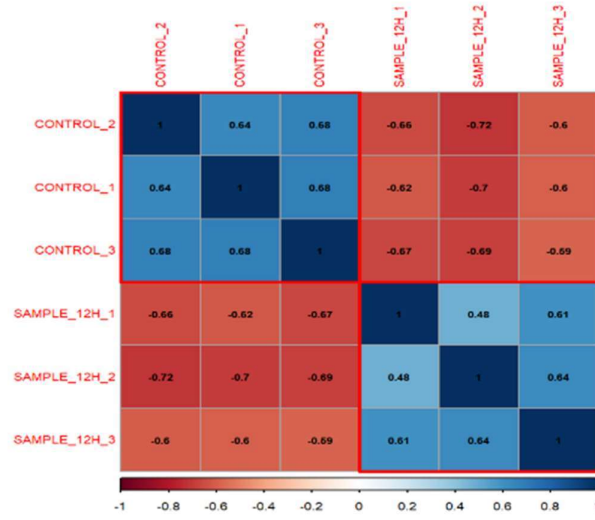
Figure 3.5 Analysis of the proteome of CHIKV infected U4.4 cells. A) Principal component analysis PCA of triplicate samples of uninfected, 12 hpi and 60 hpi U4.4 samples. B) Z-score analysis of triplicate samples of uninfected, 12 hpi, and 60 hpi CHIKV infected U4.4 cell lysate.

The comparison of 12 hpi and untreated, 60 hpi and untreated, and 60 hpi and 12 hpi have shown a similar trend in Z-score analysis. The correlation analysis has shown that triplicate samples of untreated, 12 hpi, and 60 hpi were positively correlated, whereas these different time points were negatively correlated among each other (Figure 3.6).

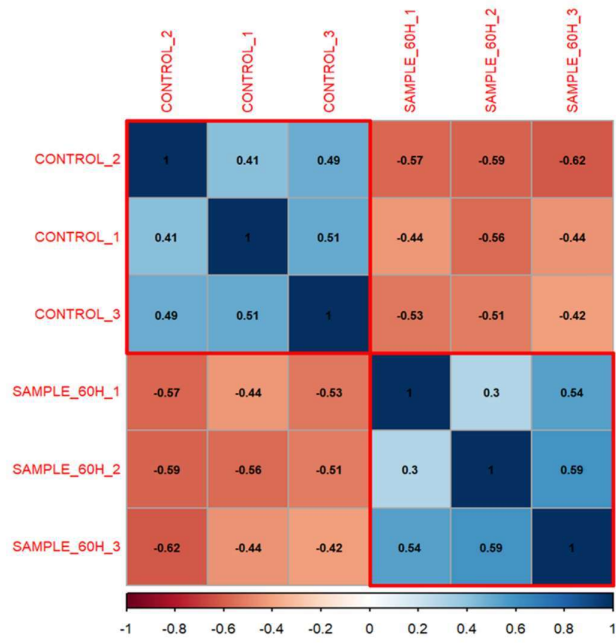
Next, the global level impact of CHIKV infection on U4.4 cells' proteome was evaluated. It was found that at 12 hpi, 195 proteins were upregulated and 134 proteins downregulated. At 60 hpi, 906 proteins were upregulated and 412 proteins were downregulated. The comparative analysis of 60 hpi with 12 hpi showed that 510 proteins were upregulated at 60 hpi as compared to 12 hpi while 152 proteins were downregulated at 60 hpi as compared to 12 hpi (Figure 3.7 and Supplementary information 1).



D



E



F

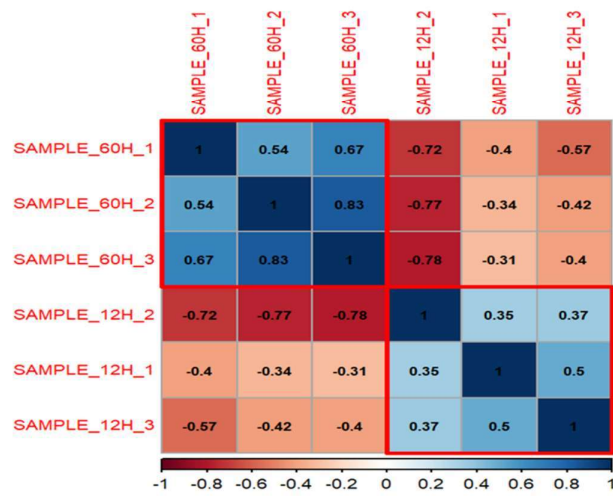


Figure 3.6 Comparison of global abundance of U4.4 cell proteins among triplicates. A) Heat map of global comparison of 12 hpi triplicates with control triplicates (uninfected), B) Heat map of global comparison of 60 hpi triplicates with control triplicates (uninfected); C) Heat map of global comparison of 60 hpi triplicate samples with 12 hpi triplicate samples; D) Correlation coefficient analysis of 12 hpi and control sample; E) Correlation coefficient analysis of 60 hpi and control sample, and F) Correlation coefficient analysis of 60 hpi and 12 hpi triplicate samples.

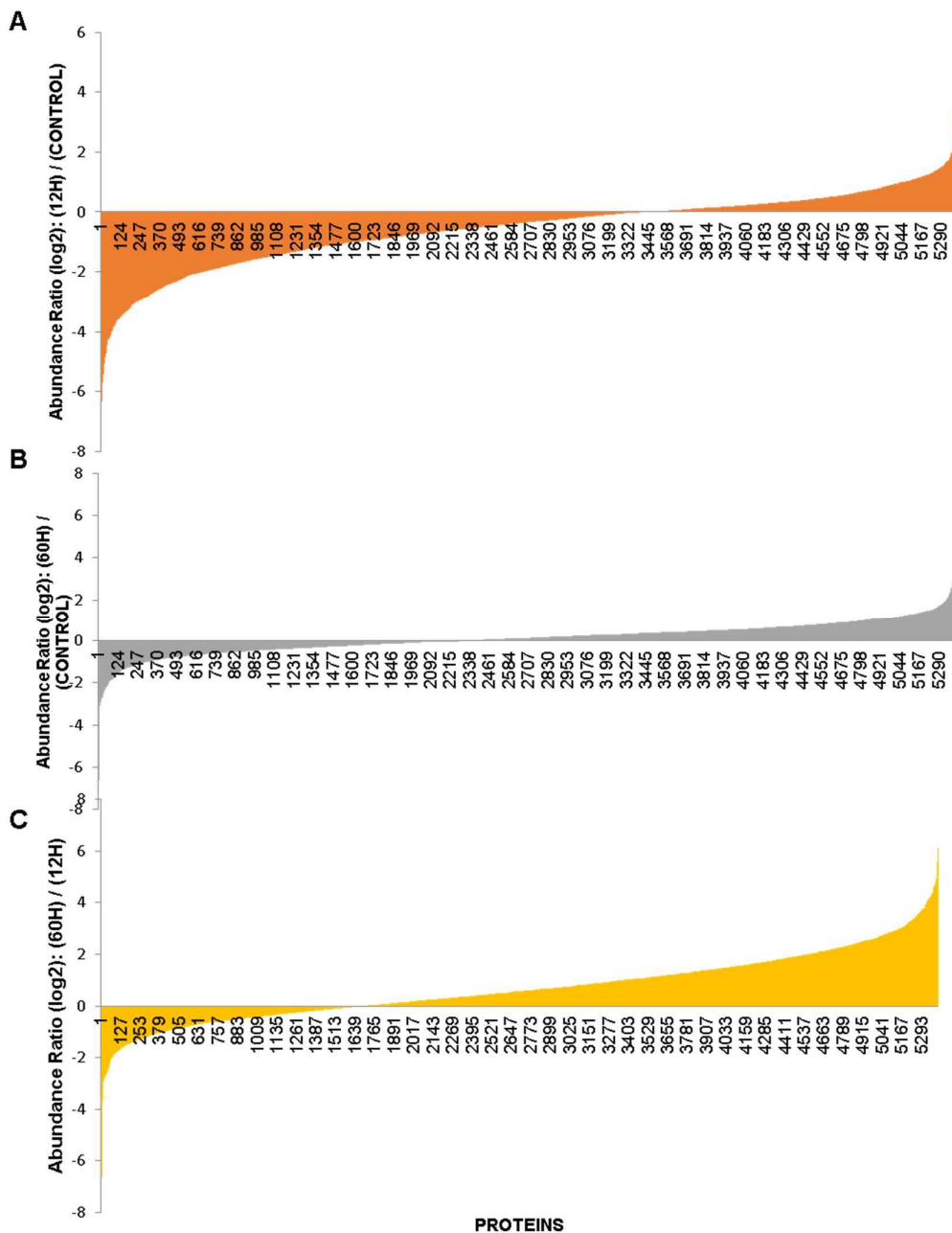


Figure 3.7 Comparison of abundance of U4.4 cell proteins at 12 hpi and 60 hpi. **A)** The log₂ abundance comparison of 12 hpi/untreated U4.4 cell proteins upon CHIKV infection, **B)** The log₂ abundance comparison of 60 hpi/untreated U4.4 cell proteins upon CHIKV infection, **C)** The log₂ abundance comparison of 60 hpi/ 12 hpi U4.4 cell proteins upon CHIKV infection.

3.2.4. Pathway analysis of U4.4 cell proteins during CHIKV infection

The CHIKV infection was found to upregulate as well as downregulate proteins in the initial as well as late infection time points. The pathway analysis reveal that at 12 hpi pathways such as **a) gene expression** AALF000803 (60S ribosomal protein L4), AALF002644 (40S ribosomal protein S2), AALF003471 (ribosomal protein L6), AALF006336 (60S ribosomal protein L9), AALF007059 (Putative 60S ribosomal protein L23), AALF010173 (RNA cytidine acetyltransferase), AALF016776 (DNA directed RNA polymerase), AALF026097 (FIP1 like 1 protein (Pre mRNA 3'-end processing factor) translation AALF011345 (ribosomal L23eN domain containing protein), AALF013833 (40S ribosomal protein S11), AALF014390 (40S ribosomal protein S4), AALF016123 (40S ribosomal protein S7), **b) RNA processing** AALF010205 (THO complex subunit 2), AALF013153 (ribosome production factor 2 homolog), AALF028554 (SAM_MT_RSMB_NOP domain containing protein), **c) microtubule based movement** AALF001770 (kinesin like protein), AALF005696 (kinesin motor domain containing protein), **d) mRNA export from nucleus** AALF005953 (WD_REPEATS_REDION domain containing protein), AALF026989 (nucleoporin GLE1), **e) heterochromatin organization** AALF008498 (ATP-dependent DNA helicase), AALF011047 (DNA topoisomerase), AALF020133 (bifunctional lysine-specific demethylase and histidyl-hydroxylase) were downregulated. In case of upregulated pathway, **a) oxidation reduction process** AALF002514 (cytochrome-b5 reductase), AALF003077 (thioredoxin domain-containing protein), **b) regulation of autophagy** AALF008411 (phosphatidylinositol -3-phosphate phosphatase), **c) NADP/H metabolic process** AALF006456 (NAD(+) kinase), **e) transport** AALF000726 (GDP-fucose transporter 1), AALF003105 (transmembrane protein 30A), AALF004603 (SEC domain containing protein), AALF005817 (calcium channel flower), AALF006714 (signal recognition particle 9kDa protein) (Figure 3.8).

At 60 hpi, the downregulated pathways include **a) cellular metabolic process** AALF002024 (aurora kinase), AALF002047 (uridine/cytidine kinase), AALF002047 (ULP_protease domain containing protein), AALF003124 (protein MAK10 homolog), AALF003666 (eukaryotic translation initiation factor 5), AALF004050 (serine/threonine-protein kinase RIO3), AALF004188 (nicotinate phosphoribosyltransferase), AALF005069 (peptidylpropyl isomerase), AALF005515 (histone acetyltransferase type B catalytic subunit), AALF006821 (asparagine synthetase), **b) phosphorous metabolic process** AALF001440 (2-deoxy-D-ribose 5-phosphate aldolase), AALF009801 (adenine phosphoribosyltransferase), AALF010115 (3'-phosphoadenosine-5'-phosphosulfate synthase), AALF011221 (adenylsuccinate lyase), **c) cytoplasmic translation** AALF000668 (eukaryotic translation initiation factor 3 subunit F), AALF007705 (eukaryotic translation initiation factor 3 subunit D), AALF008592 (eukaryotic translation initiation factor 3 subunit C), AALF010660 (eukaryotic translation initiation factor 3 subunit K), AALF014786 (eukaryotic translation initiation factor 3 subunit I), AALF017000 (eukaryotic translation initiation factor 3 subunit G), AALF019400 (eukaryotic translation initiation factor 3 subunit B), AALF023524 (eukaryotic translation initiation factor 3 subunit A). At 60 hpi, the upregulated pathways included **a) RNA processing** AALF000368 (tRNA (adenine(58)-N(1))-methyltransferase non-catalytic subunit TRM6), AALF000393 (Pre mRNA processing factor 6) , AALF000910 (small nuclear ribonucleoprotein E), AALF001573 (small nuclear ribonucleoprotein sm D1), AALF001576 (cleavage and polyadenylation specificity factor subunit 5), RNA splicing AALF002793 (U6 snRNA-associated Sm-like protein LSm3), AALF004524 (putative nuclear mRNA splicing via spliceosome), AALF008858 (Pre-mRNA-splicing factor 18) **b) ribonucleoprotein complex biogenesis** AALF013153 (ribosome production factor 2 homolog), AALF013154 (RRP15-like protein), AALF013709 (KKR-R motif containing protein 1), AALF015138 (Pre-mRNA processing factor 31), AALF017275 (SCA7 domain-containing protein), **c) ncRNA processing** AALF002462 (tRNA(cytosine(34)-C(5))-methyltransferase), AALF005020 (probable tRNA(His)guanylyltransferase), AALF007329 (integrator complex subunit 10), **d) transcription DNA templated** AALF000489 (DNA directed RNA polymerase subunit beta), AALF000727 (DNA directed RNA polymerase III subunit RC3), **e) chromosome organization** AALF000354 (FCS type domain containing protein) AALF000490 (DNA helicase), AALF004593 (Zinc hook

domain containing protein), AALF0046243 (nuclear pore complex protein), AALF006549 (DNA replication licensing factor MCM7), AALF007687 (probable lysine specific histone demethylase 1), AALF010323 (nibrin), AALF013028 (histone deacetylase), AALF017609 (histone-lysine N-methyltransferase), AALF018472 (ATP dependent DNA helicase 2 subunit 1), AALF020325 (E3 ubiquitin protein ligase RING 3), AALF024525 (structural maintenance of chromosome), AALF024804 (general transcription and DNA repair factor IIIH), AALF025662 (RNA polymerase II associated factor 1 homolog), **f) cellular metabolic process** AALF000490 (exonuclease domain containing protein), AALF000727 (DNA-directed RNA polymerase III subunit RPC3), AALF000910 (small nuclear ribonucleoprotein E (snRNP-E)), AALF001602 (poly (ADP -ribose) polymerase), AALF003192 (signal peptidase complex subunit 3), AALF004120 (palmitoyl protein hydrolase), AALF004388 (pyruvate carboxylase), AALF004605 (putative cytochrome C oxidase subunit vb), AALF004987 (non-specific serine/threonine protein kinase), AALF005111 (NADH dehydrogenase (ubiquinone) 1 alpha), AALF005529 (proteasome subunit alpha type), AALF006073 (peptide-propyl cis-trans isomerase), AALF008197 (endoribonuclease), AALF008432 (proteasome endopeptidase complex), AALF009033 (ribosomal RNA-processing protein 43), AALF009424 (heme oxygenase) (Figure 3.8).

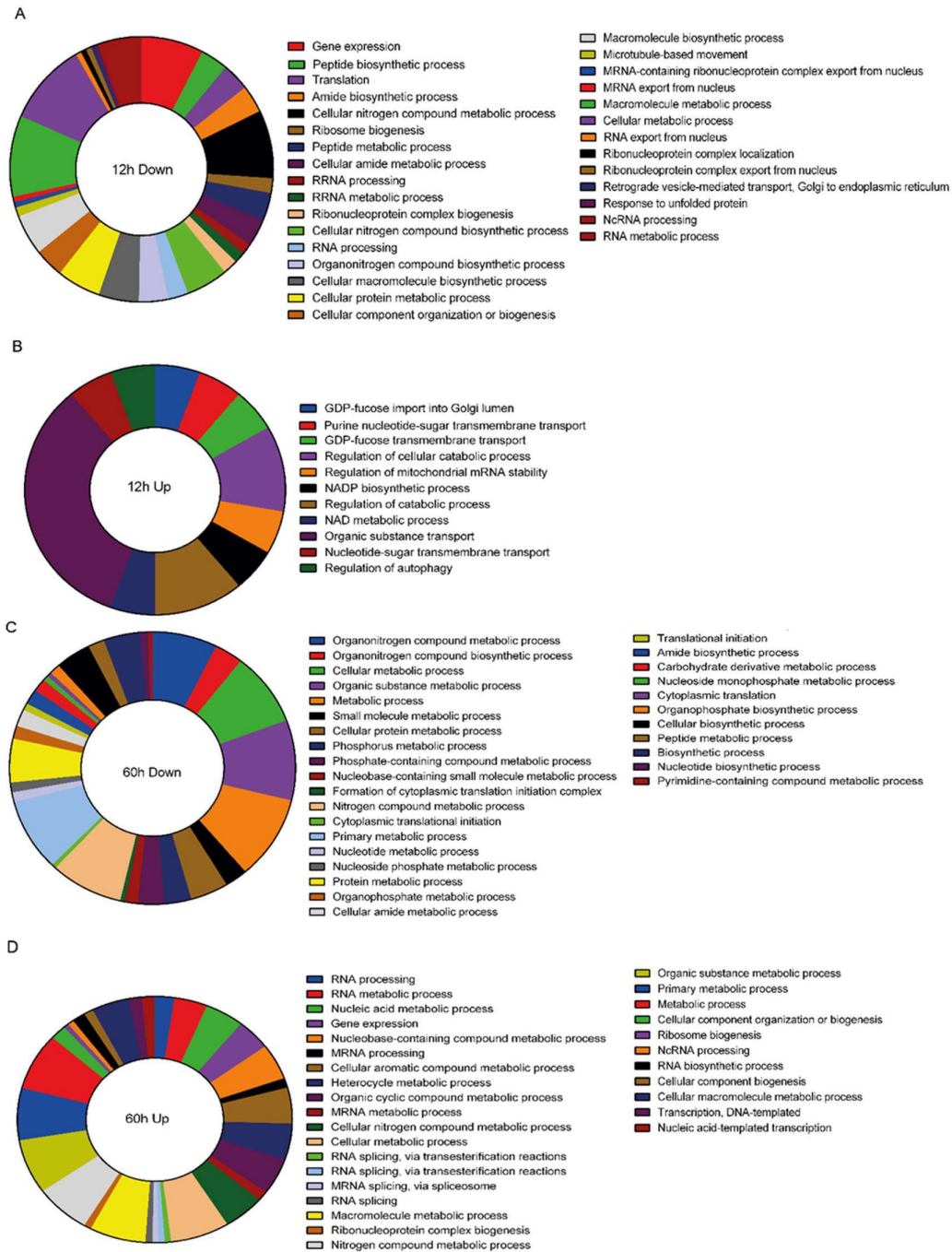


Figure 3.8 Pathway analysis of CHIKV infected U4.4 cells. A) Downregulated pathways at 12 hpi in comparison to uninfected cells; B) Upregulated pathways at 12 hpi in comparison to uninfected cells; C) Downregulated pathways at 60 hpi in comparison to uninfected cells; and D) Upregulated pathways at 60 hpi in comparison to uninfected cells.

3.2.5. Comparative analysis of upregulated and downregulated proteins at early and late infection time points

Comparative analysis of proteins upregulated and downregulated at 12 hpi and 60 hpi as compared to uninfected was done. It was found that 121 proteins were downregulated exclusively at 12 hpi while 399 proteins were downregulated exclusively at 60 hpi. 13 proteins were commonly downregulated at 12 hpi as well as 60 hpi (Figure 3.9). The proteins which were commonly downregulated were involved in microtubule-based movement process (AALF005696 and AALF010622), Organic cyclic compound binding (AALF002791, AALF002941, AALF015210, AALF016979, AALF022185, and AALF022252), ATP binding (AALF016979 and AALF017330).

The comparative analysis showed that 153 proteins were upregulated at 12 hpi and 864 were upregulated at 60 hpi, whereas 42 proteins were upregulated at 12 hpi and 60 hpi. The 42 proteins which were common were involved in fucose transport into Golgi lumen (AALF000726, AALF007632), nitrogen metabolism (AALF020908 and AALF025639), ribosome biogenesis (AALF008344 and AALF022486), and protein kinase complex (AALF018184 AALF026217).

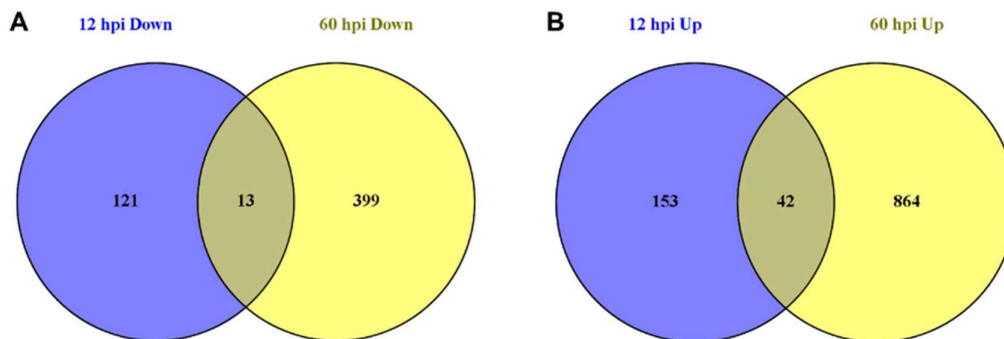


Figure 3.9 Comparative analysis of proteins. A) Comparison of exclusive downregulated proteins at 12 hpi (blue color) and 60 hpi (yellow color) and proteins downregulated at both 12 hpi and 60 hpi show at the center of two circles. B) Comparison of exclusive upregulated proteins at 12 hpi (blue color) and 60 hpi (yellow color) and proteins upregulated at both 12 hpi and 60 hpi show at the center of two circles.

The comparison of 12 hpi with 60 hpi have shown the pathways/proteins which continued to be upregulated or downregulated. It was found that 511 proteins were upregulated at 60 hpi as compared to 12 hpi. The major pathways which were modulated included **a) RNA processing** with proteins involved as AALF000393 (Pre mRNA processing factor 6), AALF000753 (Histone acetyltransferase), AALF001576 (Cleavage and polyadenylation specificity factor), AALF002792 (H/ACA ribonucleoprotein complex subunit) AALF004151 (TAF domain containing protein) AALF007191(Small nuclear ribonucleoprotein Sm D3)), **b) ribosome biogenesis** AALF013153 (Ribosome production factor 2 homolog), AALF014955 (Nucleolar GTP-binding protein 1)), **c) mRNA processing** AALF010205 (THO complex subunit 2), AALF011344 (PWI domain containing protein), AALF014937(Pre mRNA splicing factor RBM22) AALF016189 (Pre mRNA splicing factor 19), AALF016914 (XRN2-binding domain-containing protein), AALF017462 (U1 small nuclear ribonucleoprotein 70 kDa)), **d) gene expression** AALF000368 (tRNA (adenine(58)-(1))-methyltransferase), AALF000806 (HRDC domain-containing protein), AALF004104 (60S ribosomal protein L8), AALF004899 (HMG box domain-containing protein), AALF005953 (WD_REPEATS REGION domain-containing), AALF007329 AALF008423 (Ribosomal protein L15), AALF011384 (DNA-directed RNA polymerase subunit beta)), and **e) protein containing complex biogenesis** AALF004593 (Zinc-hook domain containing protein), AALF005506 (Myosin motor domain containing protein) AALF005594 (Double strand break repair protein), AALF006069 (Proteasome subunit beta), AALF007138 (Histone 2A) AALF015086 (Putative mediator of RNA polymerase II), AALF015312 (Replication factor C subunit 1) AALF016772 (Mediator of RNA polymerase II transcription), and AALF018182 (Structural maintenance of chromosome protein).

The analysis revealed that there were 152 downregulated proteins at 60 hpi with respect to 12 hpi and major pathways included **a) protein ubiquitination** AALF006339 (HECT-type E3 ubiquitin transferase), AALF012286 (PEST proteolytic signal-containing nuclear protein) AALF014219 (E3 ubiquitin-protein ligase) AALF014351 (UBC core-containing protein), **b) cellular protein metabolic process** AALF001347 (SERPIN domain containing protein), AALF006714 (Signal recognition particle 9kDa protein) AALF006747 (Glutamyl tRNA aminotransferase subunit A), AALF008079 (Focal AT domain containing protein) AALF008381

(Tyrosine protein kinase), AALF008580 (Ubiquitin thioesterase), AALF011382 (Putative serine/threonine protein phosphatase), AALF022452 (Metallophos domain-containing protein) AALF024907 (Eukaryotic translation initiation factor 2 subunit), **c) mitochondrial respiratory chain complex**, AALF021781 (Complex I-B17 (NADH dehydrogenase), AALF022264 (NADH dehydrogenase (ubiquinone) 1 alpha), **d) phosphorus metabolic process** AALF000130 (dNK domain containing protein) AALF002635 (CHK domain containing protein) AALF002832 (GDP-4-keto-6-deoxy-D-mannose-3,5-epimerase -4-reductase) AALF003795 (PP28 domain-containing protein), AALF005923 (diphosphomevalonate decarboxylase), AALF012826 (arginine kinase), AALF017331 (amidophosphoribosyltransferase), and AALF019693 (trehalose 6-phosphate phosphatase), AALF022264 (NADH dehydrogenase 1 alpha sub complex subunit 8).

3.3. Discussion

Viruses are known to infect the host cell and control their machinery to support their replication. These include host ribosomes and other factors which are recruited to viral RNAs, which help them in their translation (Walsh & Mohr, 2011). Virus infections induces oxidative stress, which induces stress granule (SG) formation. These granules are a host defense mechanism to control viral replication by entrapping host proteins involved in translation, such as ribosomes and other RNA binding factors, thus reducing their availability in the cytoplasm. The stress granules formation is accompanied by translation arrest due to phosphorylation of eukaryotic initiation factor 2a (eIF2a). Additionally, host immune pathways are also activated, which include Toll-like receptor (TLR) and RIG-1 like receptor (RLR), which recognize viral RNA and lead to activation of NF- κ B and cytokines, which helps in virus clearance (Seth et al., 2006). In the case of mosquitoes, several innate pathways such as RNAi, IMD pathways, and TOLL pathways are involved in protection from viruses (Kumar et al., 2018). The aim of this study was to study the response of U4.4 cells upon CHIKV infection.

In this study, CHIKV E1 protein was expressed in *E. coli*, and an antibody was generated to study the viral kinetics to study the viral growth pattern. From the expression profiling and viral plaque data, it was observed that probably virus has entered the log phase at 12 hpi and peaked at 36 to 48 hpi. At this phase, viral number

inside cells is very low, and many of the cells are not even infected, as evident from confocal images, thus may not have an active immune system. As the viral titer peaked at 36-48 hpi, thereafter, it entered into decline phases. The late infection time point (60 hpi) was chosen to study the impact on *Aedes* cells when the cells' immune pathways are active and have controlled the virus propagation to some extent.

The pathways analysis revealed that at 12 hpi, crucial pathways were downregulated and included ribonucleoprotein complex export from the nucleus, mRNA export from the nucleus, gene expression, and heterochromatin organization were downregulated. This was similar to data obtained from Figure 3.7A. It has been reported that CHIKV infection induces oxidative stress, which favors stress granule formation at initial infection time points. The formation of SGs is coupled with translational arrest, but as the infection progresses, the nsP3 amount increases, which disperse the stress granules, and the virus uses the translation components for its replication (Fros et al., 2012; Jayabalan et al., 2021). In the case of upregulated pathways at 12 hpi, important ones are the oxidation-reduction process, autophagy regulation, RNA stability, and transport. These pathways have a crucial role in virus growth as these help in controlling well as its spreading. For example, the redox process, transport of molecules, and autophagy. This indicates that metabolic remodeling was happening as the virus increases its number while U4.4 cells activate pathways to counteract viral growth.

At 60 hpi, the virus started to decline its number after reaching the peak, and cells are exhausted after long exposure to the virus, which was indicated by western blot data of CHIKV E1, plaque data of viral titer of different time points as well as from previous studies (Lee & Chu, 2015; Vasconcellos et al., 2020; Xin et al., 2017). This might have resulted in the downregulation of pathways such as cellular metabolic process, phosphorus metabolic process, and translation. Several subunits of eIF3 such as eIF3B, eIF3C, eIF3D, eIF3F, eIF3G, eIF3I, and eIF3K were downregulated. eIF3 plays central role in recruitment of pre-initiation complex to mRNA (Aitken et al., 2016). Thus, downregulation of eIF subunits might cause translational downregulation. The upregulated pathways at 60 hpi included RNA metabolic process such as Pre mRNA processing factor 6), small nuclear ribonucleoprotein E, small nuclear ribonucleoprotein sm D1, cleavage and polyadenylation specificity factor subunit 5, and those involved in RNA splicing such as U6 snRNA-associated Sm-like

protein LSM3, Pre-mRNA-splicing factor 18, and other processes such as ribonucleoprotein complex biogenesis, ncRNA processing, transcription DNA templated were upregulated. Upregulation of these pathways indicates that U4.4 cells are trying to maintain homeostasis and activating pathways to control virus growth and favors its survival. The comparative analysis has shown that very few common proteins were downregulated at both 12 hpi and 60 hpi, including kinesin-like protein, kinesin motor domain protein, RNA helicase, AIR carboxylase. Similarly, few proteins such as GDP fucose transporter 1, sulfite oxidase, ribosome biogenesis regulator factor, and some other uncharacterized proteins were upregulated from 12 hpi to 60 hpi. The analysis revealed that cells are actively manipulating their gene expression during the course of infection.

In this, the impact of CHIKV on the siRNA pathway competent *Ae. albopictus* cell line (U4.4) was studied. This study revealed that at MOI of 1 the CHIKV was reached at a peak between 36 hpi to 48 hpi. The pathway analysis showed that during initial infection time, the protein expression was downregulated for pathways such as translation, RNA processing, cellular metabolic processes, mRNA cleavage, while those of upregulated were involved in RNA stability, regulation of autophagy, GDP fucose transport to Golgi lumen, indicating that cells are trying to conserve their resources, while viruses using cells resource to multiply. The translation continued to be downregulated at 60 hpi. In contrast, other pathways such as RNA splicing, nucleic acid metabolic process, primary metabolic pathways, and ribonucleoprotein complex biogenesis were upregulated, indicating the complex interplay between mosquito cells and virus to favor their survival while controlling another one.

3.4. Materials and methods

3.4.1 Buffers and reagents

***E. coli* Lysis buffer:**

Tris-Cl pH 8.0 50 mM

NaCl 150 mM

Glycerol 5%

EDTA 1 mM

2-mercaptoethanol 2 mM

PMSF 1 mM

Lysozyme

Cell lysis buffer

Tris-Cl pH 7.4 50 mM

NaCl 150 mM

Triton-X-100 1%

SDS 0.1%

Sodium deoxycholate 0.5%

Protease inhibitor cocktail tablet

Crystal violet solution

Crystal violet (1%) 0.25%

Methanol 30%

PBS (1X) to make final volume

Carboxymethyl cellulose (CMC)

2 g CMC was suspended in 100 ml water and continuously stirred till dissolved completely. It was then autoclaved.

Other reagents:

DMEM medium, fetal bovine serum, penicillin/streptomycin, nitrocellulose membrane, anti-His-probe antibody (H-3) HRP (sc-8036 HRP), Pierce™ BCA Protein Assay Kit, SuperSignal™ West Pico PLUS Chemiluminescent substrate, coomassie brilliant blue solution, 2% CMC, anti-mice IgG HRP antibody, anti-actin HRP antibody, anti-mice alexa 488, DAPI, sterile coverslips, glass sides, and 6 well culture plates.

3.4.2 Methods

3.4.2.1 Cloning and expression of CHIKV E1 protein

RNA was isolated from Chikungunya virus (Accession no. JF950631.1) (Shrinet et al., 2012) infected *Ae. aegypti* (Aag2) cells. RNA was reverse transcribed using PrimeScript one-step kit with E1 specific primers. Forward 5'-

GCAGGTACCATGGTATTGGAGATGGA ACTACTG-3' and reverse primer 5'-GCAGGATCCTCGCACGACATGTCCGTTAAAG-3'. The reverse transcription PCR was done as shown in chapter 2 with 57°C annealing temperature and 1 min extension time. The PCR product was run on the gel, and upon confirmation of the size of around 800 bp, the bands were cut and eluted.

The PCR product and pET29a plasmid were digested with *Kpn1* and *BamH1* enzymes and again separated on 1% agarose gel. The digested plasmid and PCR product were eluted, and a ligation reaction was set up, as shown in the method section. The next day, the ligation product was transformed into competent *Escherichia coli* DH5α cells. The transformed cells were plated onto the LB agar plates having kanamycin (50 µg/ml) and incubated at 37°C for overnight growth. The next day, the plates were observed for colonies. 4-6 colonies were taken randomly and put into 10 ml LB broth with kanamycin and incubated at 37°C for 12-14 h. The plasmids were isolated from the individual tubes with a Sure spin plasmid isolation kit (Genetix). The isolated plasmids were quantified using the nanodrop 2000 system (Thermo fisher scientific).

The plasmids were digested with *Kpn1* and *BamH1* enzymes and run on the 1% agarose gel. The bands were first visualized in a UV transilluminator and then imaged in a UV gel documentation system. The plasmids which showed insert of the desired size were transformed into competent *E. coli* BL21-CodonPlus cells. The transformed cells were cultured in LB agar plates and then incubated at 37°C for overnight growth. The next day, colonies were picked and put into 10 ml LB broth with kanamycin and incubated at 37°C for 12-14 h. Glycerol stocks were prepared for future used. The detailed protocol for each of these is mentioned in chapter 2.

3.4.2.2 CHIKV E1 protein purification

The culture was inoculated from glycerol stock and put into 10-50 ml LB media having kanamycin at the desired concentration. The culture was allowed to grow at 37°C for 12-14 h at 150 rpm. The culture was transferred into a flask at a final dilution of 1% with kanamycin. It was allowed to grow and then induced at 18°C with the final concentration of IPTG at 1 mM. The culture was induced for 16h and then centrifuged and lysed in the lysis buffer using sonication. The suspension was centrifuged at 12000 g (RCF) for 30 min at 4°C. The supernatant was transferred to a fresh falcon tube or bottle and to the pellet, 8 M urea was added and incubated for 1 h

at 37°C and 150 rpm. After the incubation, the urea suspension was centrifuged, and the supernatant fraction was transferred into the fresh falcon tube.

The Ni-NTA beads were recharged with lysis and urea buffer; detailed protocol is given in chapter 2. Both supernatant fraction and urea fraction were allowed to bind to beads and eluted with increasing concentrations of imidazole in the lysis buffer or urea solution. The eluted fractions were kept on ice and run on SDS-PAGE.

3.4.2.3 SDS-PAGE, staining, and western blotting

The cell lysate was quantified using Pierce™ BCA protein assay kit following the manufacturer protocol. In each well, 20-25 µg protein lysate or 4-6 µg purified protein was loaded. The samples were separated on either 10% SDS PAGE gel (in case of lysate) or 12 % SDS-PAGE gel (in case of purified protein) at 100 V till the front dye was eluted from the other end of the gel. For purified protein half of the gel was stained with Coomassie brilliant blue stain, and the other half of the gel having similar fractions was used to run transfer onto nitrocellulose membrane for 1 h at 50 V in transfer buffer, whereas in case of lysate whole gel was proceeded for transfer. The membrane was blocked with 5% BSA in PBS and then probes with antibody (anti-CHIKV E1 IgG mice serum 1:3000 dilution in PBS+2.5% BSA overnight at 4-7 °C whereas anti-His IgG HRP 1:6000 dilution and anti-actin IgG-HRP in PBST+2.5% BSA) at RT for 1 h with shaking. The membrane was washed with PBST for 3X10 min and either probed with anti-mice IgG-HRP in PBST+2.5% BSA) at RT for 1 h with shaking (anti CHIKV E1 mice serum) followed by washing in PBST for 3X10 min or directly visualized (blots incubated with anti-actin and anti-His) after adding chemiluminescent substrate to the membrane in the Bio-rad ChemiDoc MP system.

3.4.2.4 Anti-CHIKV E1 antibody generation

The protein was injected into four female Balb/c mice with FCA (Freund's complete adjuvant) at a 100 µg/mice concentration. The booster doses of the protein (50µg/mice) were given at regular intervals, and blood was collected by puncturing retro-orbital sinus in mice or with a sterile hematocrit capillary tube. The blood was collected in an microfuge tube and kept at 37°C for 30 min to allow the blood to clot. The tube was then centrifuged at 4000 g for 3 min. The transparent serum was transferred to a fresh tube, and if there were traces of RBCs, then centrifugation was repeated. The serum was then added with sterile sodium azide at a concentration of

0.002%, aliquoted if needed, and then kept at the ice (for immediate use) or -70°C (for future use).

3.4.2.5 Chikungunya virus infection in U4.4 cells

U4.4 cells were cultured in DMEM media supplemented with 10% fetal bovine serum (FBS), tryptose phosphate, glutamine, penicillin, and streptomycin (P/S). The cells were split and plated in 6 well plates and place at 28°C with 5% CO₂. When cells reached 60-70% confluency, cells were kept in serum-free media for 1 h and then infected with chikungunya virus (Shrinet et al., 2012) grown in Vero cells at MOI of 1. The virus was allowed to enter into the cells for 1.5 h. Cells were then washed with serum-free media to remove any virus particles that had not entered the cells. Then cells were supplemented with completed media having all components like FBS, tryptose phosphate, and antibiotics. Cells are then transferred to the incubator for growth. Cells/media collected at this time were counted as 0 h. Cells/media were collected at desired time points.

3.4.2.6 RNA Isolation and Real-Time PCR

RNA isolation and real-time PCR were done as per protocol mentioned in chapter 2. Briefly, total RNA was isolated using TRIzol (Thermo Fisher Scientific Inc., Waltham, MA, USA). RNA was dissolved in DEPC-treated water, and RNA was quantified. One-step SYBR green real-time PCR was carried out on a PIKOREAL 96 real-time PCR system (Thermo Fisher Scientific Inc., Waltham, MA, USA). A total of 300 ng total RNA per reaction was used with 0.3 µM of each primer (CHIKV E1 and RPS7) with QuantiTect PCR kit (Qiagen, Hilden, Germany). The RT-PCR conditions for the one-step RT-PCR consisted of a 30 min reverse transcription step at 50 °C and then 2 min of initial denaturation at 95 °C, followed by 40 cycles of PCR at 95 °C without holding time (denaturation), 60 °C for 30 s (annealing), and 72 °C for 30 s (extension). Small subunit ribosomal protein 7 (RPS7) was used as an internal control. The sequence for real time PCR was: CHIKV E1 primer forward: TACCCATTTATGTGGGGC and reverse GCCTTTGTACACCACGATT and RPS7 was forward: GCAAGAAGGCTATCGTGATCTA and reverse: CGGAGAACTTCTTCTCCAATC.

3.4.2.7 Immunofluorescence assay

Vero/U4.4 cells were cultured in DMEM complete media in 6 well plates having sterile glass coverslips. The cells were infected with chikungunya virus at MOI 1. The cells were infected at different time points to start the next step at once. The cells were then fixed with 4% paraformaldehyde for 30 min. Cells were permeabilized with PBST (PBS+0.1% triton-X-100) for 30 min. Slides were then blocked with PBS+5% BSA for 1h. Wells were then added with anti-CHIKV E1 mice serum at 1:200 dilution in PBS+2.5% BSA overnight. The next day, washing was done with PBST (PBS+0.05% triton-X-100) for 3X10 min. The cells were then added with secondary antibody (anti-mice Alexa 488) at 1:400 dilution in PBS+2.5% BSA for 1h and then given washing of 3X10 min. Cells were briefly incubated with DAPI (1 µg/ml). Coverslips were then mounted onto glass slide having ProLong Gold Antifade Mountant. Cells were visualized in first fluorescent microscope and then in confocal microscope (Nikon).

3.4.2.8 Plaque assay

Vero cells were grown in DMEM media supplemented with FBS, glutamine, and P/S. The cells were cultured in 96 well plates for plaque assay at 37°C humidified incubator with 5% CO₂. The cell media was changed to serum-free for 1 h when the confluency was reached 100%. The supernatant collected at various time points of infection of U4.4 cells was thawed at the ice. The samples were diluted and added to the first well of the plate in triplicate. Then it was serially diluted into half in the next well. One well at the end was kept as control, having no sample addition to it. The virus was allowed to bind for 1.5 h, and then the media was changed. The wells were then added with 1% CMC and plates were transferred back to the incubator for 48 h. After the incubation, the CMC was pipetted out, and cells were fixed with 4% paraformaldehyde for 30 min. After the fixing, cells were added with crystal violet stain for 30 min. The stain was discarded after that, and wells were rinsed with tap water. Plaques were visible with naked eyes and calculated by plaque-forming units (pfu) = (No. of plaques)/(Dilution × volume of the virus).

3.4.2.9 Cell lysis

Cells were scraped using a cell scraper and collected in tubes. Cells were centrifuged at 200 g at 4°C. The cell pellet was added with RIPA buffer/IP lysis buffer in a tube.

The tubes were kept on ice for 30 min with occasional mixing for complete lysis. The cells were again centrifuged for 12000 g for 30 min at 4°C. The supernatant was transferred to a fresh vial and was quantified using a BCA protein estimation kit following manufacturer protocol. The samples were then either process further for SDS-PAGE or stored at -70°C.

3.4.2.10 Sample preparation

25 µg protein from each sample was reduced with 5 mM TCEP and further alkylated with 50 mM iodoacetamide and then digested with Trypsin (1:50, Trypsin/lysate ratio) for 16 h at 37 °C. Digests were cleaned using a C18 silica cartridge to remove the salt and dried using a speed vac. The dried pellet was resuspended in buffer A (5% acetonitrile, 0.1% formic acid).

3.4.2.11 Mass spectrometric analysis of peptide mixtures

Experiments were performed on an Ultimate 3000 RSLC nanosystem coupled with an Orbitrap Eclipse. 500 ng was loaded on C18 column 50 cm, 3.0 µm Easy-spray column (Thermo Fisher Scientific). Peptides were eluted with a 0–40% gradient of buffer B (80% acetonitrile, 0.1% formic acid) at a flow rate of 300 ml/min) and injected for MS analysis. LC gradients were run for 100 minutes. MS1 spectra were acquired in the Orbitrap (R= 240k; AGC target = 400 000; Max IT = 50 ms; RF Lens = 30%; mass range = 400–2000; centroid data). Dynamic exclusion was employed for 10 s, excluding all charge states for a given precursor. MS2 spectra were collected in either the linear ion trap (rate = turbo; AGC target = 20,000; MaxIT = 50 ms; NCEHCD= 35%).

3.4.2.12 Data Processing

All samples were processed, and RAW files generated were analyzed with Proteome Discoverer (v2.4) against the Uniprot CUSTOMIZED reference proteome database. For Sequest search, the precursor and fragment mass tolerances were set at 10 pm and 0.5 Da, respectively. The protease used to generate peptides, i.e., enzyme specificity, was set for trypsin/P (cleavage at the C terminus of "K/R: unless followed by "P") along with a maximum missed cleavages value of two. Carbamidomethyl on cysteine as fixed modification and oxidation of methionine and N-terminal acetylation were

considered as variable modifications for database search. Both peptide spectrum match and protein false discovery rate were set to 0.01 FDR.

3.4.2.13 Differential analysis

Abundance values of all samples were used for differential statistical analysis. Protein Abundance values were filtered on the basis of valid values (at least present in 8 samples). Filtered values were Log₂ transformed, followed by Z-score standardization. ANOVA was used to identify significant proteins. Statistical significance was considered for P values less than or equal to 0.05. Z score abundance values of the Significant Proteins were then used for bioinformatics data visualization using In-house R Programming Scripts. The reproducibility of replicates was accessed by Principal component analysis. The proteins which were upregulated or downregulated by 1.5 fold were included in the further analysis. The functional enrichment was done using ShinyGO v0.66 (ShinyGO v0.66: Gene Ontology Enrichment Analysis + more (sdstate.edu). The P-values cutoff (FDR) was set to 0.05. The gene details corresponding to the IDs were fetched from the Uniprot database.

3.5 References

- Abraham, R., Mudaliar, P., Jaleel, A., Srikanth, J., & Sreekumar, E. (2015). High throughput proteomic analysis and a comparative review identify the nuclear chaperone, Nucleophosmin among the common set of proteins modulated in Chikungunya virus infection. *J Proteomics*, *120*, 126-141. <https://doi.org/10.1016/j.jprot.2015.03.007>
- Abraham, R., Mudaliar, P., Padmanabhan, A., & Sreekumar, E. (2013). Induction of cytopathogenicity in human glioblastoma cells by chikungunya virus. *PLoS One*, *8*(9), e75854. <https://doi.org/10.1371/journal.pone.0075854>
- Aitken, C. E., Beznoskova, P., Vlckova, V., Chiu, W. L., Zhou, F., Valasek, L. S., . . . Lorsch, J. R. (2016). Eukaryotic translation initiation factor 3 plays distinct roles at the mRNA entry and exit channels of the ribosomal preinitiation complex. *Elife*, *5*. <https://doi.org/10.7554/eLife.20934>
- Blair, C. D. (2011). Mosquito RNAi is the major innate immune pathway controlling arbovirus infection and transmission. *Future Microbiol*, *6*(3), 265-277. <https://doi.org/10.2217/fmb.11.11>
- Bojkova, D., Klann, K., Koch, B., Widera, M., Krause, D., Ciesek, S., . . . Munch, C. (2020). Proteomics of SARS-CoV-2-infected host cells reveals therapy targets. *Nature*, *583*(7816), 469-472. <https://doi.org/10.1038/s41586-020-2332-7>
- Bosl, K., Ianevski, A., Than, T. T., Andersen, P. I., Kuivanen, S., Teppor, M., . . . Kandasamy, R. K. (2019). Common Nodes of Virus-Host Interaction Revealed Through an Integrated Network Analysis. *Front Immunol*, *10*, 2186. <https://doi.org/10.3389/fimmu.2019.02186>

- Chen, B., Tian, E. K., He, B., Tian, L., Han, R., Wang, S., . . . Cheng, W. (2020). Overview of lethal human coronaviruses. *Signal Transduct Target Ther*, *5*(1), 89. <https://doi.org/10.1038/s41392-020-0190-2>
- Cui, Y., Liu, P., Mooney, B. P., & Franz, A. W. E. (2020). Quantitative Proteomic Analysis of Chikungunya Virus-Infected *Aedes aegypti* Reveals Proteome Modulations Indicative of Persistent Infection. *J Proteome Res*, *19*(6), 2443-2456. <https://doi.org/10.1021/acs.jproteome.0c00173>
- De Clercq, E. (2002). Strategies in the design of antiviral drugs. *Nat Rev Drug Discov*, *1*(1), 13-25. <https://doi.org/10.1038/nrd703>
- De Clercq, E., & Li, G. (2016). Approved Antiviral Drugs over the Past 50 Years. *Clin Microbiol Rev*, *29*(3), 695-747. <https://doi.org/10.1128/CMR.00102-15>
- Duffy, S. (2018). Why are RNA virus mutation rates so damn high? *PLoS Biol*, *16*(8), e3000003. <https://doi.org/10.1371/journal.pbio.3000003>
- Emmott, E., Rodgers, M. A., Macdonald, A., McCrory, S., Ajuh, P., & Hiscox, J. A. (2010). Quantitative proteomics using stable isotope labeling with amino acids in cell culture reveals changes in the cytoplasmic, nuclear, and nucleolar proteomes in Vero cells infected with the coronavirus infectious bronchitis virus. *Mol Cell Proteomics*, *9*(9), 1920-1936. <https://doi.org/10.1074/mcp.M900345-MCP200>
- Fros, J. J., Domeradzka, N. E., Baggen, J., Geertsema, C., Flipse, J., Vlak, J. M., & Pijlman, G. P. (2012). Chikungunya virus nsP3 blocks stress granule assembly by recruitment of G3BP into cytoplasmic foci. *J Virol*, *86*(19), 10873-10879. <https://doi.org/10.1128/JVI.01506-12>
- Goic, B., Stapleford, K. A., Frangeul, L., Doucet, A. J., Gausson, V., Blanc, H., . . . Saleh, M. C. (2016). Virus-derived DNA drives mosquito vector tolerance to arboviral infection. *Nat Commun*, *7*, 12410. <https://doi.org/10.1038/ncomms12410>
- Gould, E. A., Coutard, B., Malet, H., Morin, B., Jamal, S., Weaver, S., . . . Canard, B. (2010). Understanding the alphaviruses: recent research on important emerging pathogens and progress towards their control. *Antiviral Res*, *87*(2), 111-124. <https://doi.org/10.1016/j.antiviral.2009.07.007>
- Jayabalan, A. K., Adivarahan, S., Koppula, A., Abraham, R., Batish, M., Zenklusen, D., . . . Leung, A. K. L. (2021). Stress granule formation, disassembly, and composition are regulated by alphavirus ADP-ribosylhydrolase activity. *Proc Natl Acad Sci U S A*, *118*(6). <https://doi.org/10.1073/pnas.2021719118>
- Kumar, A., Srivastava, P., Sirisena, P., Dubey, S. K., Kumar, R., Shrinet, J., & Sunil, S. (2018). Mosquito Innate Immunity. *Insects*, *9*(3). <https://doi.org/10.3390/insects9030095>
- Lee, R. C., & Chu, J. J. (2015). Proteomics profiling of chikungunya-infected *Aedes albopictus* C6/36 cells reveal important mosquito cell factors in virus replication. *PLoS Negl Trop Dis*, *9*(3), e0003544. <https://doi.org/10.1371/journal.pntd.0003544>
- Li, Y. G., Siripanyaphinyo, U., Tumkosit, U., Noranate, N., A. A. n., Tao, R., . . . Anantapreecha, S. (2013). Chikungunya virus induces a more moderate cytopathic effect in mosquito cells than in mammalian cells. *Intervirology*, *56*(1), 6-12. <https://doi.org/10.1159/000339985>
- Mohammadi Pour, P., Fakhri, S., Asgary, S., Farzaei, M. H., & Echeverria, J. (2019). The Signaling Pathways, and Therapeutic Targets of Antiviral Agents: Focusing on the

- Antiviral Approaches and Clinical Perspectives of Anthocyanins in the Management of Viral Diseases. *Front Pharmacol*, 10, 1207. <https://doi.org/10.3389/fphar.2019.01207>
- Nagy, P. D., & Pogany, J. (2011). The dependence of viral RNA replication on co-opted host factors. *Nat Rev Microbiol*, 10(2), 137-149. <https://doi.org/10.1038/nrmicro2692>
- Parvez, M. K., & Parveen, S. (2017). Evolution and Emergence of Pathogenic Viruses: Past, Present, and Future. *Intervirology*, 60(1-2), 1-7. <https://doi.org/10.1159/000478729>
- Seth, R. B., Sun, L., & Chen, Z. J. (2006). Antiviral innate immunity pathways. *Cell Res*, 16(2), 141-147. <https://doi.org/10.1038/sj.cr.7310019>
- Shrinet, J., Jain, S., Sharma, A., Singh, S. S., Mathur, K., Rana, V., . . . Sunil, S. (2012). Genetic characterization of Chikungunya virus from New Delhi reveal emergence of a new molecular signature in Indian isolates. *Virol J*, 9, 100. <https://doi.org/10.1186/1743-422X-9-100>
- Suhrbier, A., Jaffar-Bandjee, M. C., & Gasque, P. (2012). Arthritogenic alphaviruses--an overview. *Nat Rev Rheumatol*, 8(7), 420-429. <https://doi.org/10.1038/nrrheum.2012.64>
- Trinh, H. V., Grossmann, J., Gehrig, P., Roschitzki, B., Schlapbach, R., Greber, U. F., & Hemmi, S. (2013). iTRAQ-Based and Label-Free Proteomics Approaches for Studies of Human Adenovirus Infections. *Int J Proteomics*, 2013, 581862. <https://doi.org/10.1155/2013/581862>
- Tsetsarkin, K. A., Vanlandingham, D. L., McGee, C. E., & Higgs, S. (2007). A single mutation in chikungunya virus affects vector specificity and epidemic potential. *PLoS Pathog*, 3(12), e201. <https://doi.org/10.1371/journal.ppat.0030201>
- Varjak, M., Leggewie, M., & Schnettler, E. (2018). The antiviral piRNA response in mosquitoes? *J Gen Virol*, 99(12), 1551-1562. <https://doi.org/10.1099/jgv.0.001157>
- Vasconcellos, A. F., Mandacaru, S. C., de Oliveira, A. S., Fontes, W., Melo, R. M., de Sousa, M. V., . . . Charneau, S. (2020). Dynamic proteomic analysis of Aedes aegypti Aag-2 cells infected with Mayaro virus. *Parasit Vectors*, 13(1), 297. <https://doi.org/10.1186/s13071-020-04167-2>
- Vodovar, N., Bronkhorst, A. W., van Cleef, K. W., Miesen, P., Blanc, H., van Rij, R. P., & Saleh, M. C. (2012). Arbovirus-derived piRNAs exhibit a ping-pong signature in mosquito cells. *PLoS One*, 7(1), e30861. <https://doi.org/10.1371/journal.pone.0030861>
- Walsh, D., & Mohr, I. (2011). Viral subversion of the host protein synthesis machinery. *Nat Rev Microbiol*, 9(12), 860-875. <https://doi.org/10.1038/nrmicro2655>
- Xin, Q. L., Deng, C. L., Chen, X., Wang, J., Wang, S. B., Wang, W., . . . Zhang, L. K. (2017). Quantitative Proteomic Analysis of Mosquito C6/36 Cells Reveals Host Proteins Involved in Zika Virus Infection. *J Virol*, 91(12). <https://doi.org/10.1128/JVI.00554-17>
- Zhu, S. L., Chen, X., Wang, L. J., Wan, W. W., Xin, Q. L., Wang, W., . . . Zhang, L. K. (2017). Global quantitative proteomic analysis profiles host protein expression in response to Sendai virus infection. *Proteomics*, 17(5). <https://doi.org/10.1002/pmic.201600239>

Chapter 4

Chapter 4

Identification of CHIKV non-structural protein 3 (nsP3) interacting partners in *Ae. aegypti* (Aag2) cells

4.1. Introduction

Chikungunya virus (CHIKV), a positive-sense single-stranded RNA virus, is a member of the alphavirus family (Strauss & Strauss, 1994) and is responsible for causing outbreaks to human populations globally (Pialoux et al., 2007). The CHIKV genome is ~11.8 kb which contains 3' polyadenylation and 5'-capping. It consists of two open reading frames encoding three structural proteins (capsid, envelope glycoproteins E1 and E2), two small cleavage peptides (E3 and 6K/TF), and four non-structural proteins (nsP1, nsP2, nsP3, and nsP4). Structural proteins facilitate the entry and fusion of viral particles to the membrane of hosts (Strauss & Strauss, 1994), and the nsPs are engaged in the various steps of virus replication (Strauss & Strauss, 1994). These proteins exhibit multiple functions and enzymatic activities, e.g., methyltransferase (nsP1), protease and helicase (nsP2), ADP-ribosylhydrolase (nsP3), and RNA-dependent RNA polymerase (nsP4). They have been shown to interact actively with many host proteins to execute their functions ranging from viral RNA capping, proteolysis, replication complex formation, and RNA replication (Bourai et al., 2012) to evade the host immune system (Akhrymuk et al., 2012; Meshram et al., 2018; Wong & Chu, 2018).

Mosquitoes are the vector of various common pathogens such as plasmodium, dengue, Zika, and helminths. Among them, *Aedes sp.* (*Ae. aegypti* and *Ae. albopictus*) are involved in spreading one of the standard vector-based viral pathogens (Beerntsen et al., 2000). After the entry inside the body of the mosquito, virion disassembles, and viral RNA is translated. The viral proteins are translated as polyproteins and cleaved into individual proteins by either viral or host proteases. The viral proteins then interact or target host proteins and favor the viral growth (Leung et al., 2011). Viral proteins interact with host proteins to help in viral replication and restricting host immune pathways. Among the immune pathways, RNA interference (RNAi) serves as the primary antiviral defense mechanism in insects and is a phenomenon of post-transcriptional gene silencing in a sequence-specific manner (Agrawal et al., 2003; Gammon & Mello, 2015). Upon viral infection, Dicer (DCR), a host RNase III endonuclease, recognizes viral dsRNA and processes the dsRNA into siRNA or viRNA (Ding & Voinnet, 2007). These viRNAs/siRNAs interact with a highly specialized complex called the RNA

interference silencing complex (RISC), which ultimately degrades the viral genome (Obbard et al., 2009; Tolia & Joshua-Tor, 2007). Genome-wide screening of RNAi factors in insects revealed that Argonaute, Dicer, Droscha/Pasha, Aubergine, R2D2, and Loquacious form a core RNAi component while several other proteins, i.e., DEAD-box family of RNA helicases, chromatin factors, and proteins associated with cell cycle, ABC transporter family, metabolic factors and translational machinery components comprise auxiliary components of RNAi complex (Ghosh et al., 2014). These proteins act in a complementary manner with each other to mount an antiviral response against the invading virus. To counteract this response, viral proteins act as RNAi (VSRs) suppressors to create conditions favorable for viral replication by targeting components of the immune pathways (Obbard et al., 2009; Samuel et al., 2016). Among the CHIKV proteins, nsP3 act as a hub for interaction with host proteins due to the presence of hypervariable domain (HVD), which recruit these proteins to help the viral RNA replication and translation. Various studies in human cells have identified several host factors interacting with nsP3 ranging from G3BP, heat shock proteins, DDX proteins, etc.(Gotte et al., 2018; Lark et al., 2017)

Previous work in the lab has identified that CHIKV nsP2 and nsP3 possess viral suppressors of RNAi (VSR) activity. The nsP3 is known to form a replication complex and thus act as a hub for host interactions. CHIKV nsP3 interacting partners in *Aedes* have not identified details. The present study was undertaken to identify potential interacting partners of CHIKV-nsP3 that could be part of the *Aedes aegypti* (*Ae. aegypti*) RNAi machinery. The study from the lab also revealed that the N-terminal domain of nsP3, i.e., macro domain, acts as VSR. Macrodomains have ADP ribosylhydrolase activity. CHIKV macrodomain is known to catalyze degradation of mono ADP ribose, indicating the ADP ribose-based post-translational modification has a role in viral infection. There is no known ADP ribose polymerase in *Aedes*. The initial screening based on sequence alignment search identified three ADP ribose polymerases in *Ae. aegypti*.

4.2. Results

4.2.1. Cloning and expression of CHIKV nsP3 protein and antibody generation

CHIKV nsP3 proteins was cloned in the pET29a vector using CHIKV infected total cell RNA and CHIKV ns3 specific primers. The clone was confirmed using restriction digestion with *Kpn*1 and *Bam*H1 enzymes. The insert size came at the desired range of around 1500 bp (Figure

4.1A and 4.1B). The CHIKV nsP3-pET29a clone was transformed into *E. coli* BL21-CodonPlus cells. The expression cells were induced with 1 mM IPTG at 18°C, and culture was pelleted and then lysed with lysis buffer. After sonication, the suspension was clarified by centrifugation, and protein was purified using Ni-NTA affinity chromatography. The fractions were eluted with an increasing concentration of imidazole in lysis buffer. The eluted fractions were run on SDS-PAGE and then stained with Coomassie brilliant blue stain, and similar fractions were immunoblotted onto the nitrocellulose membrane. The membrane was blocked with 5% BSA, probed with anti-His HRP antibody for 1 h, and then washed with PBST for 3X10 min. The membrane was then briefly exposed to the chemiluminescent substrate (SuperSignal™ West Pico PLUS Chemiluminescent Substrate) and then visualized in Bio-rad Chemidoc MP System (Figure 4.1C).

The purified protein was injected into a rabbit (New Zealand White Rabbit) with the protocol mentioned in the materials and methods section of chapter 2. The blood was collected within regular intervals, and serum from blood samples was purified. The serum was tested for nsP3 specific IgG antibodies via western blot of purified recombinant protein and CHIKV infected lysate (Figure 4.1D). The serum was also tested for their ability to bind to native nsP3 via immunofluorescence assay (Figure 4.1E).

CHIKV nsP3 in pET29a vector and restriction digestion of nsP3-pET29a; C) SDS-PAGE followed by Coomassie staining and western blotting of purified recombinant CHIKV nsP3 protein (left) and pre-bleed sera testing with recombinant CHIKV nsP3 proteins via western blotting for any non-specific binding (right); D) Western blot of uninfected and CHIKV infected cell lysate with anti-CHIKV nsP3 serum (1:2000), probed with anti-rabbit HRP conjugated antibody; and E) Immunofluorescence assay of uninfected and 12 hpi and 24 hpi Vero cells at MOI of 1. The cells were probed with anti-CHIKV nsP3 serum (1:200), then incubated with Alexa 594 labelled IgG anti-rabbit antibody, and the nucleus was stained with DAPI.

4.2.2. CHIKV regulates host RNAi machinery

RNA viruses are known to infect mosquitoes and replicate within them. During their growth in the mosquitoes, the viruses hijack host machinery/pathways to support their growth. In mosquitoes, RNAi pathways are one of the major pathways to provide immunity against viruses, and the impact of the virus on mosquito cells was an important step to know the interaction as well as the impact of virus infection on the siRNA pathway at different time points of infection and different MOI. As a first step to understanding the relevance of CHIKV infection on the RNAi machinery, we sought to evaluate the expression of some important RNAi factors at different multiplicity of infections (MOIs) of CHIKV, namely, 0.1, 1, and 10 over several time points post-infection, namely, at 0 hpi, 12 hpi, 24 hpi, 36 hpi, 48 hpi, 60 hpi, and 72 hpi using plaque assays. Analysis of viral kinetics revealed that the virus replicates vigorously till 48 hpi at 0.1 and 1 MOI, and thereafter growth kinetics reduced both at 0.1 and 1 MOI. In the case of MOI of 10, virus replicated vigorously till 36 hpi, and thereafter the viral growth reached a plateau (Figure 4.2A).

Next, the profiling of CHIKV-nsP3 was done at different time points of infection at different MOIs to understand the expression of the viral transcript and the protein in relation to viral replication in Aag2 cells. Transcript expression profiling of the nsP3 gene of CHIKV during infection in Aag2 cells showed that the expression level of nsP3 begins to increase from 12 hpi and peaked at 72 hpi both in 0.1 and 1 MOIs, and thereafter expression level decreases. In contrast, in MOI of 10, it peaked at 48 hpi and then decreased. The expression of nsP3 protein during MOI of 0.1, 1, and 10 increased steadily and peaked at 72 hpi and was increased as MOI increased (Figure 4.2B and 4.2C). It was observed that there were cytopathic effects on the cells post 60 hours that might have contributed to the decrease in nsP3 transcript expression

post this time point. Taken together, these results suggested that viral replication and viral protein expression were similar at lower MOIs of 0.1 and 1, and there was a more efficient expression of nsP3 at MOI 10 at earlier time points.

Further, the expression pattern of RNAi core and auxiliary factors such as Ago2, Dicer2, FMR1, R2D2, TSN, and VIG was assessed during CHIKV infection at MOI 1 and MOI 10. The expression level of these factors unveiled that in the case of MOI 1, Dicer2 was significantly upregulated from 24 hpi to 60 hpi, while TSN and Ago-2 were significantly downregulated at 48 hpi. At MOI 10, Dicer2 was significantly upregulated at 60hpi, while Ago2 was downregulated from 48 hpi till 72 hpi. TSN, VIG, and R2D2 are significantly upregulated at 48 hpi and thereafter showed a sharp decrease in their expression (Figure 4.2D and 4.3E).

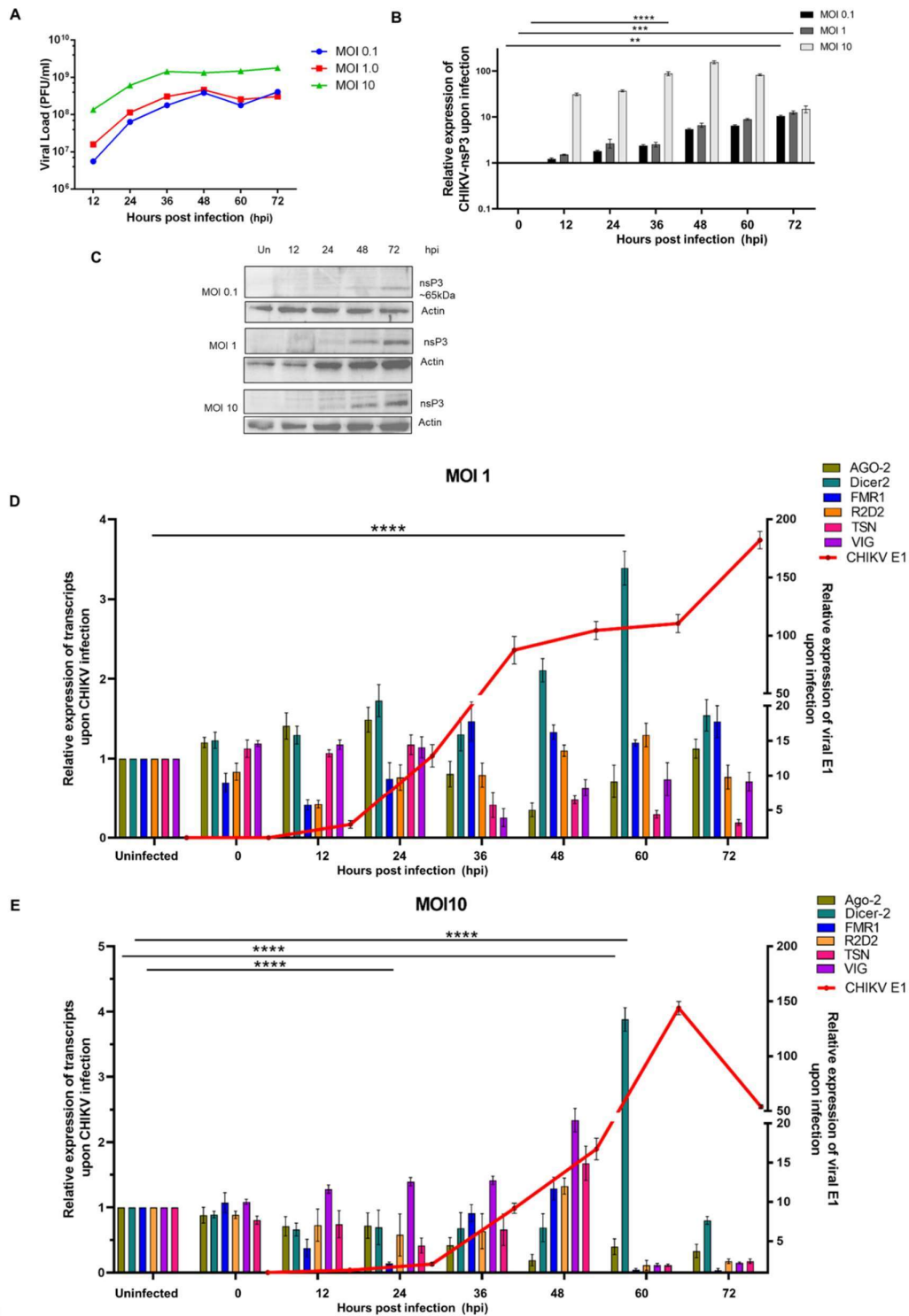


Figure 4.2 Effects of CHIKV infection on RNAi machinery. A) CHIKV viral load (Y-axis) during infection in Aag2 cells at MOI of 0.1, 1, and 10 at different time points, B) Transcripts profiling of nsP3 at MOI of 0.1, 1, and 10 at different time points and western blot analysis of nsP3 at MOI of 0.1, 1, and 10 upon CHIKV infection, C) nsP3 protein expression profiling at

MOI 0.1, 1, and 10 at different time points. D and E) Transcript profiling of Aag2 RNAi factors such as Dicer2, Ago2, R2D2, TSN, VIG, and CHIKV E1 at MOI of 1 and 10 of CHIKV at different time points (** p-value <0.007, *** p-value < 0.0008 and **** p-value < 0.0001).

4.2.3. Host interacting partners of CHIKV-nsP3

For a detailed understanding of the nsP3 interaction partners, we next analyzed the interaction of nsP3 with the *Ae. aegypti* cell (Aag2) lysate and Co-immunoprecipitation assay using purified nsP3 protein and Aag2 cell lysate. The detailed protocol is mentioned in the materials and methods section. Briefly, the agarose beads were immobilized with an anti-nsP3 antibody and then incubated with cell lysate. After washing, elutes were collected, and part of these was run on SDS-PAGE. Upon confirmation, the rest of the sample was processed for mass spectrometry.

The details of gene IDs of nsP3 specific interacting proteins were fetched from the Uniprot database. The host proteins that interacted with nsP3 were analyzed, and pathway analysis of these host proteins revealed that the interacting host proteins were involved in cellular translation, RNA metabolism, signal transduction, heat shock proteins, biomolecule transport, cellular metabolism, oxidation-reduction process, and gene expression (Table 1).

Table 1: Major pathways and their components involved in interaction with nsP3

Translation	AAEL012585 (60S ribosomal protein L7), AAEL005129 (40S ribosomal protein S30), AAEL013625 (40S ribosomal protein S5), AAEL005027 (Acidic ribosomal protein P1), AAEL006860 (Ribosomal protein S28), AAEL017198 (Ribosomal protein L37), AAEL007771 (60S ribosomal protein L22), AAEL011587 (Ribosomal protein L27), AAEL009341 (Ribosomal protein L34), AAEL000210 (Mitochondrial ribosomal protein L2), AAEL017096 (Elongation factor 1-alpha) AAEL017516 (Ribosomal protein uL23), AAEL008188 (60S ribosomal protein L6)
Heat shock protein	AAEL017980 (Heat shock protein 70 (HSP70)), AAEL011584 (chaperonin-60kD), AAEL013349 (Lethal(2)essential for life protein)
Cellular metabolism	AAEL014246 (Glucosyl/glucuronosyl transferases), AAEL010539 (Phosphodiesterase), AAEL000004 (Mannosyltransferase), AAEL000641 (Protein disulfide isomerase), AAEL003161 (Adenylosuccinate synthetase), AAEL010386 (UDP-glucuronosyltransferase)

Oxidation-reduction	AAEL010668 (Quinone oxidoreductase), AAEL004338 (Pyruvate dehydrogenase), AAEL005170 (Cytochrome c oxidase subunit iv), AAEL005538 (Mitochondrial NADH:ubiquinone oxidoreductase), AAEL006721 (2-oxoglutarate dehydrogenase), AAEL008166 (Malate dehydrogenase), AAEL010330 (Succinate dehydrogenase), AAEL000454 (Isocitrate dehydrogenase), AAEL007555 (Acyl-CoA dehydrogenase), AAEL013904 (3-hydroxyisobutyrate dehydrogenase).
Signal transduction	AAEL009287 (GTP-binding nuclear protein), AAEL013069 (Guanine nucleotide-binding protein subunit beta-like protein, Receptor for activated protein kinase c (rack1)), AAEL011116 (14-3-3 protein zeta), AAEL004902 (Ras-related protein Rab-2A)
RNA metabolism	AAEL001375 (Y-box binding protein), AAEL002083 (DEAD box ATP-dependent RNA helicase), AAEL013359 (DEAD box ATP-dependent RNA helicase), AAEL013233 (PIWI5); AAEL001371 (Pre-mRNA cleavage factor im), AAEL001769 (DEAD box ATP-dependent RNA helicase), AAEL008738 (DEAD box ATP-dependent RNA helicase), AAEL010248 (Fibrillarin), AAEL002980 (U1 small nuclear ribonucleoprotein A), AAEL009914 (Small nuclear ribonucleoprotein sm d2) AAEL003916 (Splicing factor)
Biomolecule transport	AAEL000941 (Mitochondrial inner membrane protein translocase), AAEL004438 (GrpE protein homolog), AAEL006362 (Mitochondrial solute carrier), AAEL011276 (Mitochondrial glutamate carrier protein)
Gene expression	AAEL003687 (Histone H2A), AAEL003689 (Histone H4), AAEL007496 (DNA-directed RNA polymerase III), AAEL013643 (Mitochondrial transcription factor A)
Protein metabolism	AAEL009883 (26S protease (S4) regulatory subunit), AAEL004308 (Proteasome subunit alpha type), AAEL011711 (Nascent polypeptide associated complex alpha subunit), AAEL010521 (Subunit of the oligosaccharyl transferase (OST)), AAEL011055 (Chaperone protein DNAj), AAEL010530 (Dual-specificity protein phosphatase)
Structural proteins	AAEL004172 (Tubulin alpha chain AAEL005052 (Tubulin beta chain), AAEL007439 (Myosin light chain 1), AAEL011197 (Actin)

Last decade several studies shed light on the role of ns3 on viral replication, as previously it was considered as most mysterious protein in the alphavirus genus. Most of these studies focus on human proteins interacting with nsP3 protein. Our study has found some of these factors such as YBX1, HSP70, 14-3-3 protein zeta, RPL6, RPL7, Tubulin beta chain, beta-actin, eEF1a, myosin light chain, RACK1, and DEAD-box helicases (Cristea et al., 2006; Frolova et al., 2006; Gorchakov et al., 2008; Gotte et al., 2018). These proteins help the viral replication complex formation and viral RNA replication, translation, and RNA processing. Besides these proteins, there were several proteins involved in gene expression, cellular metabolism. Viruses are known to fine-tune host pathways as well as gene expression, metabolism. Interacting and deprivation of crucial genes with nsP3 could be one of the ways to modulate host response.

Additionally, viruses induce oxidative stress, a host immune mechanism to preserve cell resources and inhibit viral growth (Miller, 2011). It promotes stress granule formation, which leads to translation repression. However, viruses encode enzymes such as proteases helicases which either cleave host immune pathway proteins or bind to viral RNA and prevent the access of host immune pathway proteins to bind to and degrade viral RNA. Viral proteins are also modified post-translationally by the host system, which affects the viral proteins positively or negatively (Burgyan & Havelda, 2011; Fros et al., 2012; Jayabalan et al., 2021).

4.2.4. Macrodomain as ADP ribosylhydrolase

The macrodomain is found among diverse organisms ranging from viruses to bacteria to humans (Li et al., 2013). We did the macrodomain sequence comparison analysis of viruses from the alphavirus family. Total 18 members of alphavirus were included in the analysis, such as Chikungunya virus, Aura virus, Bamrah forest virus, Bebaru virus, Equine encephalitis virus (EEV), Everglade virus, Getah virus, Mayaro virus, Mucambo virus, Ndumu virus, Onyong nyong virus, Rio negro virus, Ross River virus, Semliki forest virus, Sindbis virus, Una virus, Venezuelan Equine Encephalitis Virus (VEEV), and Western equine encephalomyelitis virus (WEEV). These viruses are known to cause pathogenesis in different organisms. The information of active site residues was taken from previous studies (Abraham et al., 2018; McPherson et al., 2017). The sequence comparison of macrodomain among alphaviruses showed that the active site residues such as D10, G32, T113, Y114, and R144 are most conserved in alphaviruses (Figure 4.3).

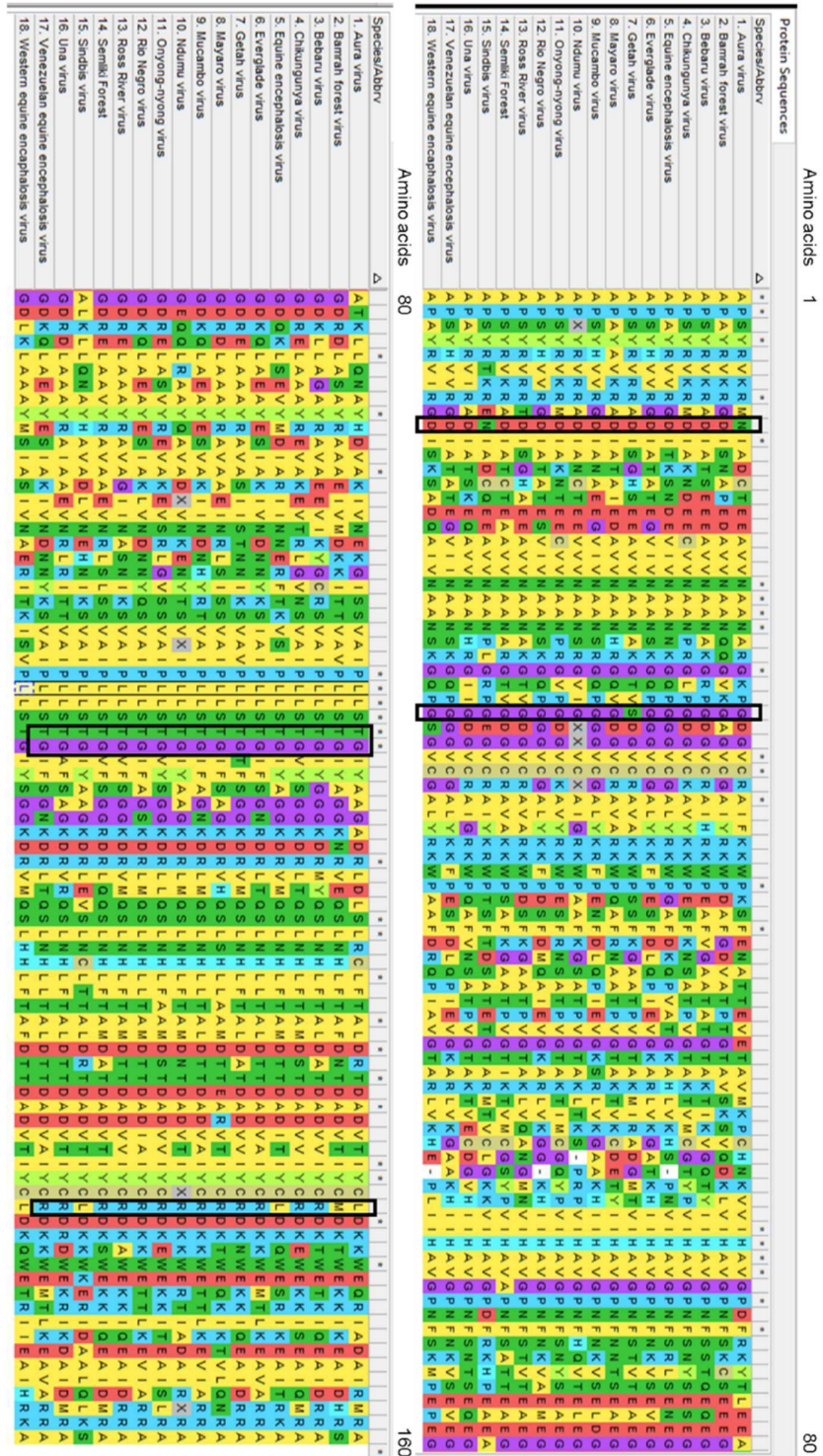


Figure 4.3 Sequence analysis of macrodomain of alphavirus family. The black rectangle encircles the active site residues. These include D10, G32, T113, Y114, and R144.

4.2.5. ADP ribose polymerases in *Ae. aegypti*

Human encodes 17 PARPs (poly ADP ribose polymerase) proteins which are categorized based on the domains. These domain variations gave them substrate diversity to which these add the ADP ribose units. Most of them are active enzymes. The sequence-based search revealed that, *Ae. aegypti* encode three ADP ribose polymerase. One of them is Tankyrase (XP_021708496.1), Poly ADP ribose polymerase (XP_001661932.1), and the third was MARP (mono ADP ribose polymerase (XP_001647568.1)). Domain analysis of these revealed that these three ADP ribose polymerases differs from each other in terms of domains these proteins contain.

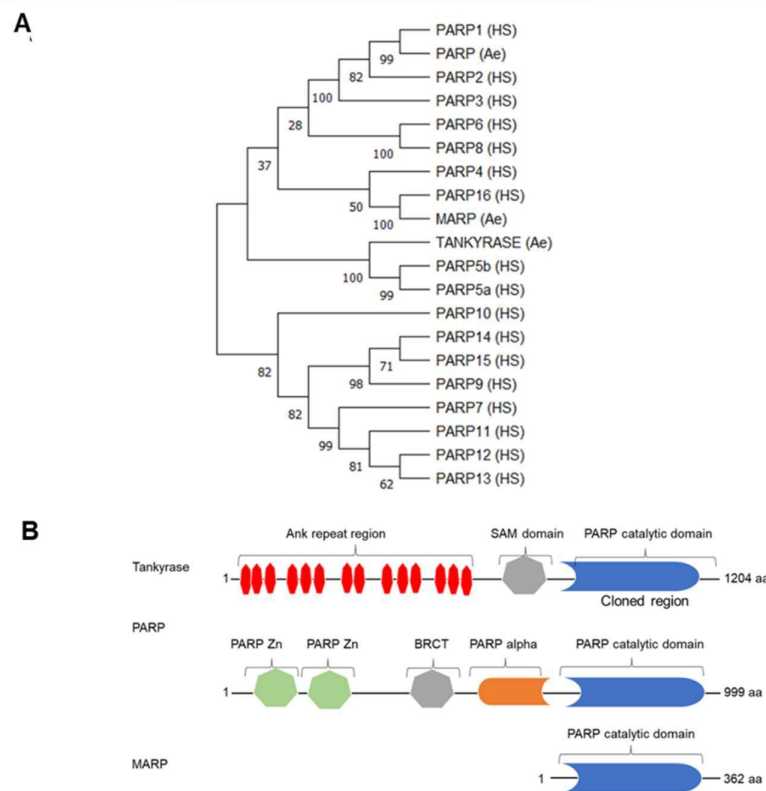


Figure 4.4 Identification of ADP ribose polymerase proteins in *Ae. aegypti*. A) Phylogenetic analysis of *Ae. aegypti* PARPs with human PARPs using MEGA software; B) Proteins sequence analysis of ADP ribose polymerase proteins for domains with ScanProsite database.

1) Tankyrase: Tankyrase has poly ADP ribose polymerase enzyme activity which indicates that it is capable of adding poly ADP ribose subunits to the proteins which are involved in processes such as gene transcription, cellular stress signaling. The length of Tankyrase protein was 1204 amino acids. The sequence comparison with humans showed 69.7% identity and 94% query coverage with poly [ADP-ribose] polymerase tankyrase-1 [Homo sapiens] in the

BLAST search (Figure 4.4A). The domain analysis revealed the presence of three types of domains: Ankyrin repeats, SMA domain, and PARP catalytic domain (Figure 4.4B).

Ankyrin repeats: These are 30-35 amino acid long motifs and have helix turn helix conformation present at the N-terminal of the protein. These motifs play a crucial role in protein-protein interactions (Li et al., 2006; Mosavi et al., 2004). The analysis revealed that the Tankyrase possesses 14 ankyrin repeats (Figure 4.4B). **SAM domain:** The sterile alpha motif (SAM) domain is involved in protein-protein interactions. These play a role in oligomerization as well as binding (Slaughter et al., 2008). There was one SAM domain in Tankyrase protein. The third domain, i.e., PARP catalytic domain, is responsible for adding the ADP ribose monomer unit. The enzyme Tankyrase is a polymerase that indicates that the protein can add a monomer unit to the end of another monomer ADP ribose unit to make a long chain of ADP ribose.

Of 1204 aa of the protein, in this study, the PARP catalytic domain of around 361 amino acids (from 843 to 1204) was cloned and expressed in *E. coli* (Figure 4.4B).

2) PARP: The other protein PARP is a poly ADP ribose polymerase in *Ae. aegypti*. The length of protein was around 1000 amino acids. From the N-terminal of the proteins, there were two PARP Zn, a Zinc finger domain. The zinc finger domain is generally localized to the nucleus and binds to DNA (Figure 4.4B). PARPs protein having zinc finger such as PARP1 are involved in DNA repair (Ali et al., 2012). The sequence alignment of *Ae. aegypti* with human PARPs revealed that, *Ae. aegypti* PARP has the highest similarity to the human PARP1 (Figure 4.4A) (44.6% with 99 % query coverage). The second domain from the N-terminal of the protein was BCRT (BRCA1 C-terminus) domain. It is a 95 amino acid long domain and is involved in cellular response, DNA repair, and cell cycle checkpoint (Leung & Glover, 2011). The other domains were PARP alpha and PARP catalytic domain. The PARP alpha domain transfers the activation signal upon binding to the site of DNA damage, while the catalytic domain adds poly ADP ribose chain to the site. All these indicate that PARP is a DNA damage repair enzyme.

3) MARP: Mono ADP ribose polymerase (MARP) is an ADP ribose polymerase enzyme that adds mono ADP ribose unit to the proteins. These proteins are not capable of adding more ADP ribose subunits to the terminals of already attached ADP ribose subunits. The *Ae. aegypti* MARP protein was only 362 amino acids long and contained only a catalytic domain (Figure 4.4B). For the protein-protein interactions, the ADP ribose chain needs to be 200 ADP ribose

subunits in length (Alvarez-Gonzalez & Jacobson, 1987). It is possible that MARP modification is involved in protein enzymatic activity. The sequence alignment search against humans revealed that the *Ae. aegypti* MARP has the highest similarity with human PARP16 (Figure 4.4A). It had 40% identity with 72% query coverage. PARP16 is a mono ADP ribose polymerase. It is an ER transmembrane protein and is involved in the activation of PERK (PKR-like ER kinase) and IRE1a (inositol requiring enzyme 1 α) in unfolded protein response (Jwa & Chang, 2012).

4.3. Discussion

CHIKV replication is known to hijack the host machinery to regulate its own replication (Fros et al., 2012). Owing to its ability to replicate in diverse organisms such as humans and the mosquito, the virus has evolved to manipulate both organisms to ensure its survival during adverse conditions. The nature of infection of the virus in both the host and the vector is hugely disparate; the virus multiplies exponentially in the human host cells that triggers a rapid launch of the host immune system, thereby resulting in faster virus clearance, whereas the virus replication is much slower in the insect cells. The virus can survive in the insect cells throughout the life of the mosquito (Burgyan & Havelda, 2011; Li et al., 2013). The virus employs multiple strategies for its survival in both the host and the insect, depending on the host's kind of defense, and the vector mounts on the virus. In the case of mosquitoes, RNAi is an important defense mechanism employed to counter viral infections (Abraham et al., 2018; McPherson et al., 2017). Several studies have shown arboviruses specifically activate the RNAi pathway in mosquitoes in addition to other innate immune systems such as the TOLL pathway, IMD pathway, and the JAK-STAT pathway (Li et al., 2006). Earlier reports have shown that in the case of arboviruses and CHIKV, RNAi was amongst the immune pathways to be activated upon virus infection (Ali et al., 2012). In the present study, transcript profiling of RNAi factors such as Ago-2, Dicer-2, FMR, TSN, and VIG upon the condition with different MOIs of the virus revealed that at lower MOIs, there was distinct regulation of RNAi factors. Some of the factors showing downregulation while others showed upregulation, whereas, in higher MOI, most of the RNAi factors were downregulated except for Dicer. Further in-depth studies to understand the possible role of Dicer-mediated cleavage of dsRNA during CHIKV infection are necessary, as observed in other arboviruses.

CHIKV-nsP3 is a vital protein owing to its multiple functions in CHIKV replication in the host and vector. In the present study, CHIKV-nsP3 was interacting with numerous proteins of

various pathways that include translation, heat shock proteins, oxidation-reduction, biomolecule transport, cellular metabolism, gene expression, protein. Such multiple interactions have been possible due to three domains in the protein, namely, macro domain, Alphavirus unique domain (AUD), and hypervariable domain (HVD). Except for the macrodomain (which has ADP ribosyl hydrolase activity), other domains don't have any enzymatic activity; however, all the domains are essential, and mutation of amino acids in these regions affects viral growth and viral replication (Jwa & Chang, 2012; Shrinet et al., 2012). Among the domains, HVD is known as the hub of host proteins binding. It helps in recruiting the host proteins when the replication complex is formed.

It is important to mention that most of the PARP-related work has been done on humans. There has been very little or no information about *Aedes* PARPs. The use of sequence alignment and BLAST tool with human PARPs have shown that there is three ADP ribose in *Aedes aegypti*. Of these, one was PARP and has zinc finger domain, and sequence alignment analysis showed it had shown the highest similarity to human PARP1, which has a role in DNA repair. The other was mono ADP ribose polymerase. The MARPs are known to add mono ADP ribose to the targets and are capable of adding poly ADP ribose. The third one was Tankyrase which had Ankyrin repeat and SAM domain. Both of which have a role in protein-protein interactions indicating that it might have a role in ADP ribosylation of target proteins.

4.4. Materials and methods

4.4.1. Cell lines and virus

Aag2 cell line was a kind gift from Dr. Alain Kohl (University of Glasgow, Scotland, UK). Cells were propagated in Leibovitz's L-15 medium (Cat no. AL011S, HiMedia, India) supplemented with 10% fetal bovine serum (FBS), glutamine, tryptose phosphate broth, and penicillin/streptomycin at 28°C and 5% CO₂. The Vero cell line (ATCC-CCL-81) and C6/36 cells were maintained in Dulbecco's Modified Eagle Media (DMEM) (Cat no: AL007A, HiMedia, India) supplemented with 10% FBS, penicillin/streptomycin at 37°C and 5% CO₂. CHIKV (Accession no. JF950631.1) was isolated and purified from a patient serum collected during an outbreak in 2010 (Shrinet et al., 2012) and propagated in both C6/36 and Vero cell lines in alternate cycles. Virus purified from Vero cells was used for Aag2 infection.

4.4.2. Virus infection

Aag2 cells were grown in 6-well plates in complete L-15 media. Cells were infected with CHIKV strain at a multiplicity of infection (MOI) of 0.1, 1, and 10. The virus was diluted in serum and antibiotic-free L-15 media, and cells were incubated at 28°C. After 2 hours post-infection (hpi), cells were washed with phosphate-buffered saline (PBS) (pH 7.4) and grown in complete L-15 media. The cells and media were collected at different time points, and cell pellets were washed once with PBS and either resuspended in TRIzol for RNA isolation or lysis buffer for western blot.

4.4.3. Plaque assay

CHIKV was quantified with plaque assay using a previously described protocol (Sirisena et al., 2018). Briefly, Vero cells were seeded in a 96-well plate in DMEM with 10% FBS. Supernatant media collected of MOI of 0.1, 1, and 10 at different time points from CHIKV infected Aag2 cells was added at different dilutions and incubated for 1 h. After the incubation, viruses containing media were removed from the wells and covered with 1% carboxymethylcellulose (CMC) in serum-free media. Cells were incubated for 48 h at 37°C. Post washing with PBS, cells were fixed with 4% formaldehyde and stained with 0.25% crystal violet in 30% methanol. Virus titer in infected cells was calculated by plaque-forming units (pfu) = (No. of plaques)/(Dilution × volume of the virus).

4.4.4. Quantitative real-time PCR

Expression profiles of RNAi factors and CHIKV genes were performed from infected cells from different time points. The sequences of RNAi factors were retrieved from ImmunoDB, and the CHIKV-nsP3 sequence was taken from CHIKV/IND/DEL/01 strain (Accession no. JF950631.1) (Shrinet et al., 2012). Primers for qPCR were made using the Prime Quest tool of Integrated DNA Technologies (IDT) with amplicon lengths ranging from 90-110 nucleotides.

Primer names	Forward Primer	Reverse Primer
Ago-2	TACCCGGCTCCAACCTATTA	CTGCATTCTCTCGTACTCCTTG
Dicer-2	TTGCTACCGTTGGGAGTTATG	GTGACAGTCGAAGGGTTGAATA
RPS17	GTGAGCGCAGAGACAACACTAC	TCCAGCTGCTTCAACATCTC
TSN	CACTGTGGTGGGAAGTGTTCA	GCCTCACGTGGAGGTTTAAT

VIG	GCCGAAAGACGCCAGATTA	CGTTTGTTCCTACTCTGTGATT
R2D2	GACGAATTGCTCTGGACGAA	CGCTGTTGTCTCGTTTCATTTC-
FMR1	AGAGCTGAACAGTGTTGATAGG	CTGGACATTTCCGTTGGATTG
CHIKV-E1	TACCCATTTATGTGGGGC	GCCTTTGTACACCACGATT
CHIKV-nsP3	AAGGCGCACTGTACTCATATC	TAGGCAGACTTGCTCATTGG

Total RNA was extracted from cells using Trizol and quantified with Nanodrop. We used 300ng RNA per reaction. The qPCR was carried out using the Quantitect SYBR green one-step real-time PCR kit (Cat. no. 204243 Qiagen). The qPCR was done with the protocol as cDNA synthesis 50°C for 30 min, initial denaturation at 95°C for 2 min, followed by 40 cycles as denaturation at 95°C for 15 s, annealing at 56°C for 30 s and extension at 72°C for 30 s, data acquisition and followed by melt curve analysis. Expression values were normalized to RPS17 housekeeping control mRNA levels. Relative log-fold expression levels were calculated using $2^{(-\Delta\Delta CT)}$ method (Schmittgen & Livak, 2008) and represented as mean \pm SD. Statistical analysis of experimental data was conducted using GraphPad Prism (version 6). Two-tailed student's t-test and Fisher's Least Significant Difference (LSD) test were performed to check the significance of the data, and p-values < 0.001 were considered significant.

4.4.5. Generation of plasmid constructs

To clone full-length CHIKV-nsP3 protein, the viral RNA was isolated using the High Pure Viral RNA Kit (Cat. no. 11858882001, Roche). Both RM62F and CHIKV-nsP3 were amplified using gene-specific primers such as CHIKV-nsP3: (Forward: 5'-GTTGGTACCATGGCACCGTCGTACCGGGTAAAAC -3'), (Reverse: 5'-CGTGGATCCACTTCTCCTGGTAAGAAGTCTCCG -3') with the PrimeScript One-Step RT PCR kit (Cat. no. RR055A, Takara, Japan) as per manufacturer instructions and cloned pET29a vector which have S-Tag at N-terminal and His-Tag in C-terminal for protein expression.

4.4.6. Protein purification

CHIKV-nsP3 was purified using a previously published protocol (George et al., 2019). Briefly, CHIKV-nsP3 was transformed into *E. coli* BL21-CodonPlus cells. CHIKV-nsP3 expressing *E. coli* cells were grown separately at 37°C and induced overnight with 1 mM IPTG at 18°C. The cells were collected and lysed in lysis buffer (50 mM Tris-Cl pH (8.0), 150 mM NaCl, 1%

NP40, 5% glycerol, 3mM β -mercaptoethanol, with 1mM PMSF and lysozyme). After sonication and centrifugation, the lysates were loaded onto an affinity column (Ni-NTA) and washed with lysis buffer containing 20 mM Imidazole. Proteins were eluted with a lysis buffer having 300 mM imidazole. The elution fraction was confirmed with SDS-PAGE and Western blot for proteins. Eluted fractions containing purified CHIKV-nsP3 were confirmed by Western blot and concentrated. The proteins were used for further assays.

4.4.7. Antibody generation

Antibodies against proteins were raised in-house in New Zealand white rabbit. The pre-bleed was collected at day 0. Purified CHIKV-nsP3 protein were injected into rabbits with Freund's complete adjuvant. Booster doses of respective proteins with Freund's incomplete adjuvant were given in regular intervals, and serum were collected. Antibody specificity was checked against purified protein with pre-bleed as well as bleeds collected at different time points and later against cell lysate to confirm the reactivity. Detailed protocol is given in chapter 2.

4.4.8. Co-immunoprecipitation (Co-IP)

To identify the interacting partners of CHIKV-nsP3 with *Ae. aegypti* co-immunoprecipitation assay Aag2 lysate with nsP3 protein was done with purified nsP3 protein using Pierce co-immunoprecipitation kit (Thermo Scientific, USA) as per the manufacturer's instructions. Briefly, 100 μ l Protein A beads were incubated with CHIKV-nsP3 specific antibody, and after wash, these were incubated with purified nsP3 protein (100 μ g) and allowed to bind overnight to antibody at 4°C. For negative control, antibody immobilized beads were directly incubated with Aag2 cell lysate. Beads were washed with IP wash buffer and incubated with Aag2 lysate (1 mg) for 4 h. After washing, elution fractions were processed for western blot and mass spectrometry.

4.4.9. Mass spectrometry

25 μ l samples were taken and reduced with 5 mM TCEP and further alkylated with 50 mM iodoacetamide and then digested with Trypsin (1:50, Trypsin/lysate ratio) for 16 h at 37°C. Digests were cleaned using a C18 silica cartridge to remove the salt and dried using a speed vac. The dried pellet was resuspended in buffer A (5% acetonitrile, 0.1% formic acid).

4.4.10. Mass spectrometric analysis of peptide mixtures

All the experiment was performed using EASY-nLC 1000 system (Thermo Fisher Scientific) coupled to Thermo Fisher-QExactive equipped with nanoelectrospray ion source. 1.0 µg of the peptide mixture was resolved using 20 cm PicoFrit column (360 µm outer diameter, 75 µm inner diameter, 10 µm tip) filled with 1.9 µm of C18-resin (Dr Maeisch, Germany). The peptides were loaded with buffer A and eluted with a 0–40% gradient of buffer B (95% acetonitrile, 0.1% formic acid) at a flow rate of 300 ml/min for 100 min. MS data were acquired using a data-dependent top10 method dynamically choosing the most abundant precursor ions from the survey scan.

4.4.11. Data processing

All samples were processed, and RAW files generated were analyzed with Proteome Discoverer (v2.2) against the Uniprot Human, Chikungunya, and *Ae. aegypti* reference proteome database. For Sequest search, the precursor and fragment mass tolerances were set at 10 pm and 0.5 Da, respectively. The protease used to generate peptides, i.e., enzyme specificity, was set for trypsin/P (cleavage at the C terminus of "K/R: unless followed by "P") along with a maximum missed cleavages value of two. Carbamidomethyl on cysteine as fixed modification and oxidation of methionine and N-terminal acetylation were considered as variable modifications for database search. Both peptide spectrum match and protein false discovery rate were set to 0.01 FDR.

The proteins which were present in the sample after removing the one which was also present in negative control were taken. The functional enrichment was done using ShinyGO v0.66 ([ShinyGO v0.66: Gene Ontology Enrichment Analysis + more \(sdstate.edu\)](https://shinygo.ucdavis.edu/)). The P-values cutoff (FDR) was set to 0.05. The gene details corresponding to the IDs were fetched from the Uniprot database.

4.4.12. Western blot assay

Protein sample concentration was determined by Bradford's reagent and plotted against bovine serum albumin (BSA) standards of known concentrations. An equal amount of protein samples was loaded in 10% SDS-PAGE gels and run at 100 V till the dye front reaches the other end. Proteins were then transferred onto the nitrocellulose membrane. The membrane was then blocked with PBS (pH 7.4) + 5% BSA for 1hr at RT (room temperature). The membrane was then incubated with primary antibodies (1:2,000 dilution) in PBS+2.5% BSA overnight at 4°C. The membrane was then washed with PBS+ 0.1% Tween-20 for 10 min and repeated thrice. It was then incubated with anti-mice IgG HRP secondary antibodies (1:5,000 dilution) in

PBST+2.5% BSA for 1h at RT. The membrane was then washed with PBS+ 0.1% Tween-20 for 3 X 10 min. The membrane was then visualized in Chemidoc MP (Bio-Rad) after brief incubation with SuperSignal West Pico Chemiluminescent Substrate (Thermo Scientific).

4.4.13. Protein sequence analysis of *Aedes aegypti* PARPs

The proteins sequences of *Ae. aegypti* ADP ribose polymerases were retrieved from the NCBI database by direct name search on Home - Protein - NCBI (nih.gov) and BLAST search against human PARPs. For the analysis of the domain of the proteins' sequences were submitted to the online database at ScanProsite (expasy.org).

4.4.14. Multiple sequence alignment of alphavirus macrodomain

The protein sequences macrodomain of alphaviruses were retrieved from the NCBI database. The multiple sequence alignment and phylogenetic analysis was done in the MEGA 11 software.

4.4.15. Immunofluorescence assay

Cells were grown in the respective temperature and media conditions. For the assay, the cells were grown in 6 well plates with sterile glass coverslips at 30% confluency. The cells were infected with CHIKV at MOI of 1 for respective time points. Cells were then fixed with 4% paraformaldehyde and permeabilized with PBST (PBS+0.1% Triton-X-100). Cells were then blocked with 5% BSA and then probed with rabbit-raised anti-CHIKV nsP3 antibody overnight at 4°C. The cells were washed with PBST (PBS+0.1% Triton-X-100) for 3X10 min and then incubated with anti-rabbit Alexa 594 labelled IgG antibody at 1:400 dilution in PBST (PBS+0.1% Triton-X-100) with 2.5% BSA for 1 h at room temperature. The cells were washed with PBST (PBS+0.1% Triton-X-100) for 3X10 min. Cells were incubated with DAPI solution briefly, and then coverslips were mounted on a glass slide for visualization in a fluorescence microscope.

4.5. References

- Abraham, R., Hauer, D., McPherson, R. L., Utt, A., Kirby, I. T., Cohen, M. S., . . . Griffin, D. E. (2018). ADP-ribosyl-binding and hydrolase activities of the alphavirus nsP3 macrodomain are critical for initiation of virus replication. *Proc Natl Acad Sci U S A*, *115*(44), E10457-E10466. <https://doi.org/10.1073/pnas.1812130115>
- Agrawal, N., Dasaradhi, P. V., Mohmmed, A., Malhotra, P., Bhatnagar, R. K., & Mukherjee, S. K. (2003). RNA interference: biology, mechanism, and applications. *Microbiol Mol Biol Rev*, *67*(4), 657-685. <https://doi.org/10.1128/mubr.67.4.657-685.2003>

- Akhrymuk, I., Kulemzin, S. V., & Frolova, E. I. (2012). Evasion of the innate immune response: the Old World alphavirus nsP2 protein induces rapid degradation of Rpb1, a catalytic subunit of RNA polymerase II. *J Virol*, *86*(13), 7180-7191. <https://doi.org/10.1128/JVI.00541-12>
- Ali, A. A. E., Timinszky, G., Arribas-Bosacoma, R., Kozlowski, M., Hassa, P. O., Hassler, M., . . . Oliver, A. W. (2012). The zinc-finger domains of PARP1 cooperate to recognize DNA strand breaks. *Nat Struct Mol Biol*, *19*(7), 685-692. <https://doi.org/10.1038/nsmb.2335>
- Alvarez-Gonzalez, R., & Jacobson, M. K. (1987). Characterization of polymers of adenosine diphosphate ribose generated in vitro and in vivo. *Biochemistry*, *26*(11), 3218-3224. <https://doi.org/10.1021/bi00385a042>
- Berntsen, B. T., James, A. A., & Christensen, B. M. (2000). Genetics of mosquito vector competence. *Microbiol Mol Biol Rev*, *64*(1), 115-137. <https://doi.org/10.1128/MMBR.64.1.115-137.2000>
- Bourai, M., Lucas-Hourani, M., Gad, H. H., Drosten, C., Jacob, Y., Tafforeau, L., . . . Vidalain, P. O. (2012). Mapping of Chikungunya virus interactions with host proteins identified nsP2 as a highly connected viral component. *J Virol*, *86*(6), 3121-3134. <https://doi.org/10.1128/JVI.06390-11>
- Burgyan, J., & Havelda, Z. (2011). Viral suppressors of RNA silencing. *Trends Plant Sci*, *16*(5), 265-272. <https://doi.org/10.1016/j.tplants.2011.02.010>
- Cristea, I. M., Carroll, J. W., Rout, M. P., Rice, C. M., Chait, B. T., & MacDonald, M. R. (2006). Tracking and elucidating alphavirus-host protein interactions. *J Biol Chem*, *281*(40), 30269-30278. <https://doi.org/10.1074/jbc.M603980200>
- Ding, S. W., & Voinnet, O. (2007). Antiviral immunity directed by small RNAs. *Cell*, *130*(3), 413-426. <https://doi.org/10.1016/j.cell.2007.07.039>
- Frolova, E., Gorchakov, R., Garmashova, N., Atasheva, S., Vergara, L. A., & Frolov, I. (2006). Formation of nsP3-specific protein complexes during Sindbis virus replication. *J Virol*, *80*(8), 4122-4134. <https://doi.org/10.1128/JVI.80.8.4122-4134.2006>
- Fros, J. J., Domeradzka, N. E., Baggen, J., Geertsema, C., Flipse, J., Vlak, J. M., & Pijlman, G. P. (2012). Chikungunya virus nsP3 blocks stress granule assembly by recruitment of G3BP into cytoplasmic foci. *J Virol*, *86*(19), 10873-10879. <https://doi.org/10.1128/JVI.01506-12>
- Gammon, D. B., & Mello, C. C. (2015). RNA interference-mediated antiviral defense in insects. *Curr Opin Insect Sci*, *8*, 111-120. <https://doi.org/10.1016/j.cois.2015.01.006>
- George, A., Amrutha, M. S., Srivastava, P., Sai, V. V. R., Sunil, S., & Srinivasan, R. (2019). Label-Free Detection of Chikungunya Non-Structural Protein 3 Using Electrochemical Impedance Spectroscopy. *Journal of The Electrochemical Society*, *166*(14), B1356-B1363. <https://doi.org/10.1149/2.1081914jes>
- Ghosh, S., Kakumani, P. K., Kumar, A., Malhotra, P., Mukherjee, S. K., & Bhatnagar, R. K. (2014). Genome wide screening of RNAi factors of Sf21 cells reveal several novel pathway associated proteins. *BMC Genomics*, *15*, 775. <https://doi.org/10.1186/1471-2164-15-775>
- Gorchakov, R., Garmashova, N., Frolova, E., & Frolov, I. (2008). Different types of nsP3-containing protein complexes in Sindbis virus-infected cells. *J Virol*, *82*(20), 10088-10101. <https://doi.org/10.1128/JVI.01011-08>
- Gotte, B., Liu, L., & McInerney, G. M. (2018). The Enigmatic Alphavirus Non-Structural Protein 3 (nsP3) Revealing Its Secrets at Last. *Viruses*, *10*(3). <https://doi.org/10.3390/v10030105>
- Jayabalan, A. K., Adivarahan, S., Koppula, A., Abraham, R., Batish, M., Zenklusen, D., . . . Leung, A. K. L. (2021). Stress granule formation, disassembly, and composition are regulated by alphavirus ADP-ribosylhydrolase activity. *Proc Natl Acad Sci U S A*, *118*(6). <https://doi.org/10.1073/pnas.2021719118>
- Jwa, M., & Chang, P. (2012). PARP16 is a tail-anchored endoplasmic reticulum protein required for the PERK- and IRE1alpha-mediated unfolded protein response. *Nat Cell Biol*, *14*(11), 1223-1230. <https://doi.org/10.1038/ncb2593>
- Lark, T., Keck, F., & Narayanan, A. (2017). Interactions of Alphavirus nsP3 Protein with Host Proteins. *Front Microbiol*, *8*, 2652. <https://doi.org/10.3389/fmicb.2017.02652>

- Leung, C. C., & Glover, J. N. (2011). BRCT domains: easy as one, two, three. *Cell Cycle*, *10*(15), 2461-2470. <https://doi.org/10.4161/cc.10.15.16312>
- Leung, J. Y., Ng, M. M., & Chu, J. J. (2011). Replication of alphaviruses: a review on the entry process of alphaviruses into cells. *Adv Virol*, *2011*, 249640. <https://doi.org/10.1155/2011/249640>
- Li, J., Mahajan, A., & Tsai, M. D. (2006). Ankyrin repeat: a unique motif mediating protein-protein interactions. *Biochemistry*, *45*(51), 15168-15178. <https://doi.org/10.1021/bi062188q>
- Li, X., Wu, Z., & Han, W. (2013). The macrodomain family: Rethinking an ancient domain from evolutionary perspectives. *Chin Sci Bull*, *58*(9), 953-960. <https://doi.org/10.1007/s11434-013-5674-9>
- McPherson, R. L., Abraham, R., Sreekumar, E., Ong, S. E., Cheng, S. J., Baxter, V. K., . . . Leung, A. K. (2017). ADP-ribosylhydrolase activity of Chikungunya virus macrodomain is critical for virus replication and virulence. *Proc Natl Acad Sci U S A*, *114*(7), 1666-1671. <https://doi.org/10.1073/pnas.1621485114>
- Meshram, C. D., Agback, P., Shiliaev, N., Urakova, N., Mobley, J. A., Agback, T., . . . Frolov, I. (2018). Multiple Host Factors Interact with the Hypervariable Domain of Chikungunya Virus nsP3 and Determine Viral Replication in Cell-Specific Mode. *J Virol*, *92*(16). <https://doi.org/10.1128/JVI.00838-18>
- Miller, C. L. (2011). Stress Granules and Virus Replication. *Future Virol*, *6*(11), 1329-1338. <https://doi.org/10.2217/fvl.11.108>
- Mosavi, L. K., Cammett, T. J., Desrosiers, D. C., & Peng, Z. Y. (2004). The ankyrin repeat as molecular architecture for protein recognition. *Protein Sci*, *13*(6), 1435-1448. <https://doi.org/10.1110/ps.03554604>
- Obbard, D. J., Welch, J. J., Kim, K. W., & Jiggins, F. M. (2009). Quantifying adaptive evolution in the Drosophila immune system. *PLoS Genet*, *5*(10), e1000698. <https://doi.org/10.1371/journal.pgen.1000698>
- Pialoux, G., Gauzere, B. A., Jaureguiberry, S., & Strobel, M. (2007). Chikungunya, an epidemic arbovirosis. *Lancet Infect Dis*, *7*(5), 319-327. [https://doi.org/10.1016/S1473-3099\(07\)70107-X](https://doi.org/10.1016/S1473-3099(07)70107-X)
- Samuel, G. H., Wiley, M. R., Badawi, A., Adelman, Z. N., & Myles, K. M. (2016). Yellow fever virus capsid protein is a potent suppressor of RNA silencing that binds double-stranded RNA. *Proc Natl Acad Sci U S A*, *113*(48), 13863-13868. <https://doi.org/10.1073/pnas.1600544113>
- Schmittgen, T. D., & Livak, K. J. (2008). Analyzing real-time PCR data by the comparative C(T) method. *Nat Protoc*, *3*(6), 1101-1108. <https://doi.org/10.1038/nprot.2008.73>
- Shrinet, J., Jain, S., Sharma, A., Singh, S. S., Mathur, K., Rana, V., . . . Sunil, S. (2012). Genetic characterization of Chikungunya virus from New Delhi reveal emergence of a new molecular signature in Indian isolates. *Virol J*, *9*, 100. <https://doi.org/10.1186/1743-422X-9-100>
- Sirisena, P., Kumar, A., & Sunil, S. (2018). Evaluation of Aedes aegypti (Diptera: Culicidae) Life Table Attributes Upon Chikungunya Virus Replication Reveals Impact on Egg-Laying Pathways. *J Med Entomol*, *55*(6), 1580-1587. <https://doi.org/10.1093/jme/tjy097>
- Slaughter, B. D., Huff, J. M., Wiegraebe, W., Schwartz, J. W., & Li, R. (2008). SAM domain-based protein oligomerization observed by live-cell fluorescence fluctuation spectroscopy. *PLoS One*, *3*(4), e1931. <https://doi.org/10.1371/journal.pone.0001931>
- Strauss, J. H., & Strauss, E. G. (1994). The alphaviruses: gene expression, replication, and evolution. *Microbiol Rev*, *58*(3), 491-562. <https://doi.org/10.1128/mr.58.3.491-562.1994>
- Tolia, N. H., & Joshua-Tor, L. (2007). Slicer and the argonautes. *Nat Chem Biol*, *3*(1), 36-43. <https://doi.org/10.1038/nchembio848>
- Wong, K. Z., & Chu, J. J. H. (2018). The Interplay of Viral and Host Factors in Chikungunya Virus Infection: Targets for Antiviral Strategies. *Viruses*, *10*(6). <https://doi.org/10.3390/v10060294>

Chapter 5

Chapter 5

Characterization of *Ae. aegypti* interacting partners

5.1. Confirmation of nsP3 interacting partner in Aag2 cells

5.1.1. Introduction

Viral proteins interact with host proteins to facilitate their replication. Host protein helps the virus in its genome replication, translation, modifications, etc. Host immune pathways proteins are also known to target viral proteins to counter infection by targeting them to degradation (Rothenburg & Brennan, 2020). CHIKV nsP3 protein is a crucial protein of CHIKV as it forms the replication complex. The N-terminal domain, called macrodomain, has ADP ribosylhydrolase, the middle domain is called Alphavirus unique domain or AUD, and the C-terminal domain is called hypervariable domain or HVD. The macrodomain removed the ADP ribose moieties from the target proteins, whereas the exact function of AUD is not known. The HVD domain is highly variable and acts to recruit host proteins to facilitate (Gotte et al., 2018; Huang et al., 2019; Lark et al., 2017; Meshram et al., 2018). Studies on human cells have shown that protein from pathways such as translation, stress response, and RNA metabolism interact with alphavirus nsP3 protein (Gotte et al., 2018; Lark et al., 2017).

In this study the focus was on RNA-related pathways with emphasis on the RNAi pathway considering the role of the pathways in mosquito innate immunity. Of these RNAi pathway proteins, the DEAD Box helicase was of considerable interest owing to the role in siRNA pathways as well as DEAD/DExH box helicases such as DDX1, DHX9, and DDX5, play in viral replication and are known to interact with viral non-structural proteins (Cheng et al., 2018; Fu et al., 2019; Xu et al., 2010). We found that RM62F was one of the RNA helicase interacting with the nsP3 protein. The interaction was confirmed with immunoblotting of co-immunoprecipitated lysate with RM62F specific antibodies.

5.1.2. Results

5.1.2.1. CHIKV-nsP3 interacts with RM62F

Among the *Aedes* proteins interacting with the nsP3 protein after the co-immunoprecipitation (in chapter 4), the focus was given to those involved in RNAi

pathway. The analysis of mass spectrometry data revealed that RM62F, a DEAD-box ATP-dependent RNA helicase and PIWI5 interacts with nsP3 protein. Both the proteins belong to the RNAi pathway, but RM62F was chosen as it was also present in the previous analysis of nsP3 pull-down coupled with mass spectrometry (data not shown here). To understand the interaction of RM62F with CHIKV-nsP3. The N-terminal domain of RM62F was cloned in the pET29a vector, and the protein was purified from *E. coli* expression cells and tested by western blot with anti-His HRP antibody (Figure 5.1). Antibodies were generated in mice against the purified protein in balb/c mice. The serum was tested against Aag2 lysate.

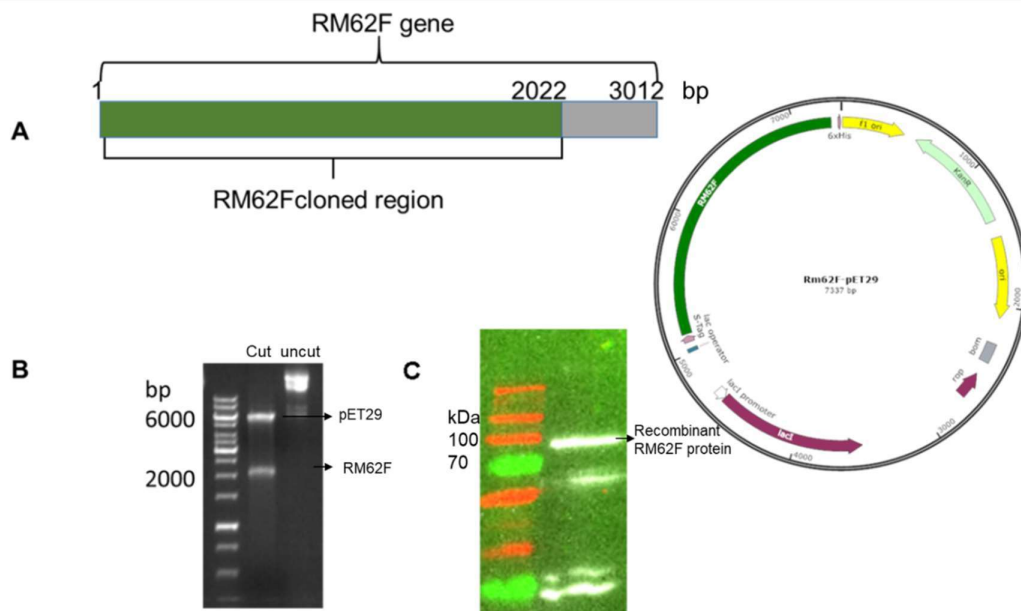


Figure 5.1 Cloning and expression of *Ae. aegypti* RM62F N terminal domain. A) RM62F region selected for cloning in pET29a vector and vector map of RM62F domain cloned in pET29a plasmid; B) Restriction digestion of RM62F cloned in pET29a. Lane 1: 1kb DNA ladder, Lane 2: double digested RM62F-pET29a and Lane 3 uncut RM62F-pET29a; and C) western blot of purified recombinant RM62F domain. For western blot, anti-His HRP tagged antibody (1:4000 dilution).

Next, the expression of RM62F transcript was evaluated during CHIKV infection in Aag2 cells at MOI of 1 and 10 over 72 hpi at 12 h intervals. At the transcript level, at MOI of 1, RM62F was overexpressed at the initial time points of infection till 24 hpi

and then reduced at 36 hpi and then increased till 72 hpi. In MOI 10, the expression reduced to 36 hpi and then increased to 72 hpi (Figure 5.2A).

In the case of protein expression, it was found that the protein level was reduced to 36 hpi as the infection proceeds and resumed slightly at 48 hpi (Figure 5.2B). The transcript level and protein profiling results revealed that RM62F was getting temporally affected during CHIKV infection in Aag2 cells. As the next step, the interaction was validated by performing a co-IP assay using antibodies against CHIKV-nsP3 in uninfected Aag2 cells. The purified protein of CHIKV-nsP3 incubated with nsP3 antibodies immobilized onto beads served as the positive control, while Aag2 lysate incubated with beads only served as the negative control in the immunoprecipitation assay. Post incubation of the lysate with CHIKV-nsP3 protein, the sample assessed for the protein confirmed the specificity of CHIKV-nsP3 as shown in lane 4 of Fig 5.2C. Co-IP assay of nsP3 using the CHIKV-nsP3 specific antibodies in Aag2 lysate and immunoblotting using CHIKV-nsP3 and RM62F specific antibodies revealed a direct interaction between these two proteins (Figure 5.2C).

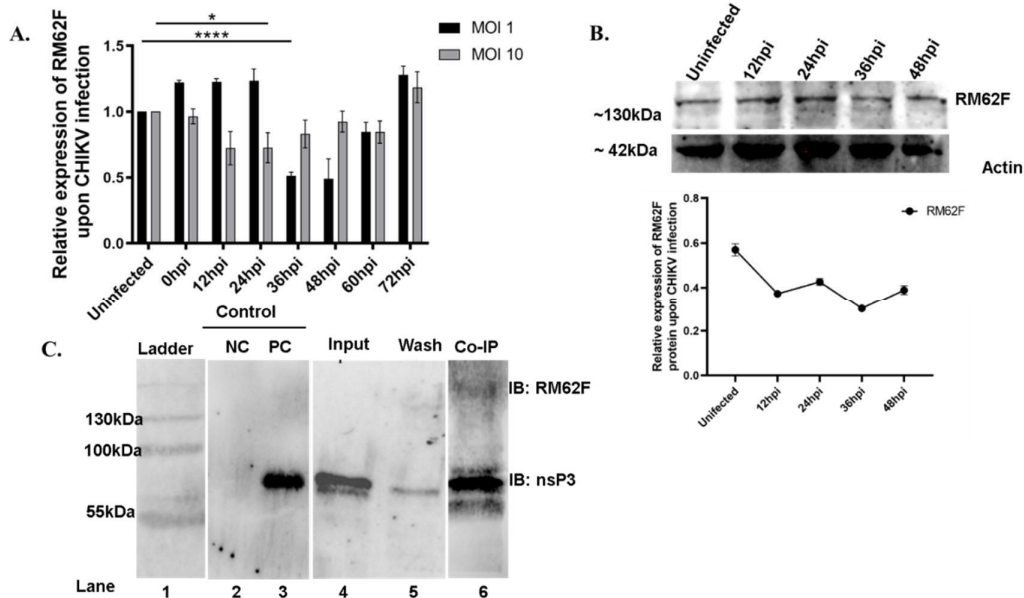


Figure 5.2 Interaction of *Ae. aegypti* host factor RM62F with CHIKV-nsP3 protein. A) Expression profiling of RM62F transcript upon CHIKV post-infection in Aag2 cells. 0 hpi samples and different infection time points like 12, 24, 36, 48, 60, and 72 hpi at MOI of 10 were checked with the antibody against RM62F and RPS17 as an

internal control. Relative comparison of RM62F expression levels at different infection time points; **B**) Expression profiling of RM62F protein upon CHIKV post-infection in Aag2 cells. Control (Uninfected) samples along with different infection time points like 12, 24, 36, and 48 hpi at MOI of 10 were checked with the antibody against RM62F and actin (as a loading control); and **C**) Co-IP of Aag2 lysate with recombinant nsP3 using anti-CHIKV nsP3 antibody. Immunoblotting was done with anti-CHIKV-nsP3 antibody and anti RM62F antibody. Lane1: Prestained protein ladder, lane 2: negative control (NC) represent elution of uninfected Aag2 lysate incubated with anti nsP3 antibody immobilized beads, and then probing with nsP3 specific antibody lane 3: positive control (PC) represent elution of recombinant nsP3 with anti-nsP3 antibody immobilized beads and probing with nsP3 specific antibody, lane 4: Pure CHIKV-nsP3 protein, probed with nsP3 specific antibody, lane 5: wash fraction after CHIKV-nsP3 incubation and lane 6: Co-IP of Aag2 lysate with recombinant nsP3 which is bound to the anti-nsP3 antibody immobilized beads and blotted with nsP3 and RM62F specific antibodies.

5.2. Isolation and characterization of catalytic domain of *Ae. aegypti* Tankyrase protein

5.2.1. Introduction

Post-translational modifications (PTMs) of proteins are essential for the cellular housekeeping functions of the cells. PTMs include adding small proteins or functional groups such as ubiquitination, lipidation, glycosylation, methylation, phosphorylation, and acetylation to specific amino acids within the protein (Rahnefeld et al., 2014; Santos & Lindner, 2017; Zhang et al., 2017). PTMs are carried out by specialized enzymes, such as ubiquitin E3 ligase, glycosyltransferase, poly ADP ribose polymerase (PARP), acetyltransferase, kinases, etc. (Bharaj et al., 2017; Santos & Lindner, 2017). PTMs enhance solubilization, conformation (by altering charge or hydrophobicity), interactions, signaling, and degradation, thus playing a crucial role in cell growth (Ryslava et al., 2013). During infection, the host overcomes viral infection by inactivating viral proteins by attaching small molecules such as ubiquitin or ubiquitin-like proteins leading to their inactivation and/or proteasomal mediated degradation and activating immune response involving interferon response to inhibit viral replication. Viruses adopt a similar approach to replicate where their proteins either cleave host proteins involved in immune response and remove PTMs from their

proteins, which otherwise hinders its replication by targeting them to proteasomal degradation (Gustin et al., 2011; Randow & Lehner, 2009; Ribet & Cossart, 2010).

ADP-ribosylation is a ubiquitous modification across all life domains ranging from the virus to eukaryotic organisms (Cohen & Chang, 2018; Grunewald et al., 2018; Hottiger et al., 2010). ADP-ribosylation utilizes nicotinamide adenine dinucleotide (NAD) as a cofactor to transfer ADP-ribose nucleotide onto proteins and DNA (Cohen & Chang, 2018). The reaction is catalyzed by the enzyme ADP-ribosyl transferases known as ARTDs (ADP-ribosyltransferase, diphtheria toxin-like) or PARPs (Poly ADP ribose polymerase) (Figure 5.3) (Cohen & Chang, 2018). Modification by PARPs occurs mainly on acidic amino acid residues such as glutamate and aspartate, but other residues such as serine, arginine, lysine, and cysteines can also be acceptors (Hottiger et al., 2010).

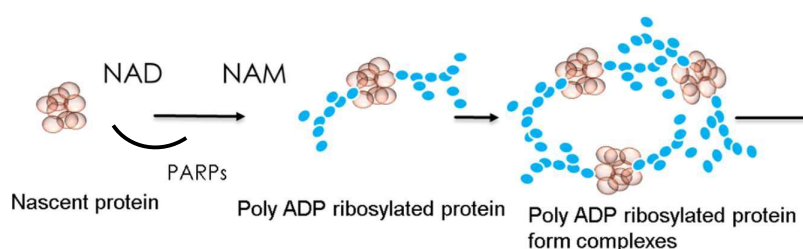


Figure 5.3 Mechanism of protein ADP ribosylation by poly ADP ribose polymerases (PARPs). PARPs modify the nascent proteins, and in the process, these enzymes use NAD (nicotinamide adenine dinucleotide) to act as a donor for ADP-ribose moieties to the proteins.

The modification plays a role in various processes like DNA damage repair, telomere maintenance, stress response and immune response, cell proliferation (Leung et al., 2011; Liu & Yu, 2015; Palazzo et al., 2019). The PAR chains promote protein complex formation by inducing phase separation and protein-protein interactions (Jin et al., 2021). The PARPs proteins localize to stress granules, affecting the assembly and disassembly of these membrane-less organelles (Isabelle et al., 2012). One of these complexes is RISC (RNA-induced silencing complex), central to the siRNA pathway. In the siRNA pathway, the host proteins bind to and cleave viral ds RNA genome into small RNAs by the action of Dicer proteins. The small RNAs are then loaded onto the RISC complex, which contains Ago2 protein and other accessory

proteins that convert dsRNA to ssRNA and then scan for complementary sequences (ssRNA genome) the target of siRNA pathways (Kumar et al., 2018). It has been found that the RNAi pathway proteins are ADP ribosylated, but detailed information is lacking about the proteins modified. During the viral infection, the expression level of the PARPs proteins increased. These possess antiviral properties, and their binding to viral RNA recruits the RNA decay factors (Bock et al., 2015).

Chikungunya virus encodes macrodomain, destabilizing the stress granules during viral infection and helps the virus in replication and growth (Jayabalan et al., 2021). This could be one of the ways other than protease and helicase-mediated viral suppression of RNA interference, a common mechanism of suppression of host immune system by viruses. CHIKV macrodomain is one of the three domains of CHIKV-nsP3 protein, is an ADP ribosylhydrolase, which can catalyze the hydrolysis of ADP ribose from polymer chain. Recent studies have highlighted that ribosylhydrolase activity was able to destabilize protein complexes (Abraham et al., 2018; Jayabalan et al., 2021; McPherson et al., 2017). The objective of this study was to identify, clone, and express the *Ae. aegypti* PARP proteins, which are essential for protein-protein interactions. Since the ADP ribosylation has an essential role in protein complexes formation, the capability of the Tankyrase catalytic domain was evaluated to add the PTM to the proteins. Additionally, the impact of the nsP3 macrodomain on PAR-modified protein was evaluated.

5.2.2. Results

5.2.2.1. Cloning and expression of *Ae. aegypti* Tankyrase protein

The literature survey provided evidence that full length PARP proteins are essential for functioning in the cells (Bai, 2015; Gupte et al., 2017; Riffell et al., 2012), but catalytic domain alone is sufficient to synthesize ADP ribose chains on the proteins. The work on human Tankyrase protein have showed that catalytic domain was monomeric in solution and need SAM domain for auto-PARylation (Fan et al., 2018).

The catalytic domain of *Ae. aegypti* Tankyrase protein was cloned into pET32a vector after amplification with specific primers (Figure 5.4A). The digested product ran at around 1100 bp in 1% agarose gel (Figure 5.4B), indicating that gene was cloned successfully in pET vector.

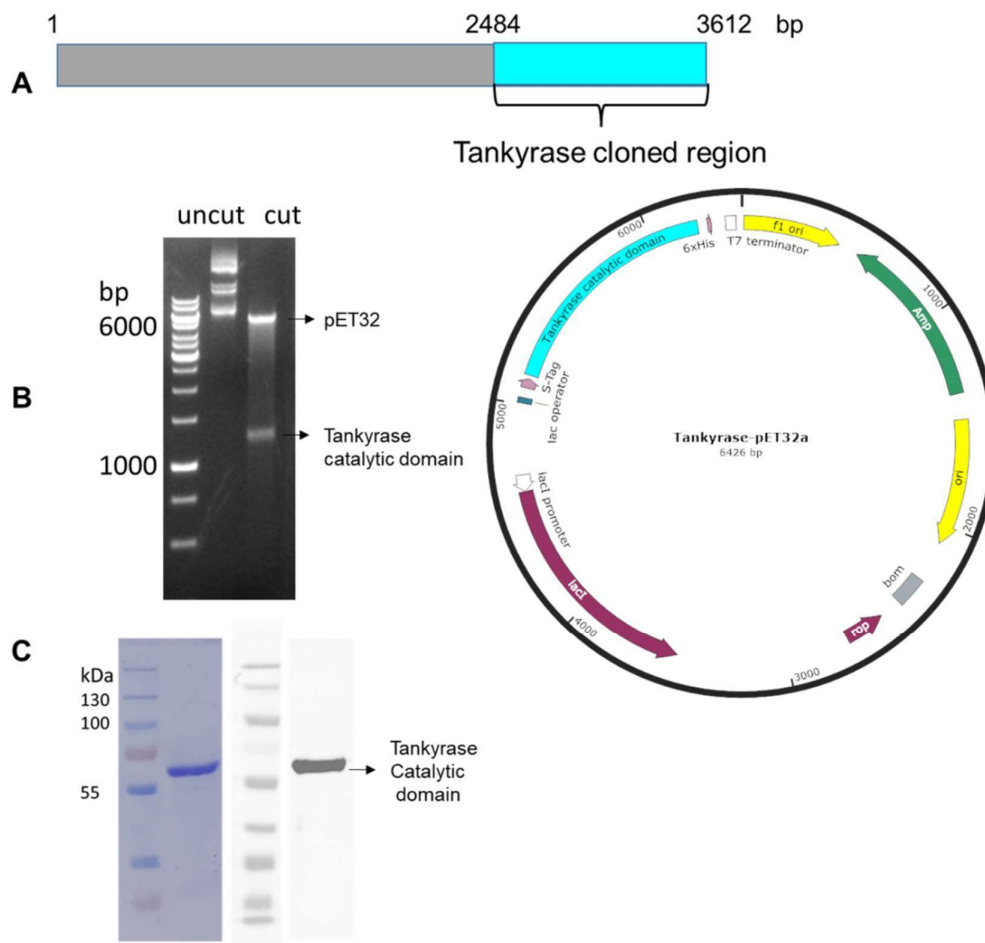


Figure 5.4 Cloning and expression of *Ae. aegypti* Tankyrase catalytic domain. A) Tankyrase region selected for cloning in pET32a vector and vector map of Tankyrase catalytic domain cloned in pET32a plasmid; B) Restriction digestion of Tankyrase catalytic domain cloned in pET32a. Lane 1: 1kb DNA ladder, Lane 2: uncut Tankyrase-pET32a, and Lane 3: double digested Tankyrase-pET32a; and C) Coomassie staining and western blot of purified recombinant Tankyrase catalytic domain. For western blot anti-His HRP tagged antibody (1:4000 dilution). Lane 1: Prestained protein ladder and Lane 2: Purified Tankyrase protein.

The clone was then transformed into *E. coli* BL21-CodonPlus expression cells. The expression cells were grown in LB media and the secondary culture was grown in TB media till OD reached around 1.5 which will take around 6-7 h. and then induced with 1 mM IPTG at 18°C for 16 h. The culture was centrifuged and then lysed with lysis buffer. After sonication and clarification, the protein was purified using affinity chromatography. The Ni-NTA beads were eluted with increasing imidazole

concentration. The elution was separated on 10% SDS PAGE gel. The purified protein was stained with Coomassie stain and checked for purity using western blot also. The purified protein has shown band at 60 kDa (Figure 5.4C).

5.2.2.2. *In vitro* PARylation assay of Tankyrase protein

The PARP proteins are multi-domain proteins, and each of these domains is critical to functioning in cells. These proteins add long ADP ribose chains of varying lengths to the target proteins (Figure 5.5A). The catalytic domains are sufficient to add ADP ribose subunits, although their specific activity, specificity, and auto-PARylation activity are affected by other domains. In this study, the catalytic domain of Tankyrase proteins was checked first for its ability to add ADP ribose subunits to the proteins. The PARylation assay was done as protocol mentioned in the materials and methods section.

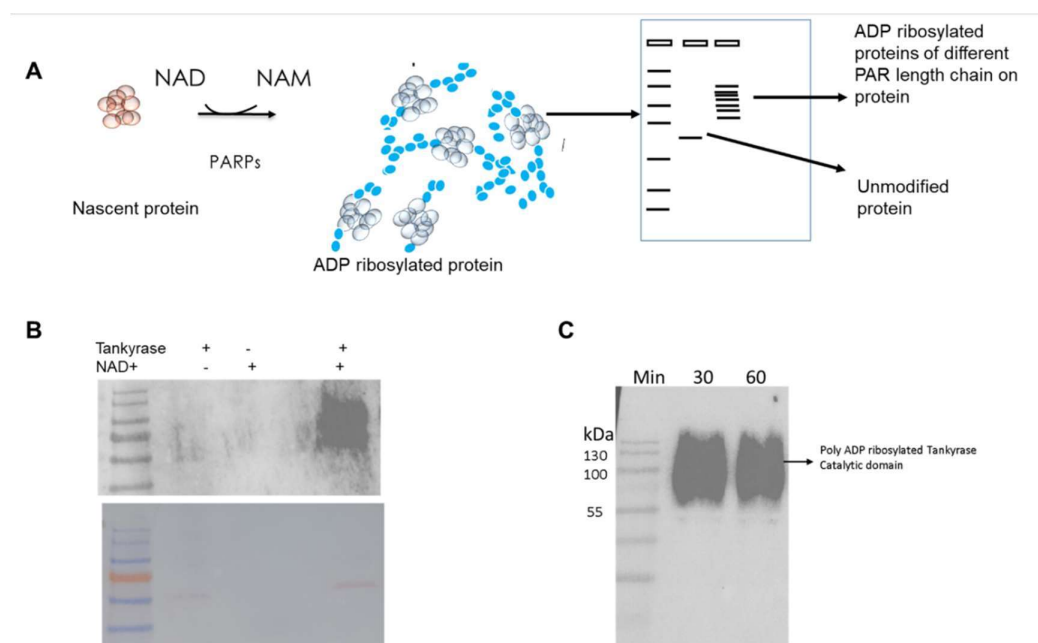


Figure 5.5 *In vitro* PARylation assay of Tankyrase catalytic domain. A) Schematic diagram of *in vitro* PARylation assay and gel run on SDS-PAGE of unmodified and ADP ribose modified sample; B) *In vitro* PARylation assay with Tankyrase alone (negative control), NAD⁺ alone (negative control) and Tankyrase with NAD⁺. The samples were run on SDS-PAGE and transferred onto nitrocellulose membrane and probed with mice anti-pADPr antibody; and C) Western blot of time points (30 and 60 min) of *in vitro* PARylated Tankyrase catalytic domain. The samples were separated on SDS-PAGE and then transferred onto a nitrocellulose membrane. The membrane

was then probed with an anti-pADPr mice antibody. It was then incubated with an anti-mice IgG HRP antibody, washed, and visualized in the gel documentation system after brief exposure to the chemiluminescent substrate.

The PARylation assay was done in 1.5 ml microfuge tubes at 28°C in a water bath for 5 min. The samples were run on SDS-PAGE gel and transferred onto the nitrocellulose membrane. The membrane was blocked and then incubated overnight with an anti-poly ADP ribose antibody. Anti-mice HRP tagged IgG secondary antibody was used for the detection of anti-pADPr antibody. After washing with PBST, the membrane was briefly incubated with chemiluminescent substrate and then visualized. Tankyrase run alone showed no bands in western blot as well as NAD⁺, whereas when mixed together Tankyrase with NAD⁺, indicating that the Tankyrase catalytic domain was able to add PTM in presence of NAD⁺ only (Figure 5.5B). A thick smear band appeared when reaction time was extended to 30 min and 60 min. The size of bands ranged from 60 kDa to more than 200 kDa, indicating that the protein was modified with ADP ribose with varying lengths of subunits (Figure 5.5C).

5.2.2.3. Effect of CHIKV nsP3 macrodomain on PARylation activity of Tankyrase

The *in vitro* PARylation assay showed that catalytic domain of Tankyrase was able to add the ADP ribose units. Previous work from lab by Mathur et al. 2016, have shown that CHIKV nsP3 macrodomain act as viral suppressor of RNAi. I was interested to know whether CHIKV viral macrodomain, which is known to remove to mono-ADP ribose moieties (Ecke et al., 2017), have impact on the Tankyrase mediated ADP ribosylation. To study the impact of the nsP3 macrodomain on Tankyrase mediated ADP ribosylation, the *in vitro* assay was done. In this assay, in addition to the PARylation reaction mixture, as NAD⁺ alone (negative control), Tankyrase with NAD⁺ (positive control), CHIKV nsp3 with NAD⁺ (negative control protein) and with Tankyrase, NAD⁺ and recombinant CHIKV nsP3 protein, and the reaction was carried out for 1 h to see the time-dependent effect of nsP3 protein on PARylation (Figure 5.6A). There was no band in NAD⁺ and nsP3 with NAD⁺, whereas there was intense band in Tankyrase and NAD⁺. Although band intensity was very faint when Tankyrase and NAD⁺ were mixed with recombinant nsP3. The ponceau stained blot showed that proteins loaded in the respective wells. Next PARylation assay was done with Tankyrase and NAD⁺ mixed with nsP3 for 30 and 60 min. It was found that the

PARylation was significant (as seen by band intensity), when Tankyrase was incubated alone with NAD⁺, but the intensity reduced significantly as the time of incubation was increasing till 1 h upon the incubation of nsP3 protein. The PAR chains number/length (indicated by chemiluminescent signal intensity which was directly co-related to PAR chain/length, as the PAR specific antibody used in western blot was specific to PAR chains only) was less at 30 min after the incubation of nsP3 protein and reduced significantly at 1 h of incubation compared to the 30 and 60 min of PARylated samples only (Figure 5.6B).

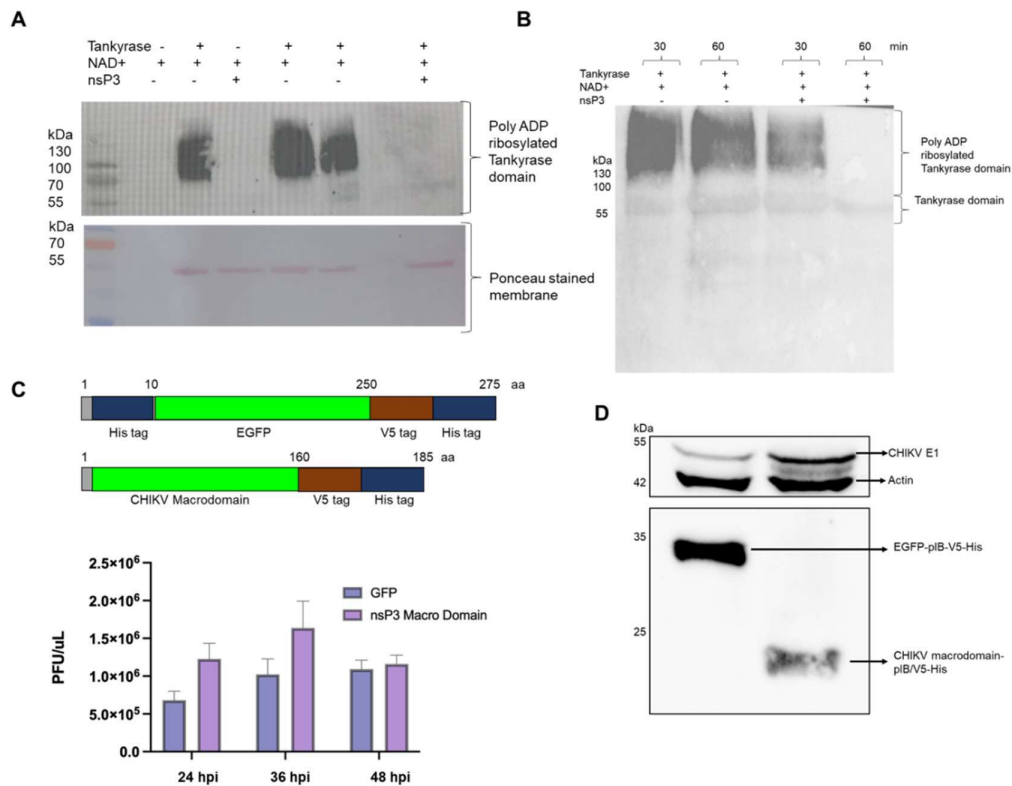


Figure 5.6 *In vitro* PARylation assay and effect of CHIKV nsP3 on PARylation. A) *In vitro* PARylation assay was done with NAD⁺ alone (lane 1) as negative control, Tankyrase with NAD⁺ (lane 2) as positive control, CHIKV nsP3 with NAD⁺ as negative protein control (lane 3), Tankyrase with NAD⁺ for 15 min (lane 4 and 5), and Tankyrase with nsP3 and NAD⁺ (lane 6); B) The *in vitro* PARylation assay was performed for 30 and 60 min (lane 1 and lane 2 from the left side). The impact of nsP3 protein on PARylation was checked by co-incubation of nsP3 protein and PARylation buffer having Tankyrase protein for 30 and 60 min (lane 3 and 4). The reaction mixture was run on SDS PAGE and transferred to a nitrocellulose membrane.

The membrane was probed with anti-pADPr antibody. The membrane was then incubated with anti-mice HRP antibody, and then it was visualized in the ChemiDoc MP system; C) diagram of EGFP and CHIKV macrodomain cloned in insect vector (pIB/V5-His). These two EGFP and CHIKV nsP3 macrodomain-pIB clones were transfected into Aag2 cells separately and then infected with CHIKV at MOI of 1 for different time points to observe the impact on viral growth via plaque assay; and D) the cells collected at 36 hpi were lysed and protein lysate was separated on SDS-PAGE which was then transferred and blotted with different antibodies such as anti-V5 antibody for EGFP and CHIKV macrodomain, house raised anti-CHIKV E1 mice sera for CHIKV E1 protein and anti-actin HRP antibody for actin protein.

The impact of macrodomain alone on CHIKV viral replication was also studied in CHIKV infected Aag2 cells. Aag2 cells were transfected with EGFP and CHIKV Macrodomain cloned in pIB/V5/His vector (Figure 5.6C). For this, the macrodomain and EGFP (control) transfected Aag2 cells were infected with CHIKV at MOI 1 and cells and/or supernatant were collected at 24 hpi, 36 hpi, and 48 hpi. The plaque assay has shown that as compared to control (EGFP transfected), the viral titre was high in macrodomain transfected cells at 24 h and 36 h, whereas at 48 h, the difference between control and macrodomain was insignificant and the expression level was coming down (Figure 5.6C). Similar trend was also observed at 24 hpi in western blot analysis of CHIKV E1 protein. In case of EGFP transfection (lane 1), the CHIKV E1 protein expression was low as compared to macrodomain transfected cells (lane 2) (Figure 5.6D). These results suggest that macrodomain probably catalyzes the removal of ADP ribose from poly-ADP ribosylated proteins. Its presence in cells leads to higher viral titre implying that macrodomain favours the viral replication by hindering the activation of immune pathways.

5.3. Discussion

Owing to our specific interest in evaluating those host proteins interacting with CHIKV-nsP3 involved in the innate immune pathway, especially RNAi, we identified proteins, namely, a PIWI5, and RM62F, a DEAD Box helicase. Ribosomal proteins interact with nsP3 and are part of the replication complex that is central for viral replication more in terms of RNA binding and processing (Frolova et al., 2006). RM62F, on the other hand, is a DExH box helicase, and DEAD/DExH helicases are known to be involved in RNA metabolisms such as transcription, translation, and

small RNA generation (Cheng et al., 2018; Taschuk & Cherry, 2020; Xu et al., 2010). Further, studies have shown that RM62F is a member of the RNAi pathway and its closest homologs are known to play a role in multiple processes such as alternative splicing, RNA transport, ribosome biogenesis, micro-RNA processing, RNAi mediated silencing and antiviral RNAi (Ambrus & Frolov, 2009; Matkovic et al., 2019; Taschuk & Cherry, 2020). The existing knowledge regarding the role of this protein in host-virus interactions prompted us to choose RM62F for further evaluation with respect to its interaction with CHIKV-nsP3. The present work has established that this protein interacts with CHIKV-nsP3; more comprehensive analyses may provide a functional relevance of this interaction.

ADP ribosylation is one of the post-translational modifications. In humans, there are 17 PARPs known. These add ADP ribose specifically to either DNA, RNA, or proteins. At the same time, few have no enzymatic activity. These are also categorized based on adding mono or poly ADP ribose moieties to target molecules (Gupte et al., 2017). PARPS, which binds to DNA or RNA, have either zinc finger domain or RNA recognition motif (RRM), while those which bind to proteins have Ankyrin repeats. PARPs are involved in various processes such as DNA repair, cell signaling, and gene regulation (Gupte et al., 2017). Besides having a role in essential pathways, PARPs are also known to have a role in stress response and pathogen response. During viral infections, PARPs serve as antiviral function by targeting cellular transcripts, promoting apoptosis (Todorova et al., 2014), attenuating RISC mediated transcript silencing (Seo et al., 2013), induction of interferon-stimulated genes, and degradation of viral proteases (Zhang et al., 2015).

For this study, the catalytic domain of Tankyrase was cloned in the pET29a vector, and then protein was expressed and purified from *E. coli* cells and checked for purity in SDS-PAGE gel.

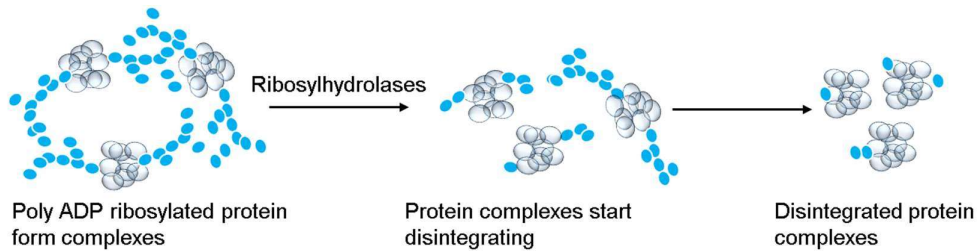


Figure 5.7 Proposed model of Macrodomain CHIKV nsP3 mediated hydrolysis of PAR chains in ADP ribosylated proteins. Poly ADP ribose modified proteins interact with each other and form protein complexes. The ADP ribosylhydrolase such as nsP3 macrodomain hydrolyzes the PAR chains, resulting in the weakened interaction leading to disintegration of complexes if protein complexes are exposed to macrodomain for a long time as virus infection.

The Tankyrase protein was checked for its ability to add PAR chain by *in vitro* auto-PARYlation. Upon running the samples in SDS-PAGE, the poly ADP ribosylated proteins appeared as smear when transferred to a membrane, and an anti-poly ADP ribose antibody was used. This indicated that Tankyrase catalytic domain was able to add PAR chains of varying lengths.

The macrodomain is known to remove the ADP ribose from the target. These are conserved in the active site region among alphaviruses, indicating the importance of the active macrodomain for viral survival. Previous studies reported that mutation in the active sites affects viral replication (Abraham et al., 2018; McPherson et al., 2017). This work showed that nsP3 protein was able to remove the ADP ribosylation from Tankyrase protein, indicating that macrodomain plays an active role during viral infection by removing the PAR chains from host proteins complexes as shown in the proposed model in Figure 5.7, which might also have a role in crucial processes like immune pathways activation, etc. Future studies will shed light on the targets and mechanism of action of macrodomain on host protein complexes.

5.4. Materials and methods

5.4.1. Reagents

Restriction enzyme (Kpn1 and BamH1, (New England Biolab)), T4 DNA ligase kit (Thermo scientific), PrimeScript One-Step RT-PCR Kit (Takara), DreamTaq DNA Polymerase (Thermo scientific), anti-His HRP antibody (Santa Cruz), Anti-pADPr Antibody (10H): sc-56198, (Santa Cruz), anti-mice HRP antibody Novus), NAD

(Nicotinamide adenine dinucleotide) (Sigma Aldrich), MgCl₂.6H₂O (Sigma Aldrich), Tris-Cl (pH 8.0), DTT, nitrocellulose membrane (Biorad), prestained protein ladder (Thermo scientific), GeneRuler 1 kb ladder (Thermo scientific), agarose, 1X TAE buffer, 1X SDS running buffer, SDS loading buffer, DMEM media, FBS, penicillin and streptomycin, L-15 medium, 2% CMC, crystal violet stain, LB broth, TB broth, RIPA buffer, PBS, bacterial cell lysis buffer, Imidazole, Ni-NTA beads, strip buffer, 1X SDS running buffer, Transfer buffer, BSA (bovine serum albumin), QuantiTect SYBR Green PCR Kit.

Cells: *E. coli* DH5a and *E. coli* BL21-CodonPlus.

5.4.2. Methods

5.4.2.1. RM62F and Tankyrase gene cloning, protein expression and purification

For cloning the catalytic domain of RM62F and Tankyrase of *Ae. aegypti*, the RNA was isolated from *Ae. aegypti* mosquitoes using Trizol. The one-step reverse transcription PCR following the manufacturer's protocol (PrimeScript One-Step RT-PCR Kit - Takara Bio) using primers: RM62F: (Forward: 5'-ATAGGTACCATGGATCCGGGAGGTTTCCGCCAC-3' and Reverse: 5'-TATGGATCCCCGTACGAAGAGCAACGGCC-3') and Tankyrase Forward primer 5'-ATAGGTACCAGCGGCACATCCATGGCCAACAG-3' and reverse primer 5'-ATAGGATCCCTCGCTGGCTCCTGGGGGCTAG-3', with annealing at 65°C and primer extension for 120 s. The PCR product was cloned after digestion with KpnI and BamHI into the pET vector. The cloned vector was transformed into an expression cell (*E. coli* BL21-CodonPlus) (See Chapter 2 Materials and methods for details).

5.4.2.2. Antibody generation

Antibodies against proteins were raised in-house. Purified RM62F proteins were injected into rabbits and mice with Freund's complete adjuvant. Booster doses of respective proteins with Freund's incomplete adjuvant were given in regular intervals, and serum samples were collected. Antibody specificity was checked against purified protein and later against cell lysate to confirm the reactivity.

5.4.2.3 Quantitative real-time PCR

Expression profiles of RM62F was performed from infected cells from different time points. The sequences of RM62F was forward primer: 5'-

GACCACAGGTTCCGGATTT-3' and Reverse primer: 5'-CAACGACGCAAGTTGGTAATG-3' and RPS17 was forward primer: 5'-GTGAGCGCAGAGACAACACTAC-3' and reverse primer: 5'-TCCAGCTGCTTCAACATCTC-3'. Primers for qPCR were made using the Prime Quest tool of Integrated DNA Technologies (IDT) with amplicon lengths ranging from 90-110 nucleotides.

Total RNA was extracted from cells using Trizol and quantified with Nanodrop. We used 300ng RNA per reaction. The qPCR was carried out using the Quantitect SYBR green one-step real-time PCR kit (Cat. no. 204243 Qiagen). The qPCR was done with the protocol as cDNA synthesis 50 °C for 30 min, initial denaturation at 95 °C for 2 min, followed by 40 cycles as denaturation at 95 °C for 15 s, annealing at 56 °C for 30 s and extension at 72 °C for 30 s, data acquisition and followed by melt curve analysis. Expression values were normalized to RPS17 housekeeping control mRNA levels. Relative log-fold expression levels were calculated using $2^{(-\Delta\Delta CT)}$ method (Schmittgen & Livak, 2008) and represented as mean \pm SD. Statistical analysis of experimental data was conducted using GraphPad Prism (version 6). Two-tailed student's t-test and Fisher's Least Significant Difference (LSD) test were performed to check the significance of the data, and p-values < 0.001 were considered significant.

5.4.2.4 Cell lines and virus

Aag2 cell line was a kind gift from Dr. Alain Kohl (University of Glasgow, Scotland, UK). Cells were propagated in Leibovitz's L-15 medium (Cat no. AL011S, HiMedia, India) supplemented with 10% fetal bovine serum (FBS), glutamine, tryptose phosphate broth, and penicillin/streptomycin at 28°C and 5% CO₂. The Vero cell line (ATCC-CCL-81) and C6/36 cells were maintained in Dulbecco's Modified Eagle Media (DMEM) (Cat no: AL007A, HiMedia, India) supplemented with 10% FBS, penicillin/streptomycin at 37°C and 5% CO₂. CHIKV (Accession no. JF950631.1) was isolated and purified from a patient serum collected during an outbreak in 2010 (Shrinet et al., 2012) and propagated in both C6/36 and Vero cell lines in alternate cycles. Virus purified from Vero cells was used for Aag2 infection.

5.4.2.5 Virus infection

Aag2 cells were grown in 6-well plates in complete L-15 media. Cells were infected with CHIKV strain at a multiplicity of infection (MOI) of 0.1, 1, and 10. The virus

was diluted in FBS and antibiotic-free L-15 media, and cells were incubated at 28°C. After 2 hours post-infection (hpi), cells were washed with phosphate-buffered saline (PBS) (pH 7.4) and grown in complete L-15 media. The cells and media were collected at different time points, and cell pellets were washed once with PBS and either resuspended in TRIzol for RNA isolation or lysis buffer for western blot.

5.4.2.6 Co-immunoprecipitation assay

To confirm the interaction of CHIKV-nsp3 with *Ae. aegypti* RM62F, co-immunoprecipitation of Aag2 lysate, was performed with purified nsp3 protein using Pierce co-immunoprecipitation kit (Thermo Scientific, USA) as per the manufacturer's instructions. Briefly, 100ul Protein A beads were incubated with CHIKV-nsp3 specific antibody, and after wash, these were incubated with purified nsp3 protein (100 µg) and allowed to bind overnight to antibody at 4°C. For negative control, antibody immobilized beads were directly incubated with Aag2 lysate. Beads were washed with IP wash buffer and incubated with Aag2 lysate (1 mg) for 4 h. After washing, elution fractions were taken for Western blot analysis using nsp3 and RM62F specific antibodies.

5.4.2.7 Western Blot Assay

Protein sample concentration was determined by Bradford's reagent and plotted against bovine serum albumin (BSA) standards of known concentrations. An equal amount of protein samples was loaded in 10% SDS-PAGE gels and run at 100 V till the dye front reaches the other end. Proteins were then transferred onto the nitrocellulose membrane. The membrane was then blocked with PBS (pH 7.4) + 5% BSA for 1hr at RT (room temperature). The membrane was then incubated with anti pADPr antibodies (1:2,000 dilution) or anti-His HRP antibody (1:4000) in PBS+2.5% BSA overnight at 4°C. The membrane was then washed with PBS+ 0.1% Tween-20 for 10 min and repeated thrice. It was then incubated with anti-mice HRP secondary antibodies (1:5,000 dilution) in PBST+2.5% BSA for 1hr at RT. The membrane was then washed with PBS+ 0.1% Tween-20 for 3 X 10 min. The membrane was then visualized in Chemidoc MP (Bio-Rad) after brief incubation with SuperSignal West Pico Chemiluminescent Substrate (Thermo Scientific).

5.4.2.8 *In vitro* PARylation assay

The *in vitro* assay was performed as per protocol (Bisht et al., 2012). Briefly, the *E. coli* purified recombinant Tankyrase protein (8 to 12 µg) was incubated for 30 min at 28°C in PARP reaction buffer (50 mM Tris [pH 8.0], 4 mM MgCl₂, 0.2 mM DTT (dithiothreitol) containing 25 µM NAD (Sigma)).

Reactions were terminated by adding SDS loading buffer and proteins fractionated by 10% SDS-PAGE. The proteins were transferred electrophoretically to the nitrocellulose membrane and probed with an Anti-pADPr antibody (1:2000 dilution). After brief exposure to the chemiluminescent substrate, the membrane was then probed with anti-mouse HRP and visualized in the Biorad ChemiDoc MP system.

5.4.2.9 CHIKV nsP3 macrodomain co-incubation assay

The nsP3 co-incubation assay was done similarly to *in vitro* PARylation assay. In addition to the assay reagents, in the co-incubation assay, the purified recombinant CHIKV nsP3 protein (8 to 12 µg) was added to the reaction mixture.

5.5 References

- Abraham, R., Hauer, D., McPherson, R. L., Utt, A., Kirby, I. T., Cohen, M. S., . . . Griffin, D. E. (2018). ADP-ribosyl-binding and hydrolase activities of the alphavirus nsP3 macrodomain are critical for initiation of virus replication. *Proc Natl Acad Sci U S A*, *115*(44), E10457-E10466. <https://doi.org/10.1073/pnas.1812130115>
- Ambrus, A. M., & Frolov, M. V. (2009). The diverse roles of RNA helicases in RNAi. *Cell Cycle*, *8*(21), 3500-3505. <https://doi.org/10.4161/cc.8.21.9887>
- Bai, P. (2015). Biology of Poly(ADP-Ribose) Polymerases: The Factotums of Cell Maintenance. *Molecular Cell*, *58*(6), 947-958. <https://doi.org/10.1016/j.molcel.2015.01.034>
- Bharaj, P., Atkins, C., Luthra, P., Giraldo, M. I., Dawes, B. E., Miorin, L., . . . Rajsbaum, R. (2017). The Host E3-Ubiquitin Ligase TRIM6 Ubiquitinates the Ebola Virus VP35 Protein and Promotes Virus Replication. *J Virol*, *91*(18). <https://doi.org/10.1128/JVI.00833-17>
- Bisht, K. K., Dudognon, C., Chang, W. G., Sokol, E. S., Ramirez, A., & Smith, S. (2012). GDP-mannose-4,6-dehydratase is a cytosolic partner of tankyrase 1 that inhibits its poly(ADP-ribose) polymerase activity. *Mol Cell Biol*, *32*(15), 3044-3053. <https://doi.org/10.1128/MCB.00258-12>
- Bock, F. J., Todorova, T. T., & Chang, P. (2015). RNA Regulation by Poly(ADP-Ribose) Polymerases. *Mol Cell*, *58*(6), 959-969. <https://doi.org/10.1016/j.molcel.2015.01.037>
- Cheng, W., Chen, G., Jia, H., He, X., & Jing, Z. (2018). DDX5 RNA Helicases: Emerging Roles in Viral Infection. *Int J Mol Sci*, *19*(4). <https://doi.org/10.3390/ijms19041122>

- Cohen, M. S., & Chang, P. (2018). Insights into the biogenesis, function, and regulation of ADP-ribosylation. *Nat Chem Biol*, *14*(3), 236-243. <https://doi.org/10.1038/nchembio.2568>
- Ecke, L., Krieg, S., Butepage, M., Lehmann, A., Gross, A., Lippok, B., . . . Verheugd, P. (2017). The conserved macrodomains of the non-structural proteins of Chikungunya virus and other pathogenic positive strand RNA viruses function as mono-ADP-ribosylhydrolases. *Sci Rep*, *7*, 41746. <https://doi.org/10.1038/srep41746>
- Fan, C., Yarravarapu, N., Chen, H., Kulak, O., Dasari, P., Herbert, J., . . . Zhang, X. (2018). Regulation of tankyrase activity by a catalytic domain dimer interface. *Biochem Biophys Res Commun*, *503*(3), 1780-1785. <https://doi.org/10.1016/j.bbrc.2018.07.113>
- Frolova, E., Gorchakov, R., Garmashova, N., Atasheva, S., Vergara, L. A., & Frolov, I. (2006). Formation of nsP3-specific protein complexes during Sindbis virus replication. *J Virol*, *80*(8), 4122-4134. <https://doi.org/10.1128/JVI.80.8.4122-4134.2006>
- Fu, W., Verma, D., Burton, A., & Swaminathan, S. (2019). Cellular RNA Helicase DHX9 Interacts with the Essential Epstein-Barr Virus (EBV) Protein SM and Restricts EBV Lytic Replication. *J Virol*, *93*(4). <https://doi.org/10.1128/JVI.01244-18>
- Gotte, B., Liu, L., & McInerney, G. M. (2018). The Enigmatic Alphavirus Non-Structural Protein 3 (nsP3) Revealing Its Secrets at Last. *Viruses*, *10*(3). <https://doi.org/10.3390/v10030105>
- Grunewald, M. E., Fehr, A. R., Athmer, J., & Perlman, S. (2018). The coronavirus nucleocapsid protein is ADP-ribosylated. *Virology*, *517*, 62-68. <https://doi.org/10.1016/j.virol.2017.11.020>
- Gupte, R., Liu, Z., & Kraus, W. L. (2017). PARPs and ADP-ribosylation: recent advances linking molecular functions to biological outcomes. *Genes Dev*, *31*(2), 101-126. <https://doi.org/10.1101/gad.291518.116>
- Gustin, J. K., Moses, A. V., Fruh, K., & Douglas, J. L. (2011). Viral takeover of the host ubiquitin system. *Front Microbiol*, *2*, 161. <https://doi.org/10.3389/fmicb.2011.00161>
- Hottiger, M. O., Hassa, P. O., Luscher, B., Schuler, H., & Koch-Nolte, F. (2010). Toward a unified nomenclature for mammalian ADP-ribosyltransferases. *Trends Biochem Sci*, *35*(4), 208-219. <https://doi.org/10.1016/j.tibs.2009.12.003>
- Huang, Y. S., Higgs, S., & Vanlandingham, D. L. (2019). Arbovirus-Mosquito Vector-Host Interactions and the Impact on Transmission and Disease Pathogenesis of Arboviruses. *Front Microbiol*, *10*, 22. <https://doi.org/10.3389/fmicb.2019.00022>
- Isabelle, M., Gagne, J. P., Gallouzi, I. E., & Poirier, G. G. (2012). Quantitative proteomics and dynamic imaging reveal that G3BP-mediated stress granule assembly is poly(ADP-ribose)-dependent following exposure to MNNG-induced DNA alkylation. *J Cell Sci*, *125*(Pt 19), 4555-4566. <https://doi.org/10.1242/jcs.106963>
- Jayabalan, A. K., Adivarahan, S., Koppula, A., Abraham, R., Batish, M., Zenklusen, D., . . . Leung, A. K. L. (2021). Stress granule formation, disassembly, and composition are regulated by alphavirus ADP-ribosylhydrolase activity. *Proc Natl Acad Sci U S A*, *118*(6). <https://doi.org/10.1073/pnas.2021719118>

- Jin, X., Cao, X., Liu, S., & Liu, B. (2021). Functional Roles of Poly(ADP-Ribose) in Stress Granule Formation and Dynamics. *Front Cell Dev Biol*, 9, 671780. <https://doi.org/10.3389/fcell.2021.671780>
- Kumar, A., Srivastava, P., Sirisena, P., Dubey, S. K., Kumar, R., Shrinet, J., & Sunil, S. (2018). Mosquito Innate Immunity. *Insects*, 9(3). <https://doi.org/10.3390/insects9030095>
- Lark, T., Keck, F., & Narayanan, A. (2017). Interactions of Alphavirus nsP3 Protein with Host Proteins. *Front Microbiol*, 8, 2652. <https://doi.org/10.3389/fmicb.2017.02652>
- Leung, A. K., Vyas, S., Rood, J. E., Bhutkar, A., Sharp, P. A., & Chang, P. (2011). Poly(ADP-ribose) regulates stress responses and microRNA activity in the cytoplasm. *Mol Cell*, 42(4), 489-499. <https://doi.org/10.1016/j.molcel.2011.04.015>
- Liu, C., & Yu, X. (2015). ADP-ribosyltransferases and poly ADP-ribosylation. *Curr Protein Pept Sci*, 16(6), 491-501. <https://doi.org/10.2174/1389203716666150504122435>
- Matkovic, R., Bernard, E., Fontanel, S., Eldin, P., Chazal, N., Hassan Hersi, D., . . . Briant, L. (2019). The Host DHX9 DExH-Box Helicase Is Recruited to Chikungunya Virus Replication Complexes for Optimal Genomic RNA Translation. *J Virol*, 93(4). <https://doi.org/10.1128/JVI.01764-18>
- McPherson, R. L., Abraham, R., Sreekumar, E., Ong, S. E., Cheng, S. J., Baxter, V. K., . . . Leung, A. K. (2017). ADP-ribosylhydrolase activity of Chikungunya virus macrodomain is critical for virus replication and virulence. *Proc Natl Acad Sci U S A*, 114(7), 1666-1671. <https://doi.org/10.1073/pnas.1621485114>
- Meshram, C. D., Agback, P., Shiliaev, N., Urakova, N., Mobley, J. A., Agback, T., . . . Frolov, I. (2018). Multiple Host Factors Interact with the Hypervariable Domain of Chikungunya Virus nsP3 and Determine Viral Replication in Cell-Specific Mode. *J Virol*, 92(16). <https://doi.org/10.1128/JVI.00838-18>
- Palazzo, L., Mikolcevic, P., Mikoc, A., & Ahel, I. (2019). ADP-ribosylation signalling and human disease. *Open Biol*, 9(4), 190041. <https://doi.org/10.1098/rsob.190041>
- Rahnefeld, A., Klingel, K., Schuermann, A., Diny, N. L., Althof, N., Lindner, A., . . . Voigt, A. (2014). Ubiquitin-like protein ISG15 (interferon-stimulated gene of 15 kDa) in host defense against heart failure in a mouse model of virus-induced cardiomyopathy. *Circulation*, 130(18), 1589-1600. <https://doi.org/10.1161/CIRCULATIONAHA.114.009847>
- Randow, F., & Lehner, P. J. (2009). Viral avoidance and exploitation of the ubiquitin system. *Nat Cell Biol*, 11(5), 527-534. <https://doi.org/10.1038/ncb0509-527>
- Ribet, D., & Cossart, P. (2010). Pathogen-mediated posttranslational modifications: A re-emerging field. *Cell*, 143(5), 694-702. <https://doi.org/10.1016/j.cell.2010.11.019>
- Riffell, J. L., Lord, C. J., & Ashworth, A. (2012). Tankyrase-targeted therapeutics: expanding opportunities in the PARP family. *Nat Rev Drug Discov*, 11(12), 923-936. <https://doi.org/10.1038/nrd3868>
- Rothenburg, S., & Brennan, G. (2020). Species-Specific Host-Virus Interactions: Implications for Viral Host Range and Virulence. *Trends Microbiol*, 28(1), 46-56. <https://doi.org/10.1016/j.tim.2019.08.007>

- Ryslava, H., Doubnerova, V., Kavan, D., & Vanek, O. (2013). Effect of posttranslational modifications on enzyme function and assembly. *J Proteomics*, *92*, 80-109. <https://doi.org/10.1016/j.jprot.2013.03.025>
- Santos, A. L., & Lindner, A. B. (2017). Protein Posttranslational Modifications: Roles in Aging and Age-Related Disease. *Oxid Med Cell Longev*, *2017*, 5716409. <https://doi.org/10.1155/2017/5716409>
- Schmittgen, T. D., & Livak, K. J. (2008). Analyzing real-time PCR data by the comparative C(T) method. *Nat Protoc*, *3*(6), 1101-1108. <https://doi.org/10.1038/nprot.2008.73>
- Seo, G. J., Kincaid, R. P., Phanaksri, T., Burke, J. M., Pare, J. M., Cox, J. E., . . . Sullivan, C. S. (2013). Reciprocal inhibition between intracellular antiviral signaling and the RNAi machinery in mammalian cells. *Cell Host Microbe*, *14*(4), 435-445. <https://doi.org/10.1016/j.chom.2013.09.002>
- Shrinet, J., Jain, S., Sharma, A., Singh, S. S., Mathur, K., Rana, V., . . . Sunil, S. (2012). Genetic characterization of Chikungunya virus from New Delhi reveal emergence of a new molecular signature in Indian isolates. *Viol J*, *9*, 100. <https://doi.org/10.1186/1743-422X-9-100>
- Taschuk, F., & Cherry, S. (2020). DEAD-Box Helicases: Sensors, Regulators, and Effectors for Antiviral Defense. *Viruses*, *12*(2). <https://doi.org/10.3390/v12020181>
- Todorova, T., Bock, F. J., & Chang, P. (2014). PARP13 regulates cellular mRNA post-transcriptionally and functions as a pro-apoptotic factor by destabilizing TRAILR4 transcript. *Nat Commun*, *5*, 5362. <https://doi.org/10.1038/ncomms6362>
- Xu, L., Khadijah, S., Fang, S., Wang, L., Tay, F. P., & Liu, D. X. (2010). The cellular RNA helicase DDX1 interacts with coronavirus nonstructural protein 14 and enhances viral replication. *J Virol*, *84*(17), 8571-8583. <https://doi.org/10.1128/JVI.00392-10>
- Zhang, T., Ye, Z., Yang, X., Qin, Y., Hu, Y., Tong, X., . . . Ye, X. (2017). NEDDylation of PB2 Reduces Its Stability and Blocks the Replication of Influenza A Virus. *Sci Rep*, *7*, 43691. <https://doi.org/10.1038/srep43691>
- Zhang, Y., Mao, D., Roswit, W. T., Jin, X., Patel, A. C., Patel, D. A., . . . Holtzman, M. J. (2015). PARP9-DTX3L ubiquitin ligase targets host histone H2BJ and viral 3C protease to enhance interferon signaling and control viral infection. *Nat Immunol*, *16*(12), 1215-1227. <https://doi.org/10.1038/ni.3279>

Chapter 6

Chapter 6

Conclusion from the thesis and future prospective

6.1. Conclusion from the thesis

Various microscopic pathogens, including bacteria, viruses, fungus, are known to infect living organisms. These pathogens enter inside the body of the host and start their amplification. These are dependent on the host for resources such as temperature or nutrients (in the case of bacteria and fungus) or even their proteins (in cases of viruses). Being the smallest entity, the viruses' lacks the whole machinery required for their replication cycle. They negatively affect the host during their replication, suggesting the importance of a defense mechanism to protect the organism from these pathogens. All the organisms have developed their general or specific defense mechanism to protect themselves.

Viruses are small particles with DNA or RNA as genetic material encased in structural proteins. Viruses spread through either aerosol such as influenza or coronavirus or require direct blood contact such as HIV. Some viruses, such as dengue and CHIKV, are transmitted by mosquitoes. Many studies have highlighted the impact and mechanism of virus infection in humans, including fever, joint pain, and rashes. Every year hundreds of thousands of cases are reported. Also, outbreaks are reported where there is the rapid spread of the virus among the population either due to lack of hygiene or rapid urbanization or water lodging during the rainy season. All these promote virus spread to a large population, thus affecting people physiologically and economically.

Chikungunya virus is an arbovirus having positive-sense ssRNA genome and infect human. It is transmitted from human to human by female mosquito bites during blood meals, and mosquitoes act as a vector for the virus transmission. Since the virus also infects and grows inside the mosquito, it also impacts the mosquito. Recently few studies came where they have either shown the impact of CHIKV on whole mosquito or other alphaviruses on *Aedes* cells. This is the first study where the proteome impact of CHIKV on siRNA competent cells was observed. To study the impact of the virus on cells, early and late infection time points were selected based on viral plaque titer

and CHIKV E1 protein quantitation. The quantitative analysis revealed that the viral titer peaked at 36 hpi to 48 hpi and then become persistent.

The mass spectrometry analysis revealed that at the initial time of infection of 12 hpi, various pathways such as gene expression, RNA processing, mRNA export from the nucleus were downregulated. Pathways such as oxidation-reduction, autophagy, and transport were upregulated. Upon entry inside the cells, viruses are known to induce oxidative stress, leading to stress granules that inhibit translation. Stress granules sequester various translation factors as well as RNA binding proteins, thus inhibiting viral translation. At a later point of infection, it was observed that pathways such as translation, cellular metabolic process, phosphorous metabolic process, nucleotide metabolic process, etc., were downregulated. In contrast, gene expression, transcription, RNA processing, and ncRNA processing were upregulated. The comparative analysis of downregulated and upregulated proteins at 12 hpi and 60 hpi showed that a few proteins were continuously downregulated or upregulated from 12 hpi to 60 hpi, indicating that during infection, cells are rewiring their gene expression to promote their survival and control virus infection.

One of the CHIKV proteins, nsP3, interacts with host proteins and forms a replication complex. Previously, various studies have identified human proteins that interact with viral proteins, thereby giving more information on how host and virus interact. Its interacting partners in *Aedes* are not known. The co-IP of nsP3 interacting proteins identified several proteins belonging to several pathways such as metabolism, oxidation-reduction, cellular metabolism, and RNA metabolism. Previous work has shown that nsP3 acts as a suppressor of the RNAi pathway. The focus of the study was to find the proteins of the RNAi pathway. RM62F was one of them. The interaction was also confirmed by immunoblotting.

CHIKV nsP3 has the three domains, i.e., macrodomain, AUD, and HVD. The macrodomain is an ADP ribosylhydrolase that removes ADP ribosylation. ADP ribosylation is one of the important modifications. It plays a role in gene expression, apoptosis, DNA repair, and cell signaling. Poly ADP ribose polymerases are the proteins that add the ADP ribose to the target protein/DNA. Poly ADP ribose chains of proteins interact with each other weakly, thereby favoring the formation of multi-protein complexes, which are important to cells' survival. In order to ensure their

replication, viruses encode proteins such as proteases (which cleaves host immune pathway or signaling pathway proteins) or helicases (which bind to RNA and affect the transcription process). Recently studies have reported that viral macrodomain is crucial for viral replication, and mutations in the active site of macrodomain negatively impact viral replication, as also indicated by highly conserved residues among alphaviruses. The sequence homology analysis with human PARPs revealed that, *Ae. aegypti* have three PARP proteins. Of the three PARPs, Tankyrase proteins have the domain needed for interaction with proteins. The *in vitro* PARylation assay of the Tankyrase domain revealed that the catalytic domain was capable of auto-PARylation. It was also found that CHIKV nsP3 could hydrolyze the PAR chains indicating that the macrodomain hydrolyzes the PAR chains and destabilizes the interactions between poly ADP ribosylated proteins in the polyprotein complex. The macrodomain alone was able to affect the viral growth in Aag2 cells, indicating that macrodomain have significant role in viral growth.

6.2. Future prospective

Viruses are the causative agents of many deadly diseases leading to a huge burden to the human population. The regular outbreaks of viruses in different parts of the world make it necessary to study how viruses interact and impact the host. Some viruses, such as arboviruses, use mosquitoes to move between hosts. The global proteome analysis of CHIKV infected U4.4 cells at early and late time points of infection showed significantly modulated pathways. Future work could help to identify major proteins of these pathways which affect viral replication. During the viral infection, host proteins are known to be regulated; identifying them and their role of either antiviral or proviral will give detailed information about the role of other proteins in *Aedes* during CHIKV infection. CHIKV nsP3 protein interacts with multiple *Ae. aegypti* proteins, although their role is not known in CHIKV infection. It will be important to know whether these proteins help the virus in replication or nsP3 proteins sequester them to control host immune pathways, metabolic pathways, or signaling pathways. Future studies will help to know how this domain favors the virus and impact mosquito. It will be interesting to know the target pathways of macrodomain as information about the role of macrodomain as a suppressor of host immune pathways is limited.

Supplementary information 1 for Chapter 3: *Ae. albopictus* (U4.4) upregulated and downregulated proteins upon CHIKV infection

1. 12 hpi upregulated proteins: Total proteins =195

AALF000120,AALF000277,AALF000498,AALF000726,AALF000824,AALF000831,AALF000833,AALF000946,AALF000947,AALF001195,AALF001269,AALF001477,AALF002514,AALF002516,AALF002599,AALF002635,AALF002881,AALF002936,AALF003077,AALF003105,AALF003588,AALF003591,AALF003837,AALF004064,AALF004285,AALF004520,AALF004603,AALF004775,AALF004974,AALF004979,AALF005020,AALF005359,AALF005644,AALF005817,AALF006101,AALF006301,AALF006382,AALF006402,AALF006456,AALF006714,AALF006719,AALF006747,AALF006785,AALF006820,AALF007016,AALF007074,AALF007261,AALF007309,AALF007372,AALF007395,AALF007582,AALF007632,AALF007929,AALF007997,AALF008036,AALF008038,AALF008119,AALF008264,AALF008331,AALF008344,AALF008381,AALF008411,AALF008452,AALF008589,AALF008678,AALF008762,AALF008962,AALF009032,AALF009221,AALF009332,AALF009360,AALF009509,AALF009678,AALF009770,AALF009867,AALF009955,AALF010007,AALF010132,AALF010377,AALF010417,AALF010427,AALF010544,AALF010933,AALF011026,AALF011048,AALF011172,AALF011255,AALF011313,AALF011414,AALF011843,AALF012046,AALF012062,AALF012257,AALF012284,AALF012286,AALF012329,AALF012376,AALF012590,AALF012726,AALF013060,AALF013062,AALF013237,AALF013248,AALF013431,AALF013643,AALF013831,AALF013928,AALF013979,AALF014166,AALF014497,AALF014817,AALF014911,AALF015041,AALF015060,AALF015181,AALF015332,AALF015406,AALF015441,AALF015483,AALF015696,AALF016021,AALF016114,AALF016308,AALF016668,AALF016814,AALF017036,AALF017072,AALF017221,AALF017418,AALF017764,AALF017935,AALF018184,AALF018237,AALF018289,AALF018648,AALF019111,AALF019606,AALF019743,AALF020021,AALF020161,AALF020262,AALF020341,AALF020465,AALF020790,AALF020799,AALF020853,AALF020908,AALF020954,AALF020955,AALF020966,AALF021152,AALF021583,AALF021709,AALF022068,AALF022155,AALF022264,AALF022441,AALF022452,AALF022486,AALF022710,AALF022754,AALF022976,AALF023336,AALF023338,AALF023621,AALF023646,AALF023682,AALF024142,AALF024777,AALF02534

4,AALF025390,AALF025396,AALF025489,AALF025579,AALF025639,AALF025699,AALF025927,AALF026069,AALF026217,AALF026658,AALF026819,AALF026901,AALF027156,AALF027208,AALF027571,AALF027575,AALF027745,AALF027934,AALF028004,AALF028028,AALF028091,AALF028181,AALF028467,AALF028575,AALF028628

2. 12 hpi downregulated proteins: Total proteins=134

AALF021605,AALF015139,AALF008525,AALF028554,AALF003825,AALF002644,AALF020028,AALF011980,AALF002941,AALF003471,AALF005374,AALF017749,AALF000803,AALF011616,AALF003102,AALF026130,AALF008498,AALF028042,AALF010205,AALF007783,AALF027040,AALF011344,AALF019080,AALF024825,AALF020987,AALF006336,AALF020267,AALF012391,AALF002791,AALF025307,AALF001159,AALF026729,AALF010624,AALF021042,AALF005696,AALF011533,AALF011047,AALF008136,AALF027420,AALF024437,AALF008938,AALF003720,AALF022185,AALF022190,AALF008801,AALF028095,AALF006677,AALF021215,AALF002735,AALF004218,AALF014784,AALF016123,AALF002564,AALF013292,AALF018204,AALF017480,AALF021671,AALF026989,AALF013616,AALF016912,AALF028644,AALF000753,AALF010622,AALF003898,AALF026002,AALF017334,AALF022562,AALF014165,AALF016669,AALF013414,AALF010797,AALF021885,AALF011670,AALF007059,AALF014390,AALF010173,AALF014955,AALF005355,AALF004221,AALF005517,AALF010262,AALF016979,AALF009370,AALF019844,AALF005953,AALF016776,AALF010177,AALF004041,AALF015086,AALF007316,AALF011345,AALF027222,AALF020133,AALF013554,AALF012302,AALF008423,AALF024605,AALF027818,AALF026097,AALF021789,AALF017330,AALF018477,AALF025691,AALF016817,AALF018022,AALF013833,AALF001770,AALF010979,AALF014859,AALF011675,AALF020516,AALF022252,AALF026971,AALF016958,AALF022600,AALF026230,AALF019796,AALF022370,AALF002780,AALF008970,AALF022229,AALF022527,AALF005065,AALF018287,AALF007138,AALF013153,AALF010646,AALF028388,AALF014824,AALF026816,AALF009734,AALF022258,AALF005506,AALF015210

3. 60 hpi upregulated proteins: Total proteins=906

AALF028603,AALF028600,AALF028579,AALF028554,AALF028513,AALF028465,AALF028430,AALF028429,AALF028405,AALF028369,AALF028156,AALF028130,AALF028127,AALF028090,AALF028042,AALF028031,AALF028014,AALF027965,AALF027908,AALF027907,AALF027760,AALF027745,AALF027736,AALF027723,AALF027716,AALF027713,AALF027650,AALF027649,AALF027599,AALF027585,AALF027579,AALF027486,AALF027448,AALF027445,AALF027431,AALF027430,AALF027420,AALF027396,AALF027365,AALF027364,AALF027348,AALF027311,AALF027283,AALF027265,AALF027246,AALF027221,AALF027185,AALF027143,AALF027133,AALF027127,AALF027118,AALF027115,AALF027081,AALF027080,AALF027040,AALF027036,AALF026982,AALF026959,AALF026950,AALF026933,AALF026896,AALF026867,AALF026822,AALF026717,AALF026694,AALF026594,AALF026576,AALF026566,AALF026557,AALF026519,AALF026516,AALF026515,AALF026485,AALF026370,AALF026368,AALF026354,AALF026353,AALF026344,AALF026289,AALF026263,AALF026257,AALF026220,AALF026217,AALF026216,AALF026203,AALF026202,AALF026168,AALF026130,AALF026111,AALF026106,AALF026031,AALF026010,AALF026004,AALF025984,AALF025979,AALF025941,AALF025935,AALF025929,AALF025926,AALF025910,AALF025900,AALF025873,AALF025860,AALF025857,AALF025710,AALF025691,AALF025669,AALF025662,AALF025661,AALF025639,AALF025597,AALF025593,AALF025582,AALF025579,AALF025473,AALF025450,AALF025434,AALF025418,AALF025411,AALF025410,AALF025307,AALF025265,AALF025208,AALF025133,AALF025104,AALF025102,AALF025034,AALF025019,AALF024984,AALF024895,AALF024873,AALF024868,AALF024813,AALF024810,AALF024804,AALF024679,AALF024666,AALF024653,AALF024645,AALF024610,AALF024597,AALF024531,AALF024525,AALF024509,AALF024508,AALF024474,AALF024460,AALF024459,AALF024456,AALF024445,AALF024436,AALF024426,AALF024422,AALF024356,AALF024334,AALF024250,AALF024235,AALF024225,AALF024172,AALF024147,AALF024142,AALF024126,AALF024125,AALF024093,AALF023939,AALF023885,AALF023818,AALF023775,AALF023774,AALF023705,AALF023637,AALF023621,AALF023599,AALF023537,AALF023536,AALF023515,AALF023474,AALF023395,AALF023352,AALF023285,AALF023205,AALF023200,AALF023199,AALF023157,AALF023156,AALF023155,AALF023139,AAL

F023129,AALF022984,AALF022924,AALF022855,AALF022771,AALF022759,AA
LF022754,AALF022742,AALF022632,AALF022630,AALF022486,AALF022478,A
ALF022472,AALF022468,AALF022457,AALF022352,AALF022351,AALF022327,
AALF022267,AALF022234,AALF022190,AALF022119,AALF022068,AALF02201
2,AALF021922,AALF021857,AALF021851,AALF021845,AALF021834,AALF021
824,AALF021815,AALF021806,AALF021799,AALF021791,AALF021780,AALFO
21758,AALF021728,AALF021686,AALF021685,AALF021656,AALF021633,AAL
F021616,AALF021609,AALF021607,AALF021584,AALF021583,AALF021540,AA
LF021472,AALF021436,AALF021402,AALF021348,AALF021334,AALF021295,A
ALF021215,AALF021213,AALF021179,AALF021177,AALF021152,AALF021148,
AALF021141,AALF021113,AALF021045,AALF021042,AALF021037,AALF02102
4,AALF021013,AALF021012,AALF020967,AALF020955,AALF020920,AALF020
908,AALF020898,AALF020881,AALF020876,AALF020872,AALF020863,AALFO
20845,AALF020839,AALF020837,AALF020833,AALF020712,AALF020541,AAL
F020515,AALF020469,AALF020460,AALF020439,AALF020438,AALF020388,AA
LF020387,AALF020372,AALF020358,AALF020342,AALF020325,AALF020323,A
ALF020278,AALF020277,AALF020230,AALF020161,AALF020020,AALF020017,
AALF020008,AALF019905,AALF019902,AALF019901,AALF019844,AALF01983
1,AALF019830,AALF019745,AALF019698,AALF019696,AALF019668,AALF019
660,AALF019606,AALF019574,AALF019485,AALF019469,AALF019436,AALFO
19435,AALF019397,AALF019382,AALF019367,AALF019334,AALF019277,AAL
F019242,AALF019236,AALF019116,AALF019045,AALF019024,AALF018974,AA
LF018947,AALF018943,AALF018941,AALF018888,AALF018744,AALF018734,A
ALF018719,AALF018718,AALF018682,AALF018648,AALF018617,AALF018583,
AALF018478,AALF018472,AALF018467,AALF018448,AALF018447,AALF01844
3,AALF018432,AALF018398,AALF018377,AALF018368,AALF018364,AALF018
352,AALF018337,AALF018311,AALF018304,AALF018267,AALF018260,AALFO
18184,AALF018164,AALF018121,AALF018120,AALF018013,AALF017835,AAL
F017834,AALF017771,AALF017692,AALF017652,AALF017623,AALF017609,AA
LF017546,AALF017512,AALF017462,AALF017437,AALF017409,AALF017397,A
ALF017332,AALF017313,AALF017294,AALF017275,AALF017265,AALF017185,
AALF017156,AALF017141,AALF017035,AALF017013,AALF017012,AALF01691
4,AALF016912,AALF016901,AALF016772,AALF016770,AALF016754,AALF016
749,AALF016747,AALF016743,AALF016740,AALF016716,AALF016704,AALFO

16665,AALF016645,AALF016644,AALF016591,AALF016435,AALF016425,AALF016393,AALF016369,AALF016309,AALF016308,AALF016224,AALF016189,AALF016186,AALF016169,AALF016152,AALF016140,AALF016134,AALF016133,AALF016131,AALF016130,AALF016101,AALF016078,AALF016077,AALF016076,AALF015984,AALF015977,AALF015904,AALF015902,AALF015898,AALF015894,AALF015843,AALF015758,AALF015664,AALF015622,AALF015619,AALF015614,AALF015609,AALF015580,AALF015550,AALF015499,AALF015483,AALF015482,AALF015451,AALF015414,AALF015398,AALF015293,AALF015275,AALF015238,AALF015165,AALF015138,AALF015097,AALF014982,AALF014947,AALF014937,AALF014859,AALF014840,AALF014835,AALF014784,AALF014737,AALF014642,AALF014572,AALF014530,AALF014508,AALF014500,AALF014406,AALF014393,AALF014224,AALF014218,AALF014208,AALF014189,AALF014166,AALF014165,AALF014115,AALF014112,AALF014050,AALF014049,AALF014048,AALF014039,AALF013998,AALF013984,AALF013956,AALF013933,AALF013832,AALF013802,AALF013792,AALF013722,AALF013718,AALF013709,AALF013670,AALF013626,AALF013615,AALF013603,AALF013554,AALF013542,AALF013414,AALF013407,AALF013353,AALF013351,AALF013294,AALF013248,AALF013228,AALF013224,AALF013205,AALF013154,AALF013153,AALF013091,AALF013028,AALF013011,AALF013009,AALF012960,AALF012837,AALF012807,AALF012803,AALF012755,AALF012749,AALF012741,AALF012726,AALF012721,AALF012720,AALF012717,AALF012680,AALF012626,AALF012623,AALF012612,AALF012610,AALF012579,AALF012578,AALF012577,AALF012553,AALF012463,AALF012460,AALF012454,AALF012453,AALF012442,AALF012324,AALF012323,AALF012317,AALF012302,AALF012284,AALF012257,AALF012219,AALF012162,AALF012142,AALF012084,AALF012083,AALF012054,AALF011948,AALF011941,AALF011930,AALF011920,AALF011899,AALF011843,AALF011828,AALF011778,AALF011693,AALF011646,AALF011602,AALF011599,AALF011598,AALF011597,AALF011552,AALF011536,AALF011500,AALF011421,AALF011414,AALF011410,AALF011403,AALF011384,AALF011377,AALF011344,AALF011329,AALF011259,AALF011255,AALF011251,AALF011236,AALF011202,AALF011199,AALF011189,AALF011178,AALF011174,AALF011168,AALF011108,AALF011092,AALF011044,AALF011025,AALF010930,AALF010847,AALF010846,AALF010820,AALF010771,AALF010759,AALF010751,AALF010684,AALF010681,AALF010680,AALF010678,AALF010674,AALF010669,AALF010655,AALF010

624,AALF010617,AALF010600,AALF010567,AALF010559,AALF010473,AALF010452,AALF010427,AALF010423,AALF010389,AALF010323,AALF010275,AALF010265,AALF010245,AALF010237,AALF010222,AALF010205,AALF010204,AALF010190,AALF010177,AALF010175,AALF010130,AALF010121,AALF010084,AALF009896,AALF009894,AALF009842,AALF009822,AALF009805,AALF009745,AALF009741,AALF009701,AALF009688,AALF009680,AALF009641,AALF009636,AALF009538,AALF009424,AALF009402,AALF009392,AALF009332,AALF009235,AALF009229,AALF009203,AALF009201,AALF009185,AALF009167,AALF009140,AALF009136,AALF009125,AALF009033,AALF009029,AALF009011,AALF008999,AALF008976,AALF008930,AALF008914,AALF008913,AALF008896,AALF008877,AALF008869,AALF008868,AALF008858,AALF008820,AALF008815,AALF008769,AALF008759,AALF008658,AALF008632,AALF008612,AALF008578,AALF008525,AALF008513,AALF008489,AALF008432,AALF008420,AALF008344,AALF008332,AALF008283,AALF008266,AALF008238,AALF008217,AALF008216,AALF008197,AALF008136,AALF008068,AALF008010,AALF007992,AALF007976,AALF007906,AALF007827,AALF007802,AALF007783,AALF007760,AALF007755,AALF007717,AALF007690,AALF007688,AALF007687,AALF007666,AALF007650,AALF007632,AALF007630,AALF007594,AALF007579,AALF007448,AALF007402,AALF007395,AALF007394,AALF007334,AALF007330,AALF007329,AALF007271,AALF007265,AALF007264,AALF007191,AALF007149,AALF006980,AALF006964,AALF006884,AALF006878,AALF006877,AALF006845,AALF006843,AALF006832,AALF006820,AALF006817,AALF006812,AALF006810,AALF006785,AALF006708,AALF006659,AALF006639,AALF006561,AALF006549,AALF006534,AALF006484,AALF006483,AALF006436,AALF006425,AALF006402,AALF006376,AALF006243,AALF006121,AALF006120,AALF006073,AALF006070,AALF006069,AALF006047,AALF006037,AALF006021,AALF005954,AALF005953,AALF005932,AALF005683,AALF005644,AALF005641,AALF005594,AALF005554,AALF005529,AALF005498,AALF005472,AALF005408,AALF005369,AALF005357,AALF005355,AALF005315,AALF005294,AALF005246,AALF005187,AALF005124,AALF005111,AALF005088,AALF005025,AALF005021,AALF005020,AALF005016,AALF004987,AALF004972,AALF004955,AALF004946,AALF004941,AALF004938,AALF004931,AALF004927,AALF004905,AALF004839,AALF004781,AALF004743,AALF004641,AALF004636,AALF004605,AALF004593,AALF004570,AALF004563,AALF004524,AALF004520,AALF004456,AALF004453,AALF00439

0,AALF004388,AALF004242,AALF004231,AALF004228,AALF004224,AALF004162,AALF004151,AALF004138,AALF004120,AALF004116,AALF004090,AALF004053,AALF004041,AALF004004,AALF003974,AALF003955,AALF003931,AALF003866,AALF003864,AALF003837,AALF003827,AALF003825,AALF003816,AALF003766,AALF003755,AALF003747,AALF003720,AALF003634,AALF003459,AALF003449,AALF003415,AALF003391,AALF003299,AALF003192,AALF003191,AALF003171,AALF003119,AALF003078,AALF003042,AALF003039,AALF003026,AALF002793,AALF002745,AALF002710,AALF002684,AALF002611,AALF002507,AALF002506,AALF002469,AALF002464,AALF002462,AALF002440,AALF002436,AALF002373,AALF002370,AALF002311,AALF002306,AALF002219,AALF002176,AALF002115,AALF002017,AALF002001,AALF001948,AALF001636,AALF001602,AALF001576,AALF001573,AALF001566,AALF001564,AALF001509,AALF001477,AALF001476,AALF001358,AALF001336,AALF001293,AALF001271,AALF001234,AALF001204,AALF001157,AALF001120,AALF001117,AALF001116,AALF001115,AALF001072,AALF000938,AALF000927,AALF000910,AALF000824,AALF000820,AALF000806,AALF000794,AALF000783,AALF000727,AALF000726,AALF000725,AALF000710,AALF000620,AALF000617,AALF000616,AALF000613,AALF000595,AALF000569,AALF000556,AALF000533,AALF000490,AALF000489,AALF000405,AALF000396,AALF000394,AALF000393,AALF000385,AALF000368,AALF000354,AALF000266,AALF000265,AALF000248,AALF000186,AALF000183,AALF000113,AALF000105,AALF000072.

4. 60 hpi downregulated proteins: Total proteins=412

AALF010176,AALF022392,AALF003500,AALF011238,AALF003448,AALF001114,AALF008541,AALF027041,AALF006685,AALF009900,AALF016849,AALF024285,AALF006299,AALF017823,AALF023750,AALF019390,AALF013503,AALF018403,AALF013515,AALF010179,AALF027010,AALF018613,AALF024876,AALF021919,AALF012408,AALF007653,AALF004132,AALF022035,AALF026099,AALF027820,AALF022582,AALF012329,AALF018133,AALF009556,AALF018619,AALF002601,AALF017223,AALF025707,AALF000345,AALF003666,AALF005974,AALF003567,AALF015811,AALF025146,AALF011653,AALF010411,AALF008130,AALF022861,AALF011947,AALF025420,AALF016015,AALF019010,AALF023

543,AALF002418,AALF023548,AALF026862,AALF022185,AALF026316,AALF020386,AALF014501,AALF005453,AALF002047,AALF019400,AALF009852,AALF024086,AALF019383,AALF024018,AALF004333,AALF027730,AALF012786,AALF007595,AALF021377,AALF018738,AALF018807,AALF013156,AALF005936,AALF018110,AALF016123,AALF014786,AALF013465,AALF024228,AALF002941,AALF001440,AALF005256,AALF011605,AALF017095,AALF010892,AALF003480,AALF006347,AALF014116,AALF001073,AALF022758,AALF002516,AALF006720,AALF023323,AALF005515,AALF016515,AALF008657,AALF016127,AALF022910,AALF010386,AALF007705,AALF000668,AALF024710,AALF009101,AALF016555,AALF011885,AALF018205,AALF023879,AALF001502,AALF002335,AALF027719,AALF025201,AALF010660,AALF027651,AALF015612,AALF007572,AALF025054,AALF021009,AALF007470,AALF007472,AALF022407,AALF021817,AALF012279,AALF012857,AALF027260,AALF017000,AALF002449,AALF011766,AALF022387,AALF023476,AALF013614,AALF014496,AALF004175,AALF016400,AALF017331,AALF023117,AALF024496,AALF019474,AALF024561,AALF009765,AALF018252,AALF010641,AALF021193,AALF015486,AALF026256,AALF003767,AALF018728,AALF020422,AALF017128,AALF002395,AALF005017,AALF003587,AALF017526,AALF023906,AALF021952,AALF014912,AALF012494,AALF023524,AALF006775,AALF010024,AALF011376,AALF021670,AALF017993,AALF014318,AALF010115,AALF010622,AALF027652,AALF012823,AALF006139,AALF010020,AALF008026,AALF019046,AALF017279,AALF023182,AALF020195,AALF012336,AALF018108,AALF005938,AALF026259,AALF007782,AALF004050,AALF014972,AALF020473,AALF025948,AALF013910,AALF012780,AALF004188,AALF011019,AALF008663,AALF018534,AALF015565,AALF028651,AALF021147,AALF008592,AALF005195,AALF005069,AALF023368,AALF002101,AALF021709,AALF017330,AALF022002,AALF003124,AALF018729,AALF005392,AALF008152,AALF009801,AALF008250,AALF002009,AALF004064,AALF027668,AALF025493,AALF000915,AALF018586,AALF025938,AALF026564,AALF004603,AALF017693,AALF027413,AALF014148,AALF012497,AALF010388,AALF025940,AALF024926,AALF016104,AALF016478,AALF009705,AALF015210,AALF023647,AALF000273,AALF005955,AALF007758,AALF020334,AALF002709,AALF000936,AALF020054,AALF002645,AALF022252,AALF022858,AALF020806,AALF011696,AALF009512,AALF027096,AALF014674,AALF018496,AALF013775,AALF012855,AALF025950,AALF027751,AALF023951,AALF017876,AALF00901

3,AALF015160,AALF006925,AALF012003,AALF009981,AALF020140,AALF016961,AALF008891,AALF026494,AALF021046,AALF005696,AALF021243,AALF024637,AALF025604,AALF027975,AALF025043,AALF008931,AALF017833,AALF015997,AALF024232,AALF008748,AALF008801,AALF017480,AALF015929,AALF007573,AALF022834,AALF002986,AALF012528,AALF017385,AALF014219,AALF015539,AALF012468,AALF014760,AALF003187,AALF026443,AALF005143,AALF016723,AALF011144,AALF020197,AALF016861,AALF000341,AALF001347,AALF010561,AALF024240,AALF024239,AALF021953,AALF014969,AALF011175,AALF008598,AALF012590,AALF003542,AALF009347,AALF011221,AALF012779,AALF008538,AALF019098,AALF002024,AALF015250,AALF019717,AALF003541,AALF027814,AALF007467,AALF027546,AALF025023,AALF017747,AALF016188,AALF025117,AALF010107,AALF022452,AALF022710,AALF020291,AALF009662,AALF016835,AALF001572,AALF010517,AALF001119,AALF024843,AALF004005,AALF023673,AALF014171,AALF014787,AALF003353,AALF016095,AALF021760,AALF025795,AALF017733,AALF006339,AALF019876,AALF016365,AALF008584,AALF023126,AALF004225,AALF001357,AALF019695,AALF024745,AALF017935,AALF019875,AALF010144,AALF009067,AALF006361,AALF020005,AALF014350,AALF014351,AALF020805,AALF018219,AALF026321,AALF023562,AALF006821,AALF012843,AALF021331,AALF021036,AALF023971,AALF019693,AALF017663,AALF020089,AALF014689,AALF019484,AALF012688,AALF004191,AALF016221,AALF002804,AALF010685,AALF019659,AALF013298,AALF007785,AALF022326,AALF022807,AALF002300,AALF010109,AALF028372,AALF005221,AALF011145,AALF020030,AALF011983,AALF007392,AALF006341,AALF009548,AALF014260,AALF019859,AALF020799,AALF014528,AALF014559,AALF020581,AALF027350,AALF011481,AALF024605,AALF025903,AALF008765,AALF002791,AALF026527,AALF021807,AALF025212,AALF016611,AALF020841,AALF019572,AALF026224,AALF016124,AALF016955,AALF010587,AALF011938,AALF016979.

5. 12 hpi to 60 hpi upregulated protein: Total proteins=510

AALF028653,AALF028579,AALF028554,AALF028513,AALF028465,AALF028405,AALF028388,AALF028369,AALF028183,AALF028090,AALF028042,AALF028041,AALF027908,AALF027907,AALF027818,AALF027760,AALF027713,AALF027599,AALF027579,AALF027486,AALF027445,AALF027431,AALF027422,AALF027364,AALF027348,AALF027286,AALF027246,AALF027222,AALF027080,AALF027040,AALF026993,AALF026989,AALF026959,AALF026950,AALF026896,AALF026822,AALF026717,AALF026695,AALF026576,AALF026566,AALF026557,AALF026531,AALF026519,AALF026485,AALF026368,AALF026353,AALF026317,AALF026257,AALF026216,AALF026130,AALF026097,AALF026031,AALF026004,AALF025984,AALF025935,AALF025873,AALF025867,AALF025857,AALF025748,AALF025691,AALF025597,AALF025582,AALF025434,AALF025411,AALF025307,AALF025265,AALF025208,AALF025171,AALF025162,AALF025157,AALF025102,AALF025042,AALF025034,AALF025019,AALF024825,AALF024813,AALF024810,AALF024804,AALF024531,AALF024525,AALF024474,AALF024462,AALF024460,AALF024437,AALF024422,AALF024356,AALF024251,AALF024235,AALF024172,AALF024147,AALF024093,AALF023815,AALF023775,AALF023774,AALF023764,AALF023705,AALF023623,AALF023537,AALF023468,AALF023352,AALF023340,AALF023205,AALF023157,AALF023155,AALF023139,AALF023129,AALF023127,AALF023053,AALF022838,AALF022771,AALF022630,AALF022600,AALF022554,AALF022527,AALF022472,AALF022457,AALF022370,AALF022351,AALF022267,AALF022258,AALF022234,AALF022190,AALF022103,AALF022012,AALF021922,AALF021885,AALF021857,AALF021851,AALF021845,AALF021834,AALF021809,AALF021799,AALF021791,AALF021780,AALF021728,AALF021685,AALF021671,AALF021633,AALF021472,AALF021436,AALF021334,AALF021295,AALF021215,AALF021213,AALF021042,AALF020987,AALF020967,AALF020899,AALF020881,AALF020872,AALF020845,AALF020839,AALF020651,AALF020584,AALF020541,AALF020515,AALF020460,AALF020439,AALF020372,AALF020342,AALF020323,AALF020316,AALF020267,AALF020133,AALF020017,AALF019919,AALF019901,AALF019844,AALF019796,AALF019600,AALF019469,AALF019435,AALF019382,AALF019277,AALF019242,AALF019236,AALF019116,AALF019024,AALF018974,AALF018888,AALF018734,AALF018719,AALF018617,AALF018478,AALF018470,AALF018467,AALF018432,AAL

F018368,AALF018304,AALF018287,AALF018261,AALF018260,AALF018204,AA
LF018182,AALF018169,AALF018164,AALF018121,AALF017836,AALF017771,A
ALF017680,AALF017592,AALF017546,AALF017524,AALF017462,AALF017383,
AALF017332,AALF017313,AALF017185,AALF017035,AALF016958,AALF01691
4,AALF016912,AALF016901,AALF016817,AALF016815,AALF016776,AALF016
772,AALF016770,AALF016666,AALF016645,AALF016591,AALF016482,AALFO
16435,AALF016434,AALF016224,AALF016200,AALF016189,AALF016169,AAL
F016152,AALF016140,AALF016133,AALF016101,AALF016078,AALF016077,AA
LF015998,AALF015977,AALF015972,AALF015869,AALF015619,AALF015609,A
ALF015521,AALF015354,AALF015312,AALF015275,AALF015210,AALF015097,
AALF015086,AALF014955,AALF014937,AALF014859,AALF014840,AALF01482
5,AALF014824,AALF014793,AALF014784,AALF014737,AALF014731,AALF014
726,AALF014572,AALF014218,AALF014208,AALF014165,AALF014118,AALFO
14115,AALF014050,AALF014048,AALF014039,AALF014024,AALF013802,AAL
F013784,AALF013722,AALF013718,AALF013709,AALF013626,AALF013554,AA
LF013415,AALF013414,AALF013353,AALF013153,AALF013066,AALF013051,A
ALF012962,AALF012960,AALF012875,AALF012837,AALF012836,AALF012803,
AALF012741,AALF012721,AALF012720,AALF012717,AALF012680,AALF01261
2,AALF012610,AALF012579,AALF012454,AALF012442,AALF012323,AALF012
317,AALF012302,AALF012264,AALF012210,AALF012166,AALF012162,AALFO
12142,AALF011997,AALF011957,AALF011930,AALF011899,AALF011898,AAL
F011897,AALF011778,AALF011675,AALF011670,AALF011646,AALF011602,AA
LF011599,AALF011598,AALF011567,AALF011536,AALF011533,AALF011505,A
ALF011422,AALF011403,AALF011384,AALF011344,AALF011270,AALF011189,
AALF011092,AALF010979,AALF010847,AALF010820,AALF010797,AALF01077
1,AALF010684,AALF010655,AALF010646,AALF010624,AALF010559,AALF010
452,AALF010423,AALF010370,AALF010323,AALF010262,AALF010245,AALFO
10205,AALF010177,AALF010175,AALF010131,AALF010121,AALF009954,AAL
F009894,AALF009842,AALF009745,AALF009741,AALF009734,AALF009636,AA
LF009538,AALF009473,AALF009403,AALF009392,AALF009370,AALF009352,A
ALF009203,AALF009201,AALF009143,AALF009136,AALF009011,AALF008976,
AALF008970,AALF008930,AALF008878,AALF008877,AALF008769,AALF00865
8,AALF008612,AALF008591,AALF008578,AALF008525,AALF008488,AALF008
472,AALF008423,AALF008332,AALF008283,AALF008068,AALF008060,AALFO

07976,AALF007906,AALF007831,AALF007802,AALF007783,AALF007760,AALF007755,AALF007594,AALF007579,AALF007394,AALF007329,AALF007316,AALF007284,AALF007191,AALF007138,AALF006964,AALF006881,AALF006878,AALF006877,AALF006845,AALF006484,AALF006483,AALF006360,AALF006357,AALF006337,AALF006329,AALF006121,AALF006120,AALF006076,AALF006069,AALF006021,AALF005953,AALF005683,AALF005594,AALF005554,AALF005506,AALF005395,AALF005374,AALF005355,AALF005246,AALF005187,AALF005176,AALF005088,AALF005065,AALF005030,AALF005016,AALF004972,AALF004950,AALF004927,AALF004899,AALF004593,AALF004570,AALF004563,AALF004524,AALF004446,AALF004445,AALF004350,AALF004228,AALF004221,AALF004218,AALF004151,AALF004138,AALF004104,AALF004102,AALF004090,AALF004041,AALF003977,AALF003974,AALF003955,AALF003866,AALF003864,AALF003825,AALF003766,AALF003720,AALF003699,AALF003449,AALF003415,AALF003191,AALF003102,AALF003078,AALF003042,AALF003039,AALF003026,AALF002792,AALF002780,AALF002723,AALF002710,AALF002684,AALF002611,AALF002507,AALF002469,AALF002464,AALF002373,AALF002208,AALF002095,AALF001887,AALF001770,AALF001764,AALF001602,AALF001576,AALF001566,AALF001369,AALF001358,AALF001204,AALF001159,AALF001120,AALF001100,AALF000938,AALF000820,AALF000806,AALF000794,AALF000783,AALF000753,AALF000730,AALF000620,AALF000617,AALF000616,AALF000595,AALF000490,AALF000394,AALF000393,AALF000368,AALF000354,AALF000186.

6. 12hpi to 60 hpi downregulated protein: total protein=152

AALF020386,AALF016857,AALF027524,AALF013503,AALF022301,AALF002230,AALF022920,AALF014817,AALF022264,AALF027575,AALF010179,AALF008657,AALF002101,AALF006821,AALF011986,AALF020033,AALF025117,AALF005923,AALF003092,AALF024907,AALF021781,AALF003588,AALF008580,AALF025489,AALF003795,AALF017764,AALF024240,AALF006747,AALF009678,AALF007016,AALF026259,AALF025390,AALF002449,AALF028181,AALF026658,AALF028628,AALF004775,AALF006339,AALF010754,AALF026292,AALF020966,AALF025049,AALF017990,AALF000831,AALF016124,AALF011026,AALF018237,AALF013831,AALF013928,AALF020291,AALF028574,AALF014760,AALF006719,AALF027814,AALF017935,AALF008079,AALF013029,AALF012800,AALF0

25212,AALF002986,AALF002832,AALF004547,AALF012497,AALF015406,AALF028028,AALF018289,AALF019111,AALF008598,AALF011382,AALF026901,AALF012329,AALF011696,AALF012286,AALF002599,AALF005340,AALF005458,AALF014219,AALF027156,AALF006714,AALF007997,AALF013431,AALF008584,AALF007261,AALF020790,AALF024898,AALF020841,AALF008381,AALF009597,AALF008437,AALF008962,AALF000498,AALF016979,AALF002936,AALF022976,AALF001347,AALF014350,AALF023338,AALF020341,AALF004603,AALF010933,AALF008932,AALF003416,AALF021807,AALF010417,AALF028005,AALF017036,AALF016015,AALF011128,AALF004064,AALF005419,AALF011144,AALF028004,AALF013979,AALF014351,AALF020021,AALF008331,AALF007074,AALF008411,AALF012046,AALF005268,AALF024687,AALF017798,AALF017331,AALF019693,AALF019695,AALF008264,AALF019139,AALF002881,AALF027708,AALF010380,AALF027651,AALF002516,AALF022326,AALF022807,AALF021709,AALF010755,AALF026443,AALF011172,AALF020089,AALF010109,AALF001351,AALF012590,AALF002635,AALF020799,AALF016955,AALF012826,AALF022452,AALF022710,AALF000359,AALF016668,AALF000130,AALF019743.